AD_____

Award Number: DAMD17-97-1-7044

TITLE: Role of Tissue Transglutaminases in Breast Cancer

PRINCIPAL INVESTIGATOR: Zishan Haroon, M.D.
Dr. C. Greenberg

CONTRACTING ORGANIZATION: Duke University Medical Center
Durham, North Carolina 27710

REPORT DATE: July 2000

TYPE OF REPORT: Final

PREPARED FOR: U.S. Army Medical Research and Materiel Command
Fort Detrick, Maryland 21702-5012

REPORT DOCUMENTATION PAGE

Form Approved
OMB No. 074-0188

1. AGENCY USE ONLY (Leave blank)	2. REPORT DATE	3. REPORT TYPE AND DATES COVERED
	July 2000	Final (1 Jul 97 - 30 Jun 00)

4. TITLE AND SUBTITLE
Role of Tissue Transglutaminases in Breast Cancer

5. FUNDING NUMBERS
DAMD17-97-1-7044

6. AUTHOR(S)
Zishan Haroon, M.D.
Dr. C. Greenberg

7. PERFORMING ORGANIZATION NAME(S) AND ADDRESS(ES)
Duke University Medical Center
Durham, North Carolina 27710

E-MAIL:
z@radonc.duke.edu

8. PERFORMING ORGANIZATION REPORT NUMBER

9. SPONSORING / MONITORING AGENCY NAME(S) AND ADDRESS(ES)
U.S. Army Medical Research and Materiel Command
Fort Detrick, Maryland 21702-5012

10. SPONSORING / MONITORING AGENCY REPORT NUMBER

11. SUPPLEMENTARY NOTES
This report contains colored photos

12a. DISTRIBUTION / AVAILABILITY STATEMENT
Approved for public release; distribution unlimited

12b. DISTRIBUTION CODE

13. ABSTRACT ***(Maximum 200 Words)***

Angiogenesis is vital to tumor growth and metastasis. The scope of this grant was to study in detail the role of Tissue transglutaminase (tTG) during wound healing and tumorigenesis. In the first year of the grant proposal, we have described the expression, localization, molecular form and tTG's association with other major determinants of wound healing and tumorigenesis. Our findings clearly show that tTG is readily upregulated in wound healing and rat mammary adenocarcinoma and is associated with endothelial and inflammatory cells. Hypoxia, Vascular endothelial growth factor, Transforming growth factor beta and Tumor necrosis factor alpha are also upregulated alongside tTG in those cells. tTG is quickly proteolysed in the tissues and that may have important consequences as tTG can hydrolyze ATP/GTP in its fragmented form. In the second year and continuing, We have also shown that tTG can inhibit tumor growth as part of host response mechanism and identified that tTG's effects are compartmentalized i.e. host and tumor. In tumor cells, it prevents growth and metastasis at primary site and promotes establishment of metastasis once the tumor cells escape from the primary focus. We are still continuing with establishing the mechanism behind tTG effects.

14. SUBJECT TERMS
Breast Cancer

15. NUMBER OF PAGES
75

16. PRICE CODE

17. SECURITY CLASSIFICATION OF REPORT	18. SECURITY CLASSIFICATION OF THIS PAGE	19. SECURITY CLASSIFICATION OF ABSTRACT	20. LIMITATION OF ABSTRACT
Unclassified	Unclassified	Unclassified	Unlimited

FOREWORD

Opinions, interpretations, conclusions and recommendations are those of the author and are not necessarily endorsed by the U.S. Army.

___ Where copyrighted material is quoted, permission has been obtained to use such material.

___ Where material from documents designated for limited distribution is quoted, permission has been obtained to use the material.

___ Citations of commercial organizations and trade names in this report do not constitute an official Department of Army endorsement or approval of the products or services of these organizations.

X In conducting research using animals, the investigator(s) adhered to the "Guide for the Care and Use of Laboratory Animals," prepared by the Committee on Care and use of Laboratory Animals of the Institute of Laboratory Resources, national Research Council (NIH Publication No. 86-23, Revised 1985).

N/A For the protection of human subjects, the investigator(s) adhered to policies of applicable Federal Law 45 CFR 46.

N/A In conducting research utilizing recombinant DNA technology, the investigator(s) adhered to current guidelines promulgated by the National Institutes of Health.

N/A In the conduct of research utilizing recombinant DNA, the investigator(s) adhered to the NIH Guidelines for Research Involving Recombinant DNA Molecules.

N/A In the conduct of research involving hazardous organisms, the investigator(s) adhered to the CDC-NIH Guide for Biosafety in Microbiological and Biomedical Laboratories.

7/31/00

PI - Signature Date

Table of Contents

Introduction

Malignant tumors require the development of new blood vessels (angiogenesis) for progressive growth. Angiogenesis is a complex process involving degradation of the basement membrane, proliferation, migration, and remodeling of the tissues by vascular cells. The goal of my dissertation was to explore the different modalities through which tumor angiogenesis progresses and study the role of the enzyme tissue Transglutaminase (TG), a crosslinking enzyme, in tumor growth, angiogenesis and metastasis. In the light of recent advances concerning role of anti-angiogenic therapy for Breast and other carcinoma, this work would enhance our understanding and provide valuable insights to the complicated process of tumor growth and angiogenesis. Also, we wanted to investigate the role of host response in inhibiting tumor growth as a new way of restricting tumor progression.

Body:

The goal of my dissertation was to investigate the role of a crosslinking enzyme tissue transglutaminase (TG) in tumor growth and angiogenesis. Since tumors are considered wounds that do not heal, we also studied the role of this enzyme in normal wound healing. In the process of that investigation, we also looked at the relationship of hypoxia to angiogenesis during wound healing. This has provided insights to the primary stimulus of angiogenesis, which could have implications in how we approach anti-angiogenic therapy in the future. We investigated TG's role in tumor growth and metastasis from two different angles i.e. host and tumor. As a host response, TG restricts tumor growth through fibrosis. Meanwhile, as a tumor protein, it has different functions altogether. Now, I will enumerate the research accomplishments as stated in statement of work.

Technical Objective 1; Task 1-8:

We had problems in getting consistent results from fibrin gel chambers. The gel liquefied in the chamber that led to non-evaluation of chambers. This also resulted in excessive use of materials including fibrinogen. Since then, we have since altered the design of these chambers reducing the amount of materials used and added Factor XIII to stabilize the fibrin for longer time periods. We have a new protocol approved by the Duke IACUC and are proceeding with those experiments. We have already duplicated our findings of window chambers and feel comfortable in going on with studies with various mutants.

We investigated the role of TG during wound healing and have since completed the manuscript that was accepted in FASEB Journal (Appendix 1). This study details role of TG during wound healing including the cellular expression, molecular form and activity pattern, the relationship of TG to injury cytokines and its ability to induce angiogenesis.

We also investigated the role of hypoxia in induction of angiogenesis and repair and have the manuscript accepted in Annals of Surgery (Appendix 2). We showed that hypoxia may not be the primary stimulus of angiogenesis and repair and coagulation system has a much larger role to play in this aspect. Since TG is part of this first coagulation response, it gave us more impetus to study in detail its role in wound healing and angiogenesis. We also discovered that D-Dimer, a break down product of provisional fibrin matrix, is an indicator of nodal involvement of breast cancer (appendix 3).

Technical Objective 2; Task 1-2:

We have since divided the approach to technical objective 2 in two spheres i.e. TG as part of host response and TG as part of tumor tissue.

We have completed the study of TG's role as part of the host response against tumor growth in a rat mammary adenocarcinoma R3230 Ac (Appendix 4). We have shown that TG is part of the host response and acts to inhibit tumor growth by inducing a fibrotic reaction with help of TGF β.

We also investigated role of TG as part of tumor cells. We transfected murine breast carcinoma 4T1 with TG tagged with green fluorescent protein (GFP) and found that TG expression caused marked decrease in tumor growth and metastasis from the primary site and the details of the preliminary results are given in Appendix 5.

Dissertation:

I successfully defended my dissertation in June, 1999. I am still continuing the work related to the Defense grant as a Research Associate at Duke University Medical Center.

Key Research Accomplishments:

- TG is a wound healing enzyme and promotes angiogenesis.
- Hypoxia is not the critical factor in induction of angiogenesis and repair and is involved in vascular regression.
- TG is expressed as a host response to tumor growth and acts to limit tumor growth through fibrosis.
- TG enhances establishment of metastasis in murine breast carcinoma.
- TG limits tumor growth and metastasis in primary breast tumor mass.
- D-Dimer is a marker of nodal involvement of breast cancer.

Reportable Outcomes:

1. **ZA Haroon**, KG Peters, CS Greenberg and MW Dewhirst. Ch:01 Angiogenesis and Oxygen transport in the solid tumors in *Antiangiogenic Agents* (BA Teicher, ed) Humana, Totowa, NJ (*1999*).
2. **ZA Haroon**, JM Hettasch, TS Lai, RL McCauley, MW Dewhirst and CS Greenberg. Tissue Transglutaminase is expressed and active during Rat Dermal Wound Healing and Angiogenesis. *FASEB Journal 13: 1787-95, 1999.*
3. **ZA Haroon**, JA Raleigh, CS Greenberg and MW Dewhirst. Early wound healing exhibits cytokine surge without evidence of Hypoxia. *Annals of Surgery 231:137-147, 2000.*
4. **ZA Haroon**, TS Lai, JM Hettasch, RA Lindberg, MW Dewhirst and CS Greenberg. Tissue Transglutaminase is expressed as a host response and inhibits tumor growth. *Laboratory Investigation 79:1679-86, 1999.*
5. **ZA Haroon**, T Wannenburg, CS Greenberg, and DC Sane. Immunohistochemical detection of Transglutaminase, a Tissue stabilizing enzyme in atherosclerotic plaques. *AHA, Dallas, Texas, Novemeber, 1998.*
6. TS Lai, A Hausladen, TF Slaughter, JP Eu, KA Peoples, JM Hettasch, **ZA Haroon**, JS Stamler and CS Greenberg. Tissue Transglutaminase binds and releases Nitric Oxide- Role in regulating thrombogenesis of blood vessels. *40th Annual ASH, Miami, Florida, December, 1998.*
7. **ZA Haroon**, JA Raleigh, CS Greenberg and MW Dewhirst. Early wound healing exhibits cytokine surge without evidence of Hypoxia. *ASBMB, SanFrancisco, CA, May 1999.*
8. **ZA Haroon.** Hypoxia and Tissue Transglutaminase – A wound healing perspective. *Dissertation, June, 1999.* PhD awarded.
9. Research Associate at Duke University Medical Center. **Job.**
10. **Z.A. Haroon*,** S.O. Bukhari, R.D. Braun, J.A. Raleigh, C.S. Greenberg and M.W. Dewhirst Differential Hypoxia Distribution in Ectopic and Orthotopic R3230Ac Mammary Adenocarcinoma Tumor Implants**.** *RRS, NewMexico, 2000.*
11. **Platform speaker** at Era of Hope meeting, **Department of Defence** Initiative for Breast Cancer, Atlanta, GA (June, 2000).
12. Kimberly Blackwell, **ZA Haroon**, Gloria Broadwater, Donald Berry, Lyndsay Harris, J. Dirk Iglehart, Mark Dewhirst, and Charles Greenberg. Plasma d-dimer levels in operable breast cancer patients correlate with extent of disease involvement *Journal of Clinical Oncology, February, 2000.*

Conclusions:

The work to date has established TG as a wound healing enzyme that can also induce angiogenesis. TG's expression and activity is related to major injury cytokines such as TGF β and VEGF. This has provided much needed insights into the role of this enzyme in tumor biology also since tumors utilize wound healing mechanisms to propagate themselves.

This work was the lead to our investigations in TG's role in tumor biology and we have found that TG both as a host response and as part of primary tumor mass acts to inhibit tumor growth and metastasis. This is vital information that after further research could potentially be exploited to eradicate breast cancer.

Also, we established that hypoxia is not one of the critical factors for induction of angiogenesis and repair. This study can have major impact on the importance of initial coagulation response as the true source of angiogenesis trigger.

APPENDIX 01

Tissue transglutaminase is expressed, active, and directly involved in rat dermal wound healing and angiogenesis

ZISHAN A. HAROON,* JOANN M. HETTASCH,† THUNG-SHENQ LAI,† MARK W. DEWHIRST,*,‡ AND CHARLES S. GREENBERG*,†,[1]

*Department of Pathology, †Medicine and ‡Radiation Oncology, Duke University Medical Center, Durham, North Carolina 27710, USA

ABSTRACT **Tissue transglutaminase (TG) is an enzyme that stabilizes the structure of tissues by covalently ligating extracellular matrix molecules. Expression and localization of TG are not well established during wound healing. We performed punch biopsy wounds on anesthetized rats and monitored the wound healing process by histological and immunohistochemical methods. The TG antigen and activity are expressed at sites of neovascularization in the provisional fibrin matrix within 24 h of wounding. Endothelial cells, macrophages, and skeletal muscle cells expressed TG throughout the healing process. The TG antigen within the wound was active *in vivo* based on the detection of isopeptide bonds. The TG antigen increased four- to fivefold by day 3 postwounding and was proteolytically degraded. TG expression occurred in association with TGF-β, TNF-α, IL-6, and VEGF production in the wound. Recombinant TG increased vessel length density (a measure of angiogenesis) when applied topically in rat dorsal skin flap window chambers. We have established that TG is an important tissue stabilizing enzyme that is active during wound healing and can function to promote angiogenesis.—Haroon, Z. A., Hettasch, J. M., Lai, T.-S., Dewhirst, M. W., Greenberg, C. S. Tissue transglutaminase is expressed, active, and directly involved in rat dermal wound healing and angiogenesis. *FASEB J.* 13, 1787–1795 (1999)**

Key Words: tissue repair · extracellular matrix · cross-linking · endothelial cells · TGF-β

WOUND HEALING IS a complex and intricate process initiated in response to injury that restores the function and integrity of damaged tissues. Wound healing involves continuous cell–cell and cell–matrix interactions that allow the process to proceed in overlapping stages, i.e., inflammation, proliferation, and remodeling (1). Defects in any phase of wound healing can contribute to the pathology of many diseases (psoriasis, rheumatoid arthritis, etc.) and tumor growth (2). The tissue transglutaminase (TG)[2] is a calcium-dependent enzyme that covalently cross-links a wide variety of extracellular matrix (ECM) proteins, producing a protease-resistant matrix, and is reported to be expressed at sites of inflammation (3). The TG therefore appears to play a role in tissue repair and seems to be involved in several phases of wound healing.

The TG catalyzes the formation of ε-(γ-glutamyl) lysine bonds (isopeptide bond) between peptide-bound glutamine residues and the primary amine group of various amines (4). These isopeptide bonds are stable and more resistant to proteolytic degradation than noncovalent linkages. The covalent cross-linking reaction increases the resistance of proteins to chemical, enzymatic, and physical disruption (3). The list of proteins that are TG substrates is extensive and includes extracellular adhesive proteins such as fibronectin (5), collagen (6), fibrinogen (7), fibrin (8), laminin/nidogen (9), osteopontin (10), and vitronectin (11), to name a few. Recent data have implicated TG in several intra- and extracellular processes that are critical for wound healing including apoptosis (12), osteogenesis (13), cellular signaling (14), and cell adhesion (15).

Bowness et al. (16, 17) reported TG activity was present at sites of wound healing and that inhibition of TG by putrescine caused decreased breaking strength and increased solubility of the repairing wound tissue (18). However, the cellular expression, distribution, and metabolic fate of the TG at sites of wound healing in relationship to the expression of cytokines and migration of inflammatory cells were not investigated. The goal of this study was to identify the distribution of TG antigen, its activity, and the metabolic fate of TG during wound healing. In

[1] Correspondence: Box 2603, MSRB, DUMC, Durham, NC 27710, USA. E-mail: green032@mc.duke.edu

[2] Abbreviations: ECM, extracellular matrix; Ig, immunoglobulin; IL, interleukin; s.c., subcutaneous; TG, transglutaminase; TGF, tumor growth factor; TNF, tumor necrosis factor.

addition, the expression of various cytokines and inflammatory cells associated with the expression of TG was analyzed. Last, a direct effect of TG on angiogenesis was studied in an *in vivo* window chamber model. These studies and their implications add direct significance to the role of TG in wound healing and angiogenesis.

MATERIALS AND METHODS

Animal protocols

The Duke Institutional Animal Care and Use Committee approved all animal protocols.

Wounds

Fisher 344 female rats from Charles River Laboratories (Raleigh, N.C.) were anesthetized with intraperitoneal injections of pentobarbital (40 mg/kg) and ketamine (70 mg/kg), then shaved and depilated using Nair (Carter-Wallace, New York, N.Y.). Eighteen 5 mm biopsy punch wounds were made on the dorsal skin. The normal skin served as unwounded skin controls. Wounds were harvested at days 1 through 9 while animals were anesthetized. Days 0, 1, 3, 5, 7, and 9 postwounding were used in Western blots; days 0, 1, 2, 4, 6, and 8 were used for immunohistochemistry. Two rats were killed for each time point by intravenous pentobarbital overdose and the experiments were done in triplicate. Tissues were either snap-frozen in liquid nitrogen for Western blots and kept at −80°C or fixed in 10% neutral buffered formalin for paraffin embedding for immunohistochemistry.

Window chambers

Dorsal skin flap window chambers were used as described by Papenfuss et al. (19). Briefly, Fisher 344 rats were anesthetized and the skin over the back was depilated and surgically prepared. The skin flap was pulled dorsally away from the back. Two opposing 1 cm diameter windows were created on each side of the flap by surgically resecting the epidermis. One to two fascial planes were left, which contained a few preformed vessels. The resultant subcutaneous (s.c.) window was protected by glass coverslips and held away from the body of the animal by an anodized aluminum superstructure. This wounded tissue window created a visual field through which the process of wound healing could be observed noninvasively. Recombinant human TG (500 μl of 40 μg/ml or 40 μM) (20) was applied topically on the day of surgery and on days 1 and 2 postsurgery. Normal saline was used as a control. Rats were killed at day 10. Intravital microscopy was used to document the level of neovascularization at days 1 and 10. Quantitation of angiogenesis was provided by measuring vessel length density (21).

Immunohistochemistry

Immunohistochemistry was carried out using procedures described by Hsu et al. (22). Briefly, paraffin embedded tissues were sectioned (5 μ) and antigen retrieval was performed using citrate buffer from Biogenex (San Ramon, Calif.). Tissues were treated with primary antibody against tissue transglutaminase (TG100 and CUB 7402, 1:10, nonreactive to factor XIIIa: both monoclonals were epitope mapped to a region between 447–538 amino acids; unpublished results), vascular endothelial growth factor (VEGF 3; 1:100; Neomarkers, Fremont, Calif.), ED1-macrophage marker (MCA341, 1:100; Serotec, Oxford, U.K.), isopeptide (814 MAM, 1:75; CovalAB, Oullins, France) (23, 24), panspecific tumor growth factor β (TGF-β: AB-100-NA, 1:100, which recognizes the active forms of TGF-β1, 2, and 5), rat antitumor necrosis factor α (anti-TNF-α: AB-510-NA, 1:100; R&D, Minneapolis, Minn.), interleukin 6 (R-19, 1:100; Santa Cruz, Santa Cruz, Calif.), and mast cell tryptase (M7052, 1:100; DAKO, Carpinteria, Calif.). Secondary and tertiary antibodies were provided in a kit (314KLD) by Innovex (Richmond, Calif.) and the location of the reaction was visualized with 3, 3′-diaminobenzidine tetrahydrochloride Sigma (St. Louis, Mo.). Slides were counterstained with hematoxylin and mounted with coverslips. Controls for the immunohistochemistry were treated with normal mouse serum (NMUS) or mouse immunoglobulin G (IgG) (TG100, CUB 7402, 814 MAM, M7052, VEGF 3, and MCA 341), rabbit IgG (AB-100-NA), and goat IgG (IL-6, AB-510-NA) and were negative in any reactivity. Masson's trichrome and hematoxylin and eosin were carried out as described by Sheehan and Hrapchak (25).

Western blot

Wounds from days 0, 1, 3, 5, 7, and 9 were homogenized in 2 ml cold lysis buffer containing the proteolytic inhibitor mixture (#1697498; Boehringer Mannheim, Mannheim, Germany), followed by sonification. The blots were performed with four different wound sets. They were then centrifuged, and supernatant was removed and protein content was determined using Bio-Rad. Gel electrophoresis of the extracted tissue samples (50 μg/ml) was performed on an 8.5% polyacrylamide gel using the buffer system of Laemmeli. After electrophoresis, the proteins were transferred to nitrocellulose (0.2 μM). When the transfer was complete, the nitrocellulose membrane was blocked for 1 h with 5% nonfat milk dissolved in 20 mM Tris-HCl, pH 7.4, 150 mM NaCl, 0.5% Tween 20. The TG antigen was detected by incubation for 1 h using a monoclonal antibody for TG (TG 100, CUB 7402; Neomarkers) diluted 1:1000, followed by incubation for 1 h with sheep anti-mouse IgG conjugated to horseradish peroxidase. The TG antigen was visualized using chemiluminescence reagents (ECL, Amersham, Arlington Heights, Ill.) and a 30 s exposure to autoradiography film. The amount of protein on the blot was estimated with a densitometer. The data in Fig. 5*A* show one sample blot, and Fig. 5*B* contains the cumulative data for the four blots in a graphical presentation.

RESULTS

Light microscopy findings

At the earliest time point at day 1 (**Fig. 1*A***), provisional matrix with inflammatory cells (**Fig. 2*A***) and dilated blood vessels could be observed underneath a newly formed epithelial layer. Re-epithelialization was completed by day 2 postwounding. Maturation of granulation tissue was detected by day 4 (Fig. 1*B*) and characterized by the presence of new blood vessels, inflammatory cells (Fig. 2*B, C*), and collagen fibers organized into a dense connective tissue. Skel-

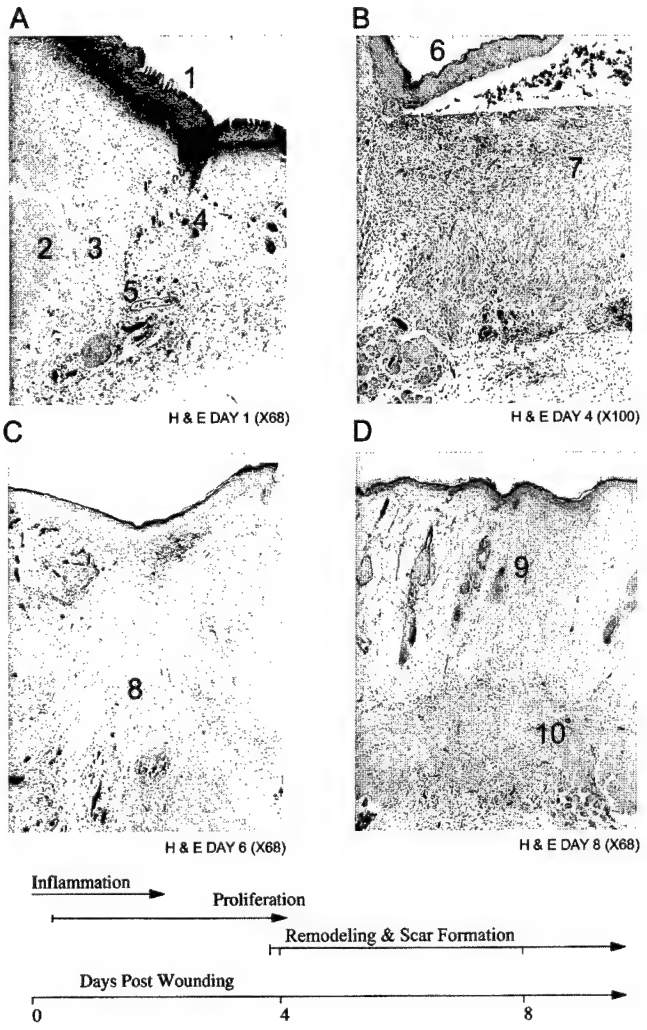

Figure 1. *A)* Light microscopic histology with hematoxylin and eosin (H&E) of normal rat dermal wound healing. New epithelium (A1) is being laid down as early as day 1 postwounding. Neovessels (A4) and dilated existing vessels (A5) can be visualized in provisional fibrin matrix. Skeletal muscle cells (A2) form a border zone (A3) between normal and wounded tissue. *B)* The epithelial later is complete by day 4 (B6) and granulation tissue (B7) has matured. *C)* The granulation tissue starts to contract (C8) by day 6. *D)* Scar tissue is visible by day 8 and the remnants of granulation tissue (D10) have moved down to the base of the wound. At the bottom of the figure is a time course illustration of normal rat dermal wound healing divided in the three stages of wound healing.

etal muscle cells that had formed a boundary between the normal and wounded tissue at earlier time points now moved to the base of the wound and closed the gap created by the injury (Fig. 1*B*). By day 6 (Fig. 1*C*), granulation tissue started to contract and increased in density. At day 8 (Fig. 1*D*) the healing was in its final stages, with remnants of granulation tissue left at the base of the wound. The injury site was filled with dense collagen tissue, with very few blood vessels. The widely recognized three stages of wound healing (1) and their time course in our model of healing are depicted at the bottom of Fig. 1.

Expression and localization of TG

The normal rat skin consistently expressed TG antigen in the blood vessels that reside in the dermis and s.c. tissue (**Fig. 3*A***). Some sebaceous glands and basal keratinocytes also showed expression, but in a sporadic fashion. The TG antigen was detected in the new blood vessels, which invaded the provisional fibrin matrix and the dilated blood vessels at day 1 postinjury (Fig. 3*B–D*). The TG antigen staining was particularly intense in macrophages adjacent to the re-epithelialization border and in the provisional matrix (Fig. 3*B, C*). Mast cells (Fig. 2*D*) were present in highest density on day 1 postwounding and exhibited TG expression. The keratinocytes involved in re-epithelialization expressed TG antigen (Fig. 3*B*). TG reactive skeletal muscle cells, macrophages, and blood vessels formed a distinct boundary between the normal and injured tissue (Fig. 3*C*). TG was also detected in the provisional fibrin matrix (Fig. 3*D*). By day 2, re-epithelialization was

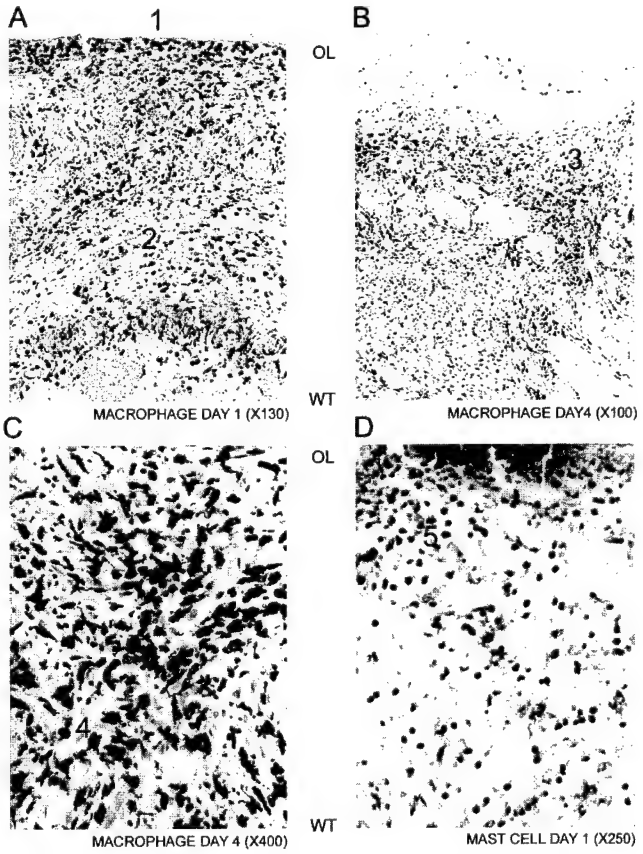

Figure 2. Expression of macrophages and mast cells is shown here. *A)* Macrophages line the re-epithelialization border (A1) and form the predominant part of provisional fibrin matrix (A2) at day 1. *B)* By day 4, macrophages have spread throughout the mature granulation tissue (B3) and could be visualized in high density (C4). Mast cells (D5) stained predominantly at day 1 only. Orientation of the figures is shown as outer layer (OL) and wounded tissue (WT).

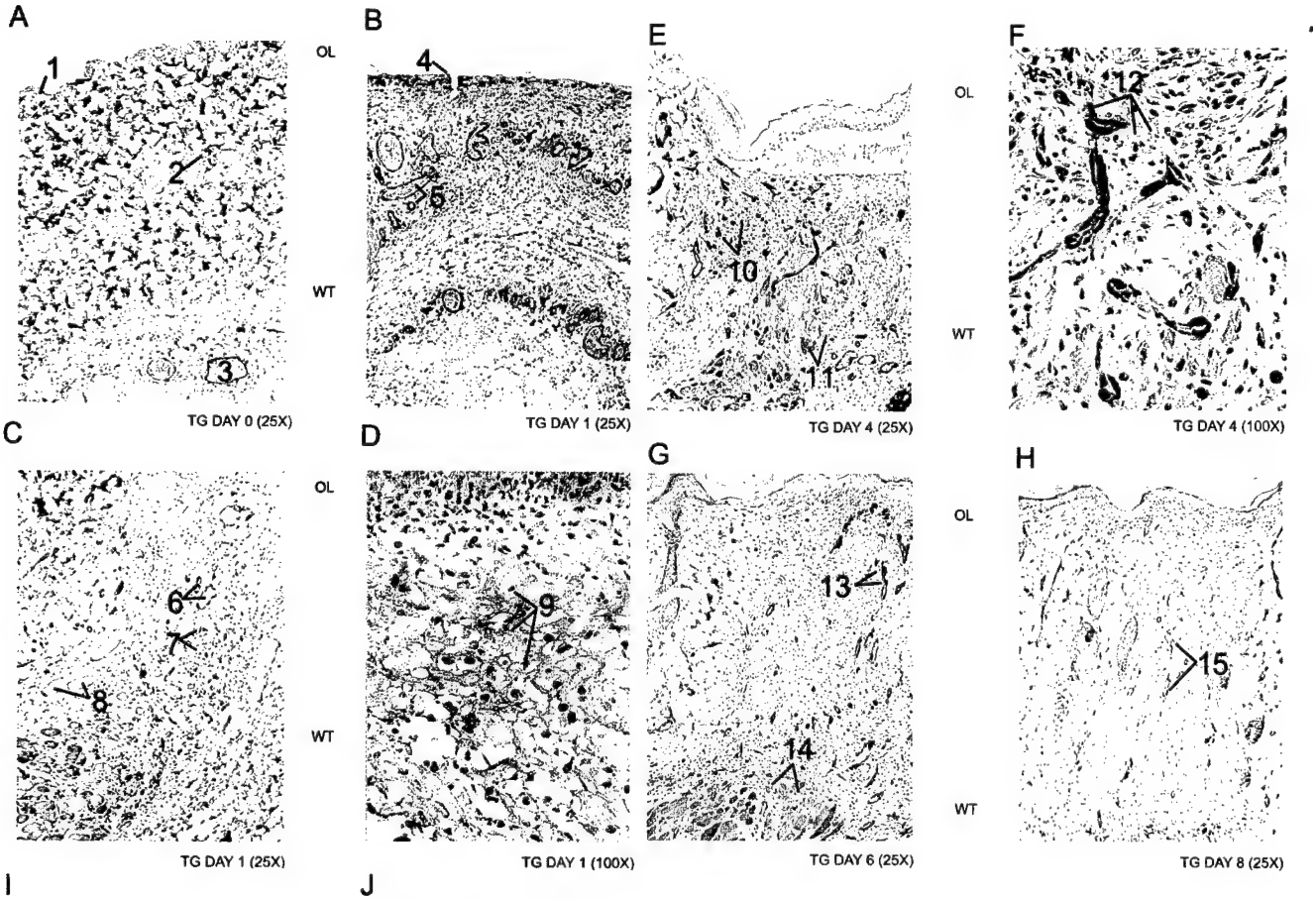

Figure 3. Immunohistochemical evidence of TG expression and activity during wound healing. Normal rat skin stained for TG is shown in panel *A*. Epithelial layer (A1) shows very little expression while blood vessels in the dermis (A2) and s.c. fascia (A3) show TG staining. Re-epithelialization zone consisting of keratinocytes and macrophages (B4) along with neovessels (B5) in provisional fibrin matrix exhibits TG staining. The border zone between normal (left) and wounded (right) tissue at day 1 (*C*) shows TG-reactive endothelial cells (C6), macrophages (C7), and skeletal muscle cells (C8). A high magnification at day 1 (*D*) exhibits the presence of TG in the provisional fibrin matrix (D9). By day 4 postwounding (*E*), expression is limited to basal keratinocytes in the epithelial layer, endothelial cells (E10), skeletal muscle cells (E11) and matrix. TG could still be detected in the granulation tissue (F12) at day 4 (F). TG continues to be detected in the blood vessels (G13) in granulation tissue and skeletal muscle cells (G14) at the base of the wound at day 6. Expression of TG is limited to the scattered blood vessels in the scar tissue (H15), with the major portion of immunoreactivity localized to the base of the wound. Isopeptide bond detection in provisional fibrin matrix (*I*) and granulation tissue (*J*) at days 1 and 4 postwounding, respectively. Isopeptide bonds could be observed in the provisional fibrin matrix (I16), basement membrane of the blood vessels (I17) at day 1. Isopeptide bonds continue to be detected in the blood vessels (J18) and granulation tissue (J19) at day 4. Orientation of the figures is shown as outer layer (OL) and wounded tissue (WT).

complete and TG expression was reduced in the epithelial layer and limited to the dermoepidermal junction. The provisional fibrin matrix was slowly replaced by granulation tissue by day 2, and the wound began to accumulate collagen and TG antigen reactivity. TG immunoreactivity in the collagen also increased as the number of endothelial cells, macrophages, and skeletal muscle cells increased in the wound.

The TG antigen (Fig. 3*E*) and macrophage (Fig. 2*B*) staining was absent from the keratinocyte layer at day 4. Macrophages, endothelial cells in the neovessels, and more mature vessels continued to stain for the TG antigen (Fig. 3*E*). The TG reactive skeletal muscle cells started to move underneath the wounded tissue to bridge the gap created by injury (Fig. 3*E*). TG was still present in the granulation tissue matrix at day 4 (Fig. 3*F*). As the granulation tissue continued to contract and the tissue was further remodeled (day 6), the highly reactive TG at

the edge of the wound vanished and TG staining became localized to the blood vessels and base of the wound (Fig. 3*G*). By day 8, the early granulation tissue was replaced with a dense collagen-rich scar. The TG antigen was predominantly expressed in blood vessels, skeletal muscles, and macrophages at the base of the wound (Fig. 3*H*). A few remaining vessels in the scar tissue also exhibited TG staining (Fig. 3*H*).

Localization of TG activity

The isopeptide bond created by TG cross-linking was detected surrounding blood vessels, newly generating epithelial layer, and fibrin by day 1 of wounding (Fig. 3*I*). The intensity of immunoreactivity of the isopeptide bond increased within the ECM of the granulation tissue, basement membrane of blood vessels, and along the epithelial region at day 4 (Fig. 3*J*). In contrast to the reduction of staining for TG and the redistribution of the TG antigen to the base of the wound, the isopeptide bond antigen continued to be detectable, but at a reduced level, during the formation of the dense scar tissue at day 8.

Expression of cytokines (TGF-β, TNF-α, IL-6, and VEGF)

TGF-β was maximally expressed at the wound surface, granulation tissue, and wound border over the entire time course examined (**Fig. 4*A***). The intensity of staining was greatest in regions where TG antigen reactivity was the highest. The one exception to this finding was in the mature epithelial layer at day 4, where TGF-β antigen was expressed but TG was absent.

Interleukin 6 (IL-6) stained intensely in the skeletal muscle cells of the dermis throughout the study (Fig. 4*B*), with less intense staining in the macrophages, fibroblasts, and endothelial cells during the early wound healing (days 1–4). IL-6 coexpressed with TG in the skeletal muscle cells at all time points examined. TNF-α stained predominantly macrophages in the wounded tissue and coexpressed with TG in those cells throughout the healing process (Fig. 4*C*). Endothelial cells and skeletal muscle cells also exhibited partial expression of this cytokine.

The endothelial cells and macrophages expressed VEGF antigen at day 1 postwounding (Fig. 4*D*), which correlated with TG expression. VEGF expression in endothelial cells and macrophages decreased in intensity even though TG continued to be expressed at high levels at day 4. By day 8, TG and VEGF coexpressed in remnant blood vessels in the scar tissue.

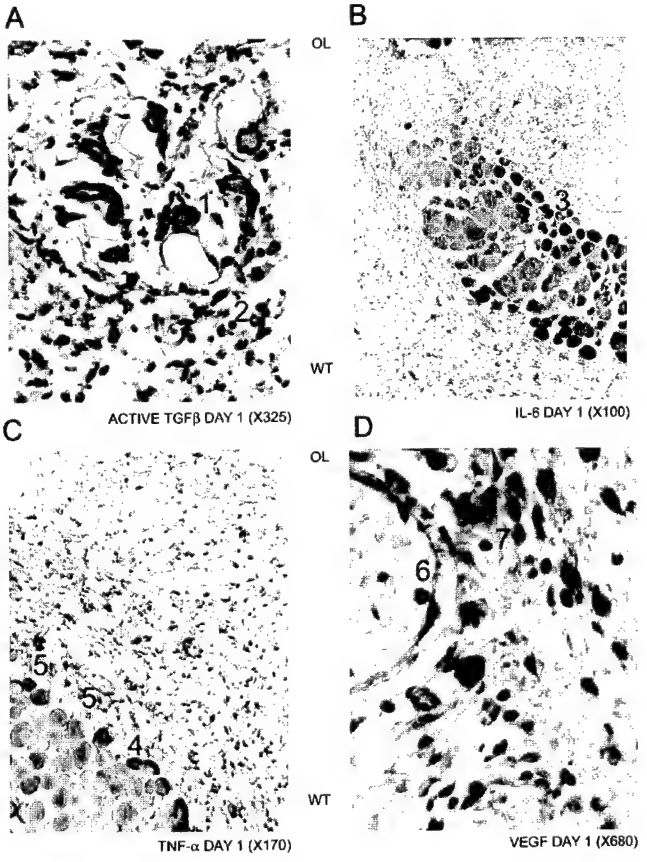

Figure 4. Cytokine expression during wound healing. *A)* Active TGF-β can be seen staining for endothelial cells (A1) and macrophages (A2) at day 1 postwounding. *B)* IL-6 exhibited intense staining in the skeletal muscle cells (B3) at day 1. *C)* TNF-α is shown here to be immunoreactive in macrophages (C4) and sporadically in endothelial cells (C5) and skeletal muscle cells. *D)* VEGF was intensely staining for endothelial cells (D6) and macrophages (D7) at day 1 postwounding. Orientation of the figures is shown as outer layer (OL) and wounded tissue (WT).

A summary of the immunohistochemical data is provided in **Table 1**.

Western blot analysis of TG antigen in wounded tissue

Sodium dodecyl sulfate-polyacrylamide gel electrophoresis and quantitative immunoblotting demonstrated that the total TG antigen increased from four- to fivefold by day 3 (**Fig. 5*A, B***). Quantitative analysis of the antigen (n=4) revealed that more than 95% of the protein was proteolytically degraded to 55, 50, and 20 kDa fragments by day 1 postwounding. The extent of proteolysis and the amount of TG antigen reached maximum by day 3, after which the full-length TG antigen was detected. The total TG antigen levels returned to baseline values by day 9. However, the amount of intact protein was still considerably reduced compared with the control skin tissue.

TABLE 1. *A summary of the immunohistochemical data described in the text*[a]

Characteristic	Time postwounding (days)					
	Control	01	02	04	06	08
Tissue transglutaminase	+	+++	+++	+++	++	+
Isopeptide	+	+++	+++	+++	++	++
Cytokines						
VEGF	+	+++	+++	++	++	+
TGF β	+	+++	+++	+++	++	++
TNF α	+	+++	+++	+++	++	+
IL-6	−	++	++	++	+	+

[a] Intensity of immunoreactivity is graded: − none, + weak, ++ strong, +++ intense.

Effect of recombinant TG on angiogenic response in rat dorsal skin flap chamber

To determine what effect the active TG had on dermal wound healing, we used the rat dorsal skin flap window chamber to administer full-length recombinant TG and measure its effects on angiogenesis. When recombinant TG was applied to fascia in the rat dorsal skin flap window chambers, a significant doubling in the vessel length density was measured at day 10 compared to controls (P=0.05) (**Fig. 6**).

DISCUSSION

The potential roles that TG plays during various stages of wound healing are summarized in **Fig. 7**. The TG could be exerting its effects during wound healing either in *1)* response to injury cytokines, *2)* stabilization of provisional fibrin matrix, *3)* migration of endothelial and inflammatory cells, and/or *4)* remodeling of the granulation tissue through apoptosis and cross-linking.

The finding that both TG expression and activity were increased very early during wound healing demonstrated that the TG gene was activated in cells that were migrating into the fibrin clot and/or remodeling the ECM. The TG gene has regulatory elements that appear to be responsive to acute-phase injury cytokines including TGF-β (26), IL-6 (27), and TNF-α (28). TG's ability to be induced by TGF-β (26), IL-6 (27), and TNF-α (28) and its association with expression of these cytokines and VEGF during wound healing indicated a pivotal role during this process. These cytokines are essential in orchestrating a defined sequence of events to complete the healing process. TG's association with these cytokines during wound healing illustrates that the TG gene could be induced by these cytokines and function to aid in tissue repair. These findings also indicate that complicated and dynamic interactions exist between the cytokines and TG.

There is an important interaction between TGF-β

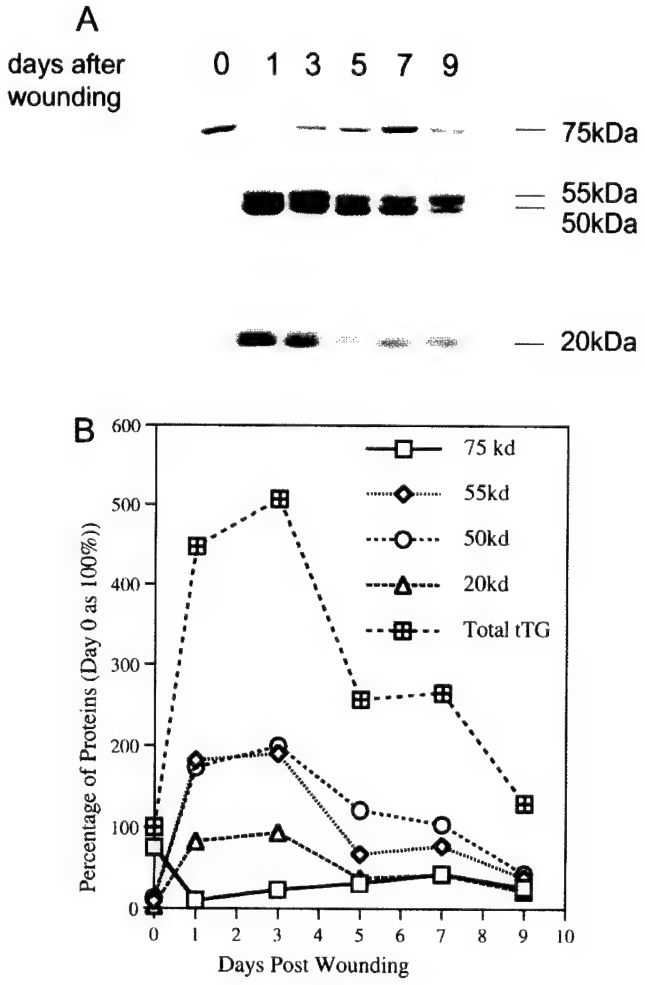

Figure 5. *A)* Western blot analysis of wounds. Normal skin shows expression of full-length TG (75 kDa) with small amounts of 55 and 50 kDa fragments. Although total TG expression increases significantly (days 1 and 3), almost all of TG is present in the form of 55, 50, and 20 kDa fragments. *B)* Quantitative analysis of Western blots (n=4). Plot shows TG and its fragments at days 0 through 9, taking total TG at day 0 (normal skin) as 100%. Total TG increases 4 to 5 times on day 1 and 3 and slowly falls to basal level by day 9. Full-length TG constitutes more than 80% of total TG at day 9, but is reduced to less than 5% by day 1 and recovers to only ~25% at day 9. The 55, 50, and 20 kDa form a minimal portion of total TG at day 0. The amount of fragmented TG increases dramatically by day 1; 55 and 50 kDa forms account for as much as 40% each of total TG. All fragments start to decline by day 5 and make up only ~25% each at day 9 of total TG.

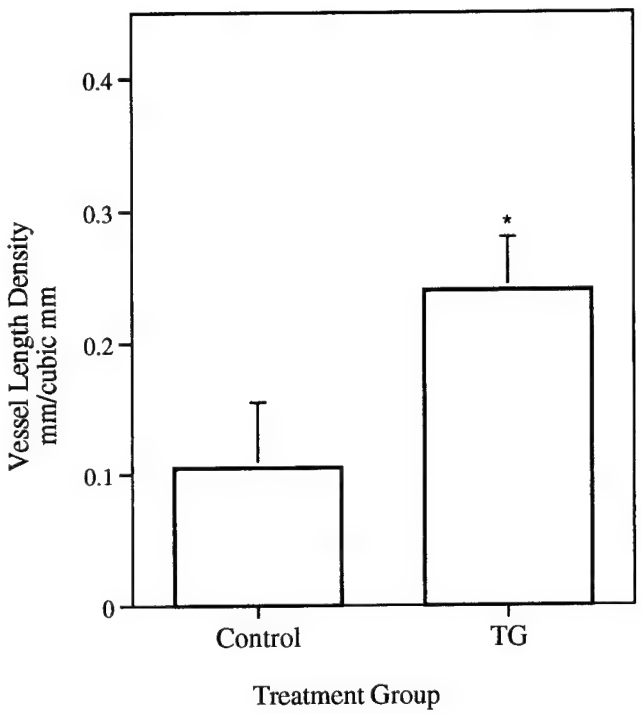

Figure 6. Vessel length density (mm^2) of rat dorsal skin flap chambers treated with saline or recombinant wild type TG. Chambers treated with wild type TG showed a significant *($P=0.05$,* two-tailed Student's *t test, $n=6$)* doubling over controls illustrating a proangiogenic effect on healing process.

and TG that could amplify production of granulation tissue. TG is bound to cell surface complexes comprised of plasminogen, uPAR, and the mannose-6-phosphate receptor (29). The function of this complex is to facilitate the conversion of latent TGF-β to its active form (29). Our immunohistochemistry results show maximal staining for active TGF-β in areas demonstrating high TG immunoreactivity when the provisional fibrin matrix is being replaced by newly synthesized connective tissue. This interaction appears to be operational in the second phase of wound healing. The increased activation of TGF-β by TG could lead to the expression of TG gene early within the fibrin clot and at sites of re-epithelialization, since the TG gene itself is induced by TGF-β. TG and TGF-β effectively complete a positive amplification loop whereby the TG increases TGF-β activation, which then induces more TGF-β activity to further amplify TGF-β activation and TG expression (Fig. 7). The end product of this process is the replacement of fibrin matrix with granulation tissue.

The early expression of TG by endothelial cells and macrophages invading the fibrin clot observed during wound healing appeared to stabilize the fibrin, since isopeptide bonds were detected in both the fibrin and the newly synthesized loose granulation tissue. Isopeptide bonds could be generated by other isoforms of TG, including factor XIIIa and epidermal transglutaminase. We cannot quantitate to what extent factor XIIIa or TG is responsible for the generation of isopeptide bonds. However, the distribution of factor XIIIa in wounds is different from that of TG antigen reported in this study (30). Earlier studies of patients with factor XIIIa deficiency have shown wound healing defects in only 20% (31), suggesting an alternate pathway of fibrin stabilization in the tissues of these patients. Factor XIIIa requires thrombin for activation while TG is synthesized in an active form (32). The factor XIIIa molecule may be responsible for the isopeptide bonds formed within the fibrin clot. Since TG does not require thrombin activation, it can catalyze the stabilization of newly formed ECM as thrombin is removed from the wounded tissue. The TG in human blood vessels catalyzes the α-α cross-links of fibrin and fibrinogen in human atherosclerotic plaques (33), demonstrating that this enzyme is active during human disease process. The stabilization of the matrix by TG could regulate assembly of the granulation tissue and the neovascularization that is essential for an effective healing response.

The transient expression of TG in the epithelial layer suggested a role of TG in re-epithelialization and keratinization, as reported by others. Raghunath et al. (34) found that TG was expressed at the dermoepidermal junction in wounds. They sug-

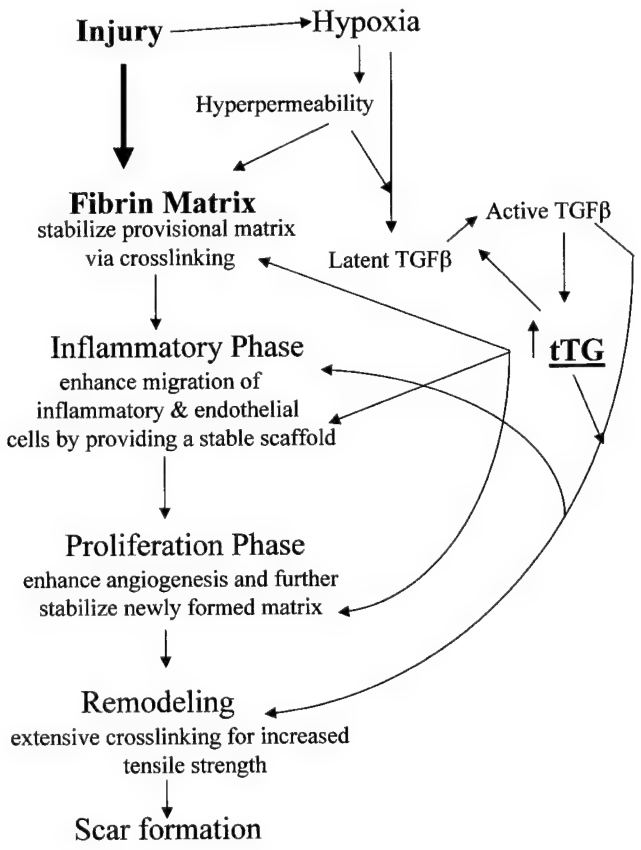

Figure 7. Schematic illustration showing TG's role and possible mechanisms of action during wound healing.

gested that TG might play a role in attaching the epithelial layer to the dermoepidermal junction. TG might be responsible for the earlier re-epithelialization episode, and epidermal transglutaminase takes over later to stabilize the mature epithelial layer as TG expression diminishes. Deficiency of epidermal transglutaminase results in ichthyosis, not a total breakdown of the skin barrier, which suggests there are other transglutaminases that can maintain epidermal integrity (35).

TG could promote wound contraction by cross-linking ECM molecules at the edge of the wound. Cohen et al. (36) suggested that the plasma factor XIII transglutaminases expressed by platelets contributed to the contraction of the fibrin clot. By ligating protein molecules throughout the wound, the TG could lead to more effective wound contraction. The TG expression by skeletal muscle cells and location of TG activity at these sites could also firmly anchor granulation tissue with the existing tissues to promote wound closure.

Migration of endothelial and inflammatory cells into fibrin forms an indispensable part of the healing process. Major proinflammatory and angiogenic cytokines such as TGF-β, TNF-α, and VEGF exert their influence by promoting migration of cells to the injured site, and the scaffolding function of fibrin has been shown to be an essential part of VEGF-mediated migration of endothelial cells (37). During migration, the stability of the provisional fibrin matrix is of utmost importance and TG's ability to stabilize the matrix that resists degradation may be vital for orchestrating tissue repair.

Adding recombinant TG to the sites of skin wound healing caused an increase in the vessel length density, a measure of neovascularization in the rat skin. The TG could be an important mediator of angiogenesis by regulating important events in vascular assembly either directly by its covalent modification of proteins or indirectly by modifying TGF-β function. TGF-β function is essential for normal vascular development (38), since defects in the TGF-β binding protein endoglin lead to the congenital vascular malformation syndrome of hereditary hemorrhagic telangiectasia (39). In ongoing experiments we have found that TG placed in a fibrin chamber enhances angiogenesis (unpublished results). Additional studies are in progress to define the mechanisms responsible for TG-mediated enhancement of angiogenesis in fibrin.

The proteolytic degradation of the TG may provide a method to regulate the duration and extent of the cross-link reaction. By degrading the TG, the positive amplification loop between TG expression and TGF-β activation would be disrupted and allow tissue remodeling to occur in the granulation tissue. Extracts from the wound could degrade recombinant TG, which demonstrated that there was proteolytic processing of the TG (unpublished results).

In conclusion, we have established that TG antigen and activity are expressed and function within the wound at sites of neovascularization and granulation tissue formation. TG appears to undergo regulation with the cytokines and directly promote angiogenesis. FJ

This work was supported by grants from Department of Defense DAMD 179717044 (Z.A.H.), the Duke SPORE on Breast Cancer P50 CA 68438 (M.W.D., C.S.G.), and NIH HL 38245 and HL 26309 (C.S.G.).

REFERENCES

1. Clark, R. A. (1993) Biology of dermal wound repair. *Dermatol. Clin.* **11,** 647–666
2. Folkman, J. (1995) Angiogenesis in cancer, vascular, rheumatoid and other disease. *Nat. Med.* **1,** 27–31
3. Greenberg, C. S., Birckbichler, P. J., and Rice, R. H. (1991) Transglutaminases: multifunctional cross-linking enzymes that stabilize tissues. *FASEB J.* **5,** 3071–3077
4. Folk, J. E. (1983) Mechanism and basis for specificity of transglutaminase catalyzed epsilon-(gamma-glutamyl) lysine bond formation. *Adv. Enzymol. Relat. Areas Mol. Biol.* **54,** 1–56
5. Barsigian, C., Stern, A. M., and Martinez, J. (1991) Tissue (type II) transglutaminase covalently incorporates itself, fibrinogen, or fibronectin into high molecular weight complexes on the extracellular surface of isolated hepatocytes. Use of 2-[(2-oxopropyl)thio] imidazolium derivatives as cellular transglutaminase inactivators. *J. Biol. Chem.* **266,** 22501–22509
6. Mosher, D. F., and Schad, P. E (1979) Cross-linking of fibronectin to collagen by blood coagulation Factor XIIIa. *J. Clin. Invest.* **64,** 781–787
7. Greenberg, C. S., Achyuthan, K. E., Borowitz, M. J., and Shuman, M. A. (1987) The transglutaminase in vascular cells and tissues could provide an alternate pathway for fibrin stabilization. *Blood* **70,** 702–709
8. Achyuthan, K. E., Rowland, T. C., Birckbichler, P. J., Lee, K. N., Bishop, P. D., and Achyuthan, A. M. (1996) Hierarchies in the binding of human factor XIII, factor XIIIa, and endothelial cell transglutaminase to human plasma fibrinogen, fibrin, and fibronectin. *Mol. Cell. Biochem.* **162,** 43–49
9. Aeschlimann, D., and Paulsson, M. (1991) Cross-linking of laminin-nidogen complexes by tissue transglutaminase. A novel mechanism for basement membrane stabilization. *J. Biol. Chem.* **266,** 15308–153017
10. Prince, C. W., Dickie, D., and Krumdieck, C. L. (1991) Osteopontin, a substrate for transglutaminase and factor XIII activity. *Biochem. Biophys. Res. Commun.* **177,** 1205–12010
11. Sane, D. C., Moser, T. L., Pippen, A. M., Parker, C. J., Achyuthan, K. E., and Greenberg, C. S. (1988) Vitronectin is a substrate for transglutaminases. *Biochem. Biophys. Res. Commun.* **157,** 115–120
12. Fesus, L., Madi, A., Balajthy, Z., Nemes, Z., and Szondy, Z (1996) Transglutaminase induction by various cell death and apoptosis pathways. *Experientia* **52,** 942–949
13. Aeschlimann, D., Mosher, D., and Paulsson, M. (1996) Tissue transglutaminase and factor XIII in cartilage and bone remodeling. *Semin. Thromb. Hemost.* **22,** 437–443
14. Im, M. J., Russell, M. A., and Feng, J. F. (1997) Transglutaminase II: a new class of GTP-binding protein with new biological functions. *Cell Signal.* **9,** 477–482
15. Kong, L., and Korthuis, R. J. (1997) Melanoma cell adhesion to injured arterioles: mechanisms of stabilized tethering. *Clin. Exp. Metastasis* **15,** 426–431
16. Bowness, J. M., Tarr, A. H., and Wong, T. (1988) Increased transglutaminase activity during skin wound healing in rats. *Biochim. Biophys. Acta* **967,** 234–240

17. Bowness, J. M., Henteleff, H., and Dolynchuk, K. N. (1987) Components of increased labelling with putrescine and fucose during healing of skin wounds. *Connect. Tissue Res.* **16,** 57–70
18. Dolynchuk, K. N., Bendor-Samuel, R., and Bowness, J. M. (1994) Effect of putrescine on tissue transglutaminase activity in wounds: decreased breaking strength and increased matrix fucoprotein solubility. *Plast. Reconstr. Surg.* **93,** 567–573
19. Papenfuss, H. D., Gross, J. F., Intaglietta, M., and Treese, F. A. (1979) A transparent access chamber for the rat dorsal skin fold. *Microvasc. Res.* **18,** 311–318
20. Lai, T. S., Slaughter, T. F., Koropchak, C. M., Haroon, Z. A., and Greenberg, C. S. (1996) C-terminal deletion of human tissue transglutaminase enhances magnesium-dependent GTP/ATPase activity. *J. Biol. Chem.* **271,** 31191–31195
21. Dewhirst, M. W., Vinuya, R. Z., Ong, E. T., Klitzman, B., Rosner, G., Secomb, T. W., and Gross, J. F. (1992) Effects of bradykinin on the hemodynamics of tumor and granulating normal tissue microvasculature. *Radiat. Res.* **130,** 345–354
22. Hsu, S. M., Raine, L., and Fanger, H. (1981) Use of avidin-biotin-peroxidase complex (ABC) in immunoperoxidase techniques: a comparison between ABC and unlabeled antibody (PAP) procedures. *J. Histochem. Cytochem.* **29,** 577–580
23. Roch, A. M., Noel, P., El-Aloui, S., Charlot, C., and Quash, G. (1991) Differential expression of isopeptide bonds N^{ε}(γ-glutamyl) lysine in benign and malignant human breast lesions: an immunohistochemical study. *Int. J. Cancer* **48,** 215–220
24. El-Alaoui, S., Grange, J., and Quash G. (1993) An immunological method for measuring N^{ε}(γ-glutamyl) lysine levels in fibrin molecules. In *Factor XIII, Second International Conference Marburg* (McDonagh, J., Seitz, R., and Egbring, R., eds) pp.135–138, Schattauer, Stuttgart, Germany
25. Sheehan, D., and Hrapchak, B. (1980) In *Theory and Practice of Histotechnology.* Battelle Press, Columbus, Ohio
26. Vollberg, T. M., George, M. D., Nervi, C., and Jetten, A. M. (1992) Regulation of type I and type II transglutaminase in normal human bronchial epithelial and lung carcinoma cells. *Am. J. Respir. Cell. Mol. Biol.* **7,** 10–18
27. Ikura, K., Shinagawa, R., Suto, N., and Sasaki, R. (1994) Increase caused by interleukin-6 in promoter activity of guinea pig liver transglutaminase gene. *Biosci. Biotechnol. Biochem.* **58,** 1540–1541
28. Kuncio, G. S., Tsyganskaya, M., Zhu, J., Liu, S. L., Nagy, L., Thomazy, V., Davies, P. J., and Zern, M. A. (1998). TNF-alpha modulates expression of the tissue transglutaminase gene in liver cells. *Am. J. Physiol.* **274,** G240–G245
29. Nunes, I., Gleizes, P. E., Metz, C. N., and Rifkin, D. B. (1997) Latent transforming growth factor-beta binding protein domains involved in activation and transglutaminase-dependent cross-linking of latent transforming growth factor-beta. *J. Cell Biol.* **136,** 1151–1163
30. Gibran, N. S., Heimbach, D. M., and Holbrook, K. A. (1995) Immunolocalization of FXIIIa+ dendritic cells in human burn wounds. *J. Surg. Res.* **59,** 378–386
31. Folk, J. E., and Finlayson, J. S. (1977) The epsilon-(gamma-glutamyl)lysine crosslink and the catalytic role of transglutaminases. *Adv. Protein Chem.* **31,** 1–133
32. Lai, T. S., Achyuthan, K. E., Santiago, M. A., and Greenberg, C. S. (1994) Carboxyl-terminal truncation of recombinant factor XIII A-chains. Characterization of minimum structural requirement for transglutaminase activity. *J. Biol. Chem.* **269,** 24596–24601
33. Valenzuela, R., Shainoff, J. R., DiBello, P. M., Urbanic, D. A., Anderson, J. M., Matsueda, G. R., and Kudryk, B. J. (1992) Immunoelectrophoretic and immunohistochemical characterizations of fibrinogen derivatives in atherosclerotic aortic intimas and vascular prosthesis pseudo-intimas. *Am. J. Pathol.* **141,** 861–880
34. Raghunath, M., Hopfner, B., Aeschlimann, D., Luthi, U., Meuli, M., Altermatt, S., Gobet, R., Bruckner-Tuderman, L., and Steinmann, B. (1996) Cross-linking of the dermo-epidermaljunction of skin regenerating from keratinocyte autografts. Anchoring fibrils are a target for tissue transglutaminase. *J. Clin. Invest.* **98,** 1174–1184
35. Jones, L. N., and Steinert, P. M. (1996) Hair keratinization in health and disease. *Dermatol. Clin.* **14,** 633–650
36. Cohen, I., Gerrard, J. M., and White, J. G. (1982) Ultrastructure of clots during isometric contraction. *J. Cell Biol.* **93,** 775–787
37. Watanabe, Y., and Dvorak, H. F. (1997) Vascular permeability factor/vascular endothelial growth factor inhibits anchorage-disruption-induced apoptosis in microvessel endothelial cells by inducing scaffold formation. *Exp. Cell Res.* **233,** 340–349
38. Pepper, M. S. (1997) Transforming growth factor-beta: vasculogenesis, angiogenesis, and vessel wall integrity. *Cytokine Growth Factor Rev.* **8,** 21–43
39. Gallione, C. J., Klaus, D. J., Yeh, E. Y., Stenzel, T. T., Xue, Y., Anthony, K. B., McAllister, K. A., Baldwin, M. A., Berg, J. N., Lux, A., Smith, J. D., Vary, C. P., Craigen, W. J., Westermann, C. J., Warner, M. L., Miller, Y. E., Iackson, C. E., Guttmacher, A. E., and Marchuk, D. A. (1998) Mutation and expression analysis of the endoglin gene in hereditary hemorrhagic telangiectasia reveals null alleles. *Hum. Mutat.* **11,** 286–294

Received for publication February 1, 1999.
Revised for publication April 8, 1999.

APPENDIX 02

Reprinted from: ANNALS OF SURGERY, Vol.231, No. 1, January 2000

Early Wound Healing Exhibits Cytokine Surge Without Evidence of Hypoxia

Zishan A. Haroon, MD, PhD,* James A. Raleigh, PhD,§ Charles S. Greenberg, MD,† and Mark W. Dewhirst, DVM, PhD‡

*From the Departments of *Pathology, †Medicine, and ‡Radiation Oncology, Duke University Medical Center, Durham, and the §Department of Radiation Oncology, University of North Carolina, School of Medicine, Chapel Hill, North Carolina*

Objective

To ascertain the spatial and temporal relation of wound hypoxia to the cell types involved, expression of selected angiogenic cytokines, the proliferative status of cells in the wound site, and angiogenesis.

Summary Background Data

Hypoxia is considered to drive the angiogenic response by upregulating angiogenic cytokines observed during wound healing. But this correlation has not been shown on a cell-to-cell basis in vivo because of limitations in measuring tissue Po_2 at the cellular level.

Methods

Using punch biopsy wounds in rats as a wound healing model, the distributions of vascular endothelial growth factor, transforming growth factor-beta, tumor necrosis factor-alpha, and pimonidazole adducts (as a hypoxia marker) were followed immunohistochemically during the healing process.

Results

Hypoxia was absent on day 1 after wounding, even though angiogenesis and maximal expression of cytokines were observed in the wounds. Hypoxia peaked in the granulation tissue stage at day 4 and correlated with increased cellularity and cellular proliferation. Hypoxia started to decrease after day 4 and was limited to the remnant blood vessels and epithelial layer in the scar tissue.

Conclusions

Induction of angiogenic cytokines early during wound healing may be due to triggering mechanisms other than hypoxia. Alternatively, the unique pattern of development and decline of cellular hypoxia as wound cellularity and proliferation regress suggest its involvement in initiating vascular regression during the later stages of healing.

Tissue hypoxia is considered a major signal that initiates and regulates angiogenic processes such as wound healing and tumor growth.[1–3] Hypoxia has been shown (in vitro) to induce several major cytokines such as vascular endothelial growth factor (VEGF),[4] transforming growth factor-beta (TGFβ),[5] tumor necrosis factor-alpha (TNFα),[6] and interleukin-8[7] from a wide variety of cells involved in tissue repair, including fibroblasts, endothelial cells, and macrophages. During wound healing, tissue Po_2 is considered to be low at the center of the wound, but it increases as the wound heals.[8–10] Wound-induced hypoxia, as suggested by the in vitro data, is thought to be a major determinant of all phases of wound healing by regulating cellular proliferation, cell migration, and extracellular matrix protein synthesis through the induction of cytokines and diverse intracellular signaling pathways. In vivo studies have demonstrated decreased Po_2 in wounds,[9–11] suggesting that conditions favorable to hypoxic stimulation of cytokine production exist.[12,13] These studies of wound tissue Po_2 have provided useful information on the kinetics of change in oxygenation after wounding. However, the methods have measured overall average tissue Po_2, whereas it is known that the diffusion distance of oxygen is on the order of a few tens of microns.[14,15] To elucidate the relation between wound hypoxia, cytokine expression, and cellular responses to wounding, we used immunohistochemical methods that allowed us to evaluate these responses on a cell-to-cell basis. The

Supported by grants from the Department of Defense DAMD 179717044 (to ZAH), the Duke SPORE on Breast Cancer P50 CA 68438 (to CSG, MWD), NIH HL 38245 & HL 26309 (to CSG), and NIH CA 40355 (to MWD).

Correspondence: Mark W. Dewhirst, PhD, Box 3455, MSRB, Duke University Medical Center, Durham, NC 27710.

Accepted for publication June 3, 1999.

object of our study was to ascertain the spatial and temporal relation of wound hypoxia to the cell types involved, expression of selected angiogenic cytokines, the proliferative status of cells in the wound site, and angiogenesis.

Pimonidazole hydrochloride belongs to a group of compounds known as 2-nitroimidazole hypoxia markers that form protein adducts under conditions of low oxygen tension (i.e., $\leq$10 mmHg) by the action of cellular nitroreductases.[16,17] The introduction of immunochemical reagents that recognize marker adducts[18] allowed the nonradioactive detection of tissue hypoxia.[19–21] Although originally developed for use in animal tumors[22,23] and human tumors,[24–26] pimonidazole hydrochloride has also been applied to the study of hypoxia and hypoxia-associated pathophysiologic changes in normal rat liver and kidney.[27–30] Of particular interest to the present study is the binding of pimonidazole to suprabasal cells in epithelial structures, including skin.[31] This binding is consistent with radiobiologic data that indicate that the skin is hypoxic.[32] The binding of pimonidazole to skin epithelium serves as a useful positive control in the present study of wound healing. Another advantage of the immunohistochemical hypoxia marker approach is that it measures cellular events with spatial resolution at the cell level without physically disturbing the tissue during the accumulation of the hypoxia signal. This is essential to the present study, and no other assay can do this in vivo. Validation of the immunohistochemical technique has been carried out in rodent tumors and human tumor xenografts tumors where correlations between pimonidazole adduct formation, oxygen electrode measurements, and radiation response have been demonstrated.[23,33] In a discussion of the scope and limitation of pimonidazole as a hypoxia marker,[23] it was noted that the bioreductive activation of pimonidazole was not dependent on specialized enzymes, nor does the concentration of P450 cytochrome enzymes in the perivascular region of rat livers, for example, override the oxygen dependence of pimonidazole activation. A cell type of specific interest to the present study is the macrophage and its bioreductive properties in terms of the oxygen-dependent activation of 2-nitroimidazole binding. Although relatively little appears to be known about this topic, Olive[34] has shown that host macrophages in rodent tumors behave as tumor cells with respect to binding hypoxia markers in the sense that binding occurred only in macrophages that were in hypoxic regions of the tumors.

We report the absence of pimonidazole adduct formation in the wound site and surrounding normal skin at day 1 after wounding, indicating the absence of tissue regions with $Po_2 \leq 10$ mmHg. Hypoxia marker intensity peaked at day 4 after wounding, which coincided with the greatest cellularity and proliferation. Hypoxia diminished as the cellularity of the wounds regressed and mature scar tissue was generated by day 8. In contrast, hypoxia-inducible cytokines such as VEGF, TGFβ, and TNFα exhibited maximal immunoreactivity at day 1, a time point where we saw no evidence of hypoxia. These results suggest there are likely to be signals present other than hypoxia that initiate tissue repair and angiogenesis during the early time points after wounding. Hypoxia reached its maximal intensity in granulation tissue at a critical juncture in the healing process when apoptosis and remodeling were being initiated. This pattern of development of hypoxia suggests that it may play a role in triggering the apoptosis and remodeling of the granulation tissue, as opposed to providing the initial stimulus for proangiogenic cytokine production in the early phases of wound healing.

METHODS

The Duke Institutional Animal Care and Use Committee approved all animal protocols.

Wounds

Fisher 344 female rats from Charles River Laboratories (Raleigh, NC) were anesthetized with intraperitoneal injections of pentobarbital (40 mg/kg) and ketamine (70 mg/kg), then shaved and depilated using Nair (Carter-Wallace, New York, NY). Sixteen 5-mm punch biopsy wounds were made in the dorsal skin immediately after depilation. The normal rat skin served as unwounded skin controls. Wounds were harvested at days 1, 2, 4, 6, and 8 while the animals were anesthetized. Two rats were killed at each time point by intravenous pentobarbital overdose, and the experiments were performed in triplicate. On average, 8 to 10 wounds were harvested at each time point. Of these, only four or five were sectioned. For hypoxia marker, $\geq$20 wounds were used for staining purposes for each time point. For the rest of the investigative work, 8 to 10 wounds were used in immunohistochemistry for each time point. Tissues were either snap-frozen using OCT in liquid nitrogen and kept at -80°C or fixed in 10% neutral buffered formalin for paraffin embedding for immunohistochemistry.

Immunohistochemistry

Immunohistochemistry was carried out using procedures described by Hsu et al.[35] Briefly, paraffin-embedded tissues were sectioned (5 microns) and antigen retrieval was performed using citrate buffer from Biogenex (San Ramon, CA). Tissues were treated with primary antibody against tissue transglutaminase (1:10; TG100; nonreactive to factor XIIIa, unpublished data) and VEGF3 (1:100; Neomarkers, Fremont, CA), ED1-macrophage marker (MCA341; 1:100); Serotec, Oxford, UK), pan-specific TGFβ (AB-100-NA, 1:100) and rat anti-TNFα (AB-510-NA, 1:100; R&D, Minneapolis, MN), Ki-67 (1:100, NCL-Ki67p; Novocastra Laboratories, Newcastle-upon-Tyne, UK), and rabbit polyclonal antisera to pimonidazole protein adducts (1:10,000, supplied by J.A. Raleigh). Secondary and tertiary antibodies were provided in a kit (314KLD; Innovex, Richmond, CA), and the location of the reaction was visualized with 3, 3′-diaminobenzidine tetrahydrochloride (Sigma, St. Louis,

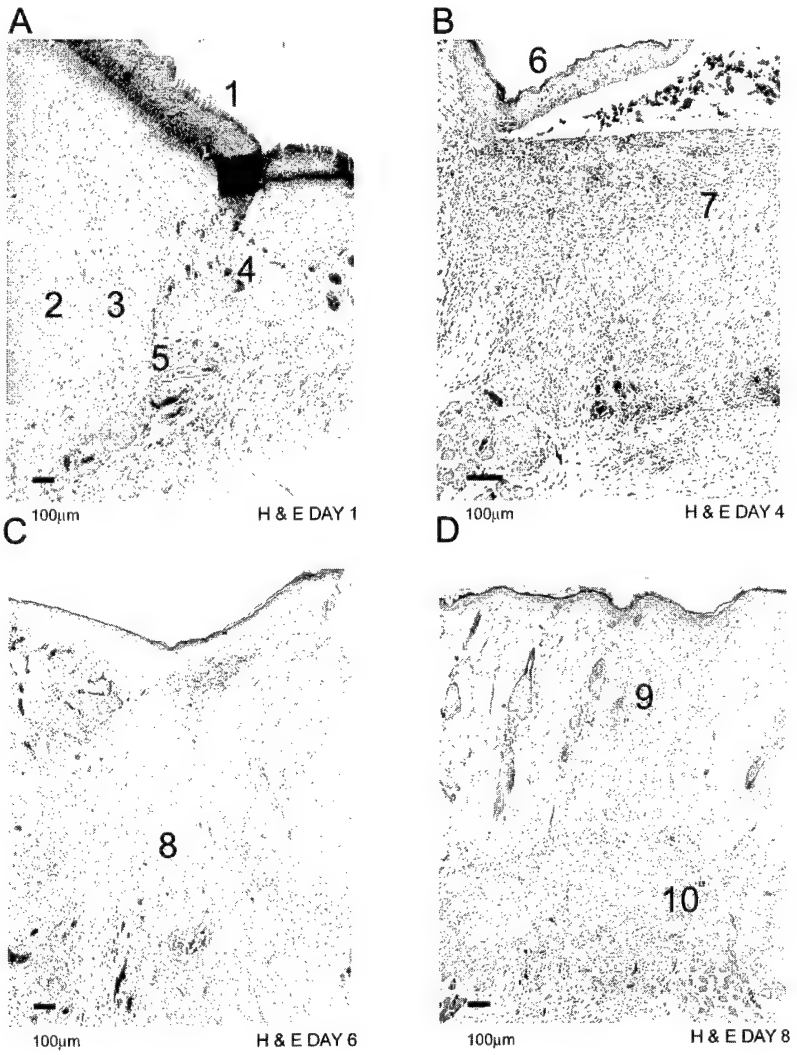

Figure 1. Light microscopic histology with hematoxylin and eosin of normal rat dermal wound healing. New epithelium (A1) is being laid down as early as day 1 after wounding (A). Neovessels (A4) and dilated existing vessels (A5) can be visualized in provisional fibrin matrix. Skeletal muscle cells (A2) form a border zone (A3) between normal and wounded tissue. By day 4 (B), the epithelial layer (B6) is complete and granulation tissue (B7) has matured. The granulation tissue starts to contract (C8) by day 6 (C). Scar tissue is visible by day 8 (D9) and the remnants of granulation tissue (D10) have moved down to the base of the wound.

MO). Slides were counterstained with hematoxylin and mounted with cover slips. Controls for the immunohistochemistry were treated with normal mouse serum (NMUS) or mouse IgG, rabbit IgG, and goat IgG and were negative for any reactivity. Masson's trichrome and hematoxylin and eosin stainings were carried out as described by Sheehan and Hrapchak.[36] The immunostaining was evaluated in a masked fashion. The stained sections were scored on the basis of the strength of the brown product (DAB) present. The designations used were no staining = −, light or weak staining = +, strong staining = ++, and intense staining covering most of the cellular tissue and matrix = +++.

Pimonidazole and Hoechst 33342 Administration

Pimonidazole hydrochloride (Hydroxyprobe-1; Natural Pharmacia International Inc., Research Triangle Park, NC; concentration 1.0 mg/100 mL in 0.9% saline) was administered at 70 mg/kg intraperitoneally 3 hours before the animal was killed. The tissues were then harvested and processed for immunohistochemistry. Hoechst 33342 (bisbenzimide; Sigma) was made at a concentration of 5 mg/mL in 0.9% NaCl and perfused through the tail vein of anesthetized rats during 45 seconds for a total dose of 12 mg/kg on days 0 and 1 after wounding only. Wounds were harvested within 5 minutes of Hoechst 33342 administration and were immediately embedded in OCT and frozen. Two rats were used for each time point. Five-micron sections were made within 2 hours, and images were visualized with the MPS Intravital Microscopy System (Carl Zeiss, Hanover, MD) attached to a color camera (ZVS 3C75DE; Optronics Eng., Goleta, CA). The images were captured with NIH image software via a CG7 frame grabber (Scion Corp., Frederick, MD).

RESULTS

Light Microscopy Findings

At the earliest time point at day 1 (Fig. 1A), provisional matrix with dilated blood vessels (Fig. 2A) and inflamma-

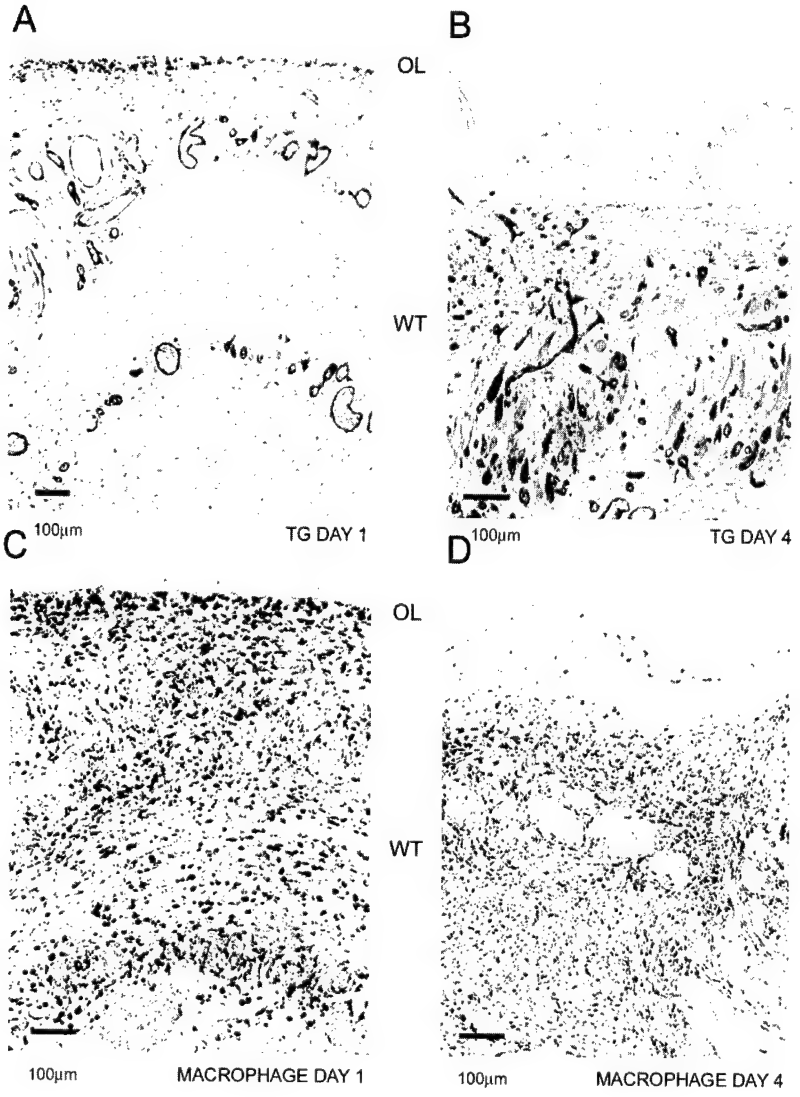

Figure 2. Localization of blood vessels and macrophages. Tissue transglutaminase was used as a blood vessel marker. Abundant blood vessels can be identified at day 1 (A) in the provisional fibrin matrix and in the granulation tissue at day 4 (B). Macrophages, as identified by ED1 marker, invade the provisional fibrin matrix (C) by day 1 and are spread throughout the granulation tissue (D). Orientation of the figures is shown as outer layer (OL) and wounded tissue (WT).

tory cells (Fig. 2C) could be observed underneath a newly generating epithelial layer. Reepithelialization was completed by day 2 after wounding. Maturation of granulation tissue was seen by day 4 (Fig. 1B), characterized by the presence of new blood vessels (Fig. 2B), inflammatory cells (Fig. 2D), and collagen fibers organized into a dense connective tissue. Skeletal muscle cells that previously formed a boundary between the normal and wounded tissue at earlier time points had moved to the base of the wound and closed the gap created by the injury (Fig. 1B). By day 6 (Fig. 1C), granulation tissue started to contract and increased in density. At day 8 (Fig. 1D), the healing was in its final stages, with remnants of granulation tissue left at the base of the wound. The injury site was filled with dense collagen tissue with few blood vessels.

Hypoxia Distribution During Wound Healing

Hypoxia was detected in the epithelial layer, sebaceous glands, and hair follicles in unwounded skin (Fig. 3A). We observed little immunoreactivity in wounds examined on day 1 for the hypoxia marker (Fig. 3B). The distribution of hypoxia in adjacent normal skin structures was ordinarily diminished at this point compared with unwounded skin. By day 2, the wounds started to exhibit some staining for hypoxia marker in the newly laid epithelial layer and the border zone between the normal and wounded tissue, a region that was infiltrated by inflammatory and endothelial cells (Fig. 3C). Immunoreactivity for hypoxia reached its highest intensity on day 4 after wounding (Figs. 3D, 3E). The keratinocytes in the epithelial layer and endothelial and inflammatory cells in the granulation tissue and the border zone stained intensely for hypoxia at day 4. As the healing process progressed, collagen became more organized and the tissue was less cellular. Hypoxia marker staining intensity was diminished in the organized collagen and more localized to the base of the wound, coinciding with residual cellularity. At day 8, hypoxia marker staining was confined to the limited cellular content of the scar tissue, such as blood vessels and macrophages, and to the granulation

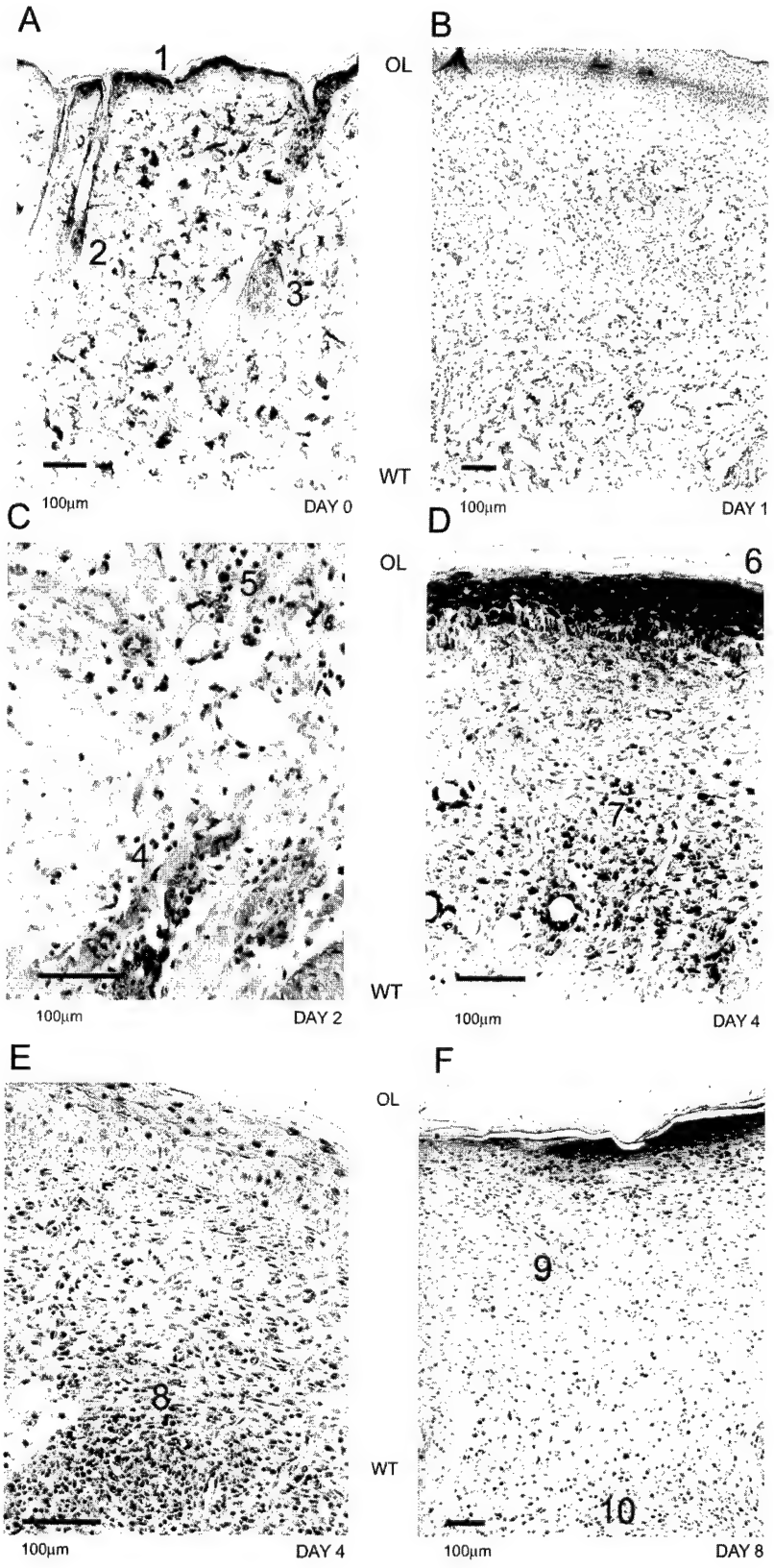

Figure 3. Immunohistochemical evidence of hypoxia during wound healing. In normal rat skin (A), the pimonidazole adducts were detected in the epithelial layer (A1), hair follicles (A2), and sebaceous glands (A3). At day 1 (B), we did not detect any reactivity for the hypoxia marker in the wounded tissue. On day 2 (C), macrophages (C4) and endothelial cells (C5) started to exhibit immunoreactivity at the border of normal and wounded tissue. By day 4 (D, E), maximal hypoxia reactivity was observed. The epithelial layer (D6) and granulation tissue both were highly reactive. Macrophages (D7) and endothelial cells (D8) in small blood vessels could be seen with evidence of pimonidazole adduct formation. By day 8 (F), the immunoreactivity was limited to the epithelial layer, remnant blood vessels (F9), and macrophages in the scar tissue. Orientation of the figures is shown as outer layer (OL) and wounded tissue (WT).

tissue at the base of the wound (Fig. 3F). The intensity of hypoxia immunoreactivity in the epithelial layer was equivalent to that in unwounded skin.

Expression of Cytokines

VEGF (Fig. 4A), TGFβ, and TNFα expression showed the same distribution as hypoxia marker binding in normal

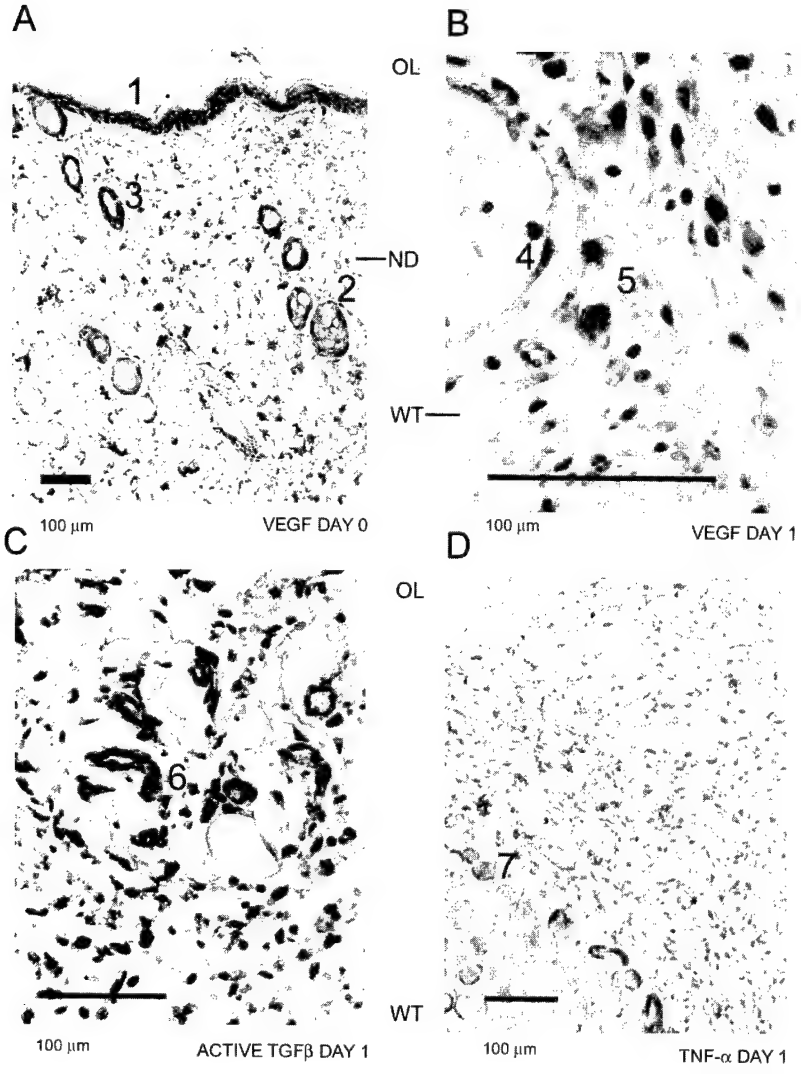

Figure 4. Cytokine expression during wound healing. Vascular endothelial growth factor (VEGF) expression could be seen in the epithelial layer (A1), sebaceous glands (A2), and hair follicles (A3) in normal rat skin (A). By day 1, VEGF expression was present in endothelial cells (B4) and macrophages (B5). Active transforming growth factor-beta expression at day 1 (C) could also be localized to endothelial cells (C6) and macrophages. Tumor necrosis factor-alpha (D) was predominantly detected in endothelial cells, macrophages, and skeletal muscle cells (D7). Orientation of the figures is shown as outer layer (OL) and wounded tissue (WT).

rat skin (i.e., epithelial layer, sebaceous glands, and hair follicles). On day 1 after wounding, VEGF (Fig. 4B), TGFβ (Fig. 4C), and TNFα (Fig. 4D) immunoreactivity was observed in the inflammatory and endothelial cells. VEGF and TGFβ were found in the provisional fibrin matrix as well (Figs. 4B, 4C). VEGF antigen started to decline after day 2, and detection was limited to endothelial cells in scar tissue and granulation tissue at the base of the wound by day 8, in a pattern similar to the distribution of hypoxia. TGFβ antigen remained at a high level and was detected throughout the healing process in the matrix, inflammatory, and endothelial cells. TNFα expression continued to be similar to that of hypoxia marker in the healing process.

Hoechst 33342 and Proliferation Marker Ki67 Distribution in Wounds

Because we observed no hypoxia marker staining on day 1, we wondered whether this might be caused by lack of marker drug delivery (perfusion). We used Hoechst 33342 dye extravasation in the wounds to determine whether perfusion was adequate. The Hoechst dye permeated the epithelial layer, the sebaceous glands, the hair follicles, and the dermis of the normal skin (Fig. 5A). We found that this dye diffused throughout the wound tissue on day 1 (Fig. 5B).

Because proliferating cells consume oxygen at rates three to five times higher than cells in G_0,[37] we hypothesized that the high intensity of hypoxia in granulation tissue may result from increased consumption. We used Ki67 as a proliferation marker, and it was detected as early as day 1 in the endothelial and epithelial cells (Fig. 6A). The immunoreactivity for Ki67 was highest at day 4 (Fig. 6B); it started to decline in intensity by day 6 and was reduced to the remnants of granulation tissue at the base of the wound by day 8.

The time course of these events is summarized in Table 1.

DISCUSSION

This is the first study to report the distribution of hypoxia at the cellular level and its association with cytokine expression and endothelial and inflammatory cells during

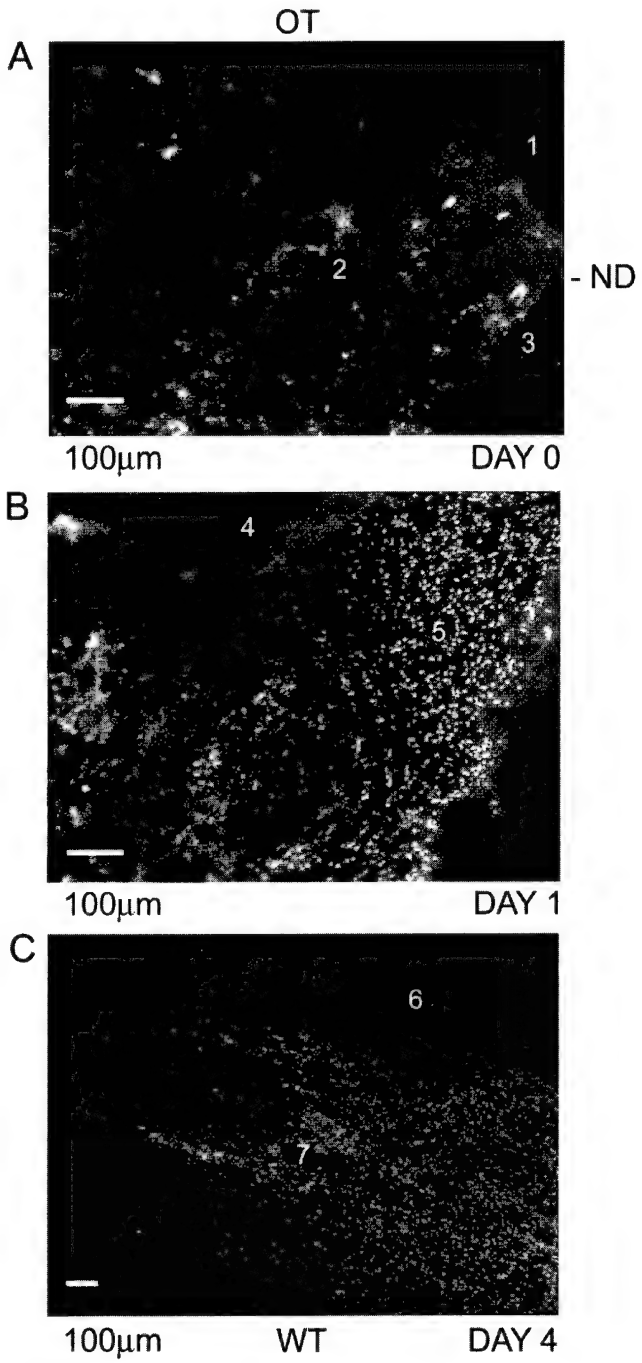

Figure 5. Hoechst dye staining of normal rat skin and wounded tissue. In normal rat skin (A), Hoechst dye stain was present in the epithelial layer (A1), sebaceous glands (A2), and hair follicles (A3). At day 1 (B), the wounded tissue was well perfused and the newly generating epithelial layer (B4) and provisional fibrin matrix (B5) exhibited the nuclear stain. Orientation of the figures is shown as outer layer (OL) and wounded tissue (WT).

wound healing. There are two interesting and unexpected findings of this study: the absence of hypoxia in the provisional fibrin matrix at day 1, a time when cytokine expression is elevated; and peak hypoxia in granulation tissue at day 4, a time when cellular proliferation is at its peak, which is followed by decreased wound cellularity and wound contraction. These results suggest that hypoxia probably does not play a role in the initial onset of cytokine expression that occurs at 1 day after wounding. Alternatively, hypoxia probably plays a role in the maintenance of the angiogenic response in the granulation tissue from day 2 forward. Also, the apparent relation between peak levels of hypoxia and the onset of decreasing cellularity seems to indicate a more prominent role of hypoxia in the initiation of remodeling during the healing process.

The absence of hypoxia in dermal wounds early during healing is readily explainable. Once breakdown of the epithelial barrier occurs, diffusion of air ($Po_2 \leq 120$ mmHg) into the open wound and the provisional fibrin matrix happens as long as scab formation or reepithelialization has not taken place. Interestingly, earlier investigators found similar results with wound fluid chambers fitted with oxygen electrodes.[8] They reported high Po_2 levels (20–30 mmHg) during the first 2 days of healing and a gradual decline in Po_2 levels down to lowest (5–8 mmHg) at 5 to 7 days after wounding. They believed that the elevated Po_2 level found in the first 2 days was an artifact caused by oxygen contamination from the air into the wound chamber. We argue that this is not an artifact. We propose that in normal dermal healing, oxygen will diffuse into the wound site by passing through the disrupted epithelial barrier from the surrounding air. Our strongest argument to support this hypothesis is based on a comparison of hypoxia marker binding in unwounded skin and in normal skin adjacent to the wound site at day 1 after wounding. In unwounded skin, strong marker binding was seen in the epithelial layer, hair follicles, and sebaceous glands. This pattern of binding was absent in normal skin surrounding the wound site at day 1. One could argue that the wound itself might have created enough vascular destruction to prevent adequate perfusion. If this were true, it is possible that the hypoxia marker drug failed to reach the target tissues. However, the strong perivascular staining with the Hoechst dye demonstrated that the tissue was adequately perfused and that the hypoxia marker would have easily reached the target tissues. Based on this evidence, we conclude that hypoxia is not responsible for the initial triggering of the repair and angiogenesis cascade. Recently, Howdieshell et al[38] have shown that wound fluid obtained from abdominal wounds was normoxic, although they detected high levels of cytokine (VEGF and TGFβ) expression.

Alternate pathways could initiate tissue repair and angiogenesis during the early stages of wound healing, which are based on the coagulation system.[39,40] Platelets are known to make up the first wave of exogenous cells to appear at an injured site.[41] In addition to initiating hemostasis and coagulation at the site of injury, they also contain a significant number of cytokines and extracellular matrix proteins and enzymes that are released from storage granules after activation. These cytokines include VEGF,[42] TGFβ,[43] TGFα,[44] and platelet-derived growth factor (PDGF).[45] Such cytokines could promote tissue repair and angiogenesis once they are released. It is known that platelet depletion leads to defective wound healing.[46] This is further evidence that

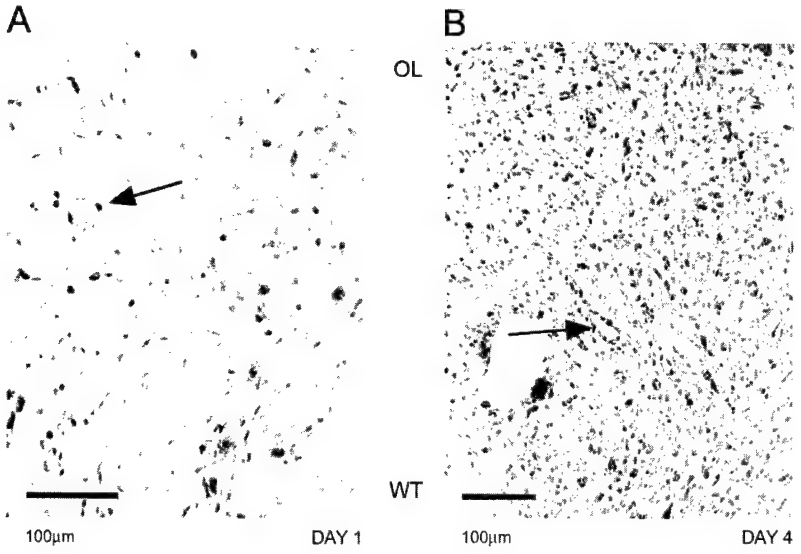

Figure 6. Ki67 proliferation marker expression in the wounded tissue. At day 1 (A), endothelial cells (arrow) could be identified as picking up the proliferation marker. The wounded tissue at day 4 (B) had high levels of Ki67 marker expression, indicating a high proliferation rate in the granulation tissue. Endothelial cells in a blood vessel were shown to be expressing the Ki67 marker (arrow). Orientation of the figures is shown as outer layer (OL) and wounded tissue (WT).

they play a role in regulation of wound healing. Our observation that hypoxia is absent during early wound healing even though angiogenic cytokine levels are elevated supports the role of platelets as being involved at this early time point. Thus, regulation of cytokines during early wound healing may be a function of the coagulation system rather than being hypoxia-driven.

The other major event during early wound healing is the generation of thrombin and formation of a provisional fibrin matrix. The provisional fibrin matrix provides the essential scaffold for the endothelial and inflammatory cells to move into the wounded tissue. Fibrin and its degradation products have diverse biologic effects on cells invading the provisional matrix and can induce various cytokines such as interleukin-8,[47] tissue factor,[48] and adhesion molecules (ICAM)[49] in those cells. This provides a second pathway for the production of cytokines to initiate repair and angiogenesis during early wound healing, because tissue factor itself can stimulate VEGF[50] in cells. Thus, there seems to be a wide array of pathways and mechanisms that may be responsible for the induction of cytokines during wound healing as an alternative to hypoxia.

The results on day 4 were also intriguing. Extensive hypoxia marker distribution correlated well with the proliferation marker Ki67, suggesting that increased oxygen consumption rates in the granulation tissue were responsible for maximal hypoxia staining. Apoptosis of endothelial cells and myofibroblasts has been shown to be responsible for the decrease in cellularity after the surge of proliferation during healing episodes.[51,52] This wave of apoptosis has been associated with CD95- and p53-related pathways.[53,54] The signals that trigger these events are not well understood, but it is well established that activation of p53-dependent apoptotic pathways is triggered by hypoxia.[55] Additional evidence implicating hypoxia in the regulation of apoptosis suggests that hypoxia may provide the essential signaling pathways for initiating apoptosis during healing.[56]

The unique pattern of emergence of hypoxia marker reactivity at the beginning of remodeling of wounded tissue and its gradual decline in the remodeled tissues suggests that the development of hypoxia may be to stimulate endothelial cell and myofibroblast apoptosis. Hypoxia might very well hold the key to the puzzle of remodeling initiation, because its progression indicates a diminished capacity for

Table 1. IMMUNOHISTOCHEMICAL DATA

Characteristic	Control	Time After Wounding (days)				
		1	2	4	6	8
Pimonidazole immunoreactivity	EP, Sg, Hf	−	+	+++	++	+
Cytokines						
VEGF		+++	+++	++	++	+
TGFβ	Same as pimonidazole	+++	+++	+++	++	++
TNFα		+++	+++	+++	++	+
Cell proliferation	−	+	++	+++	+	−
Angiogenesis	−	++	+++	+++	++	+

Intensity of immunoreactivity is graded as − none, + weak, ++ strong, +++ intense.
Ep, epidermis; Sg, sebaceous glands; Hf, hair follicle.

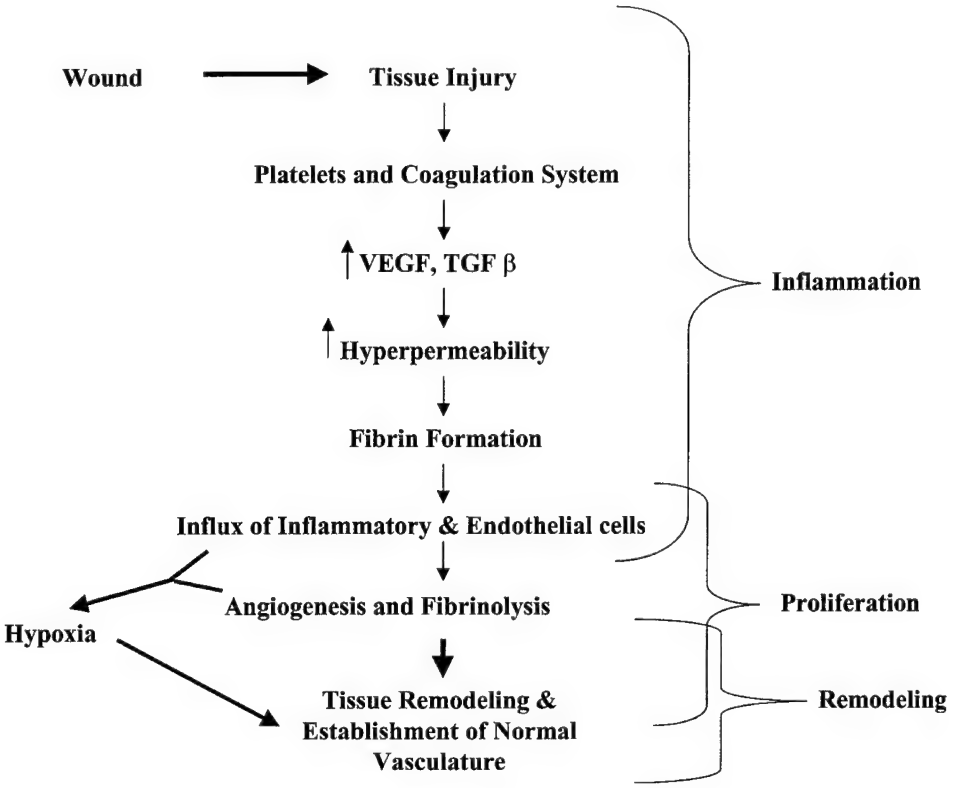

Figure 7. Proposed role of hypoxia during the wound healing cascade.

nutrient and oxygen delivery at a time that coincides with the trimming of excess cell mass by apoptosis. This is an exciting possibility that needs further investigation.

Chang et al[9] studied the oxygenation of human wounds and observed values in the range of 60 mmHg in unwounded skin. Oxygenation dropped to 40 mmHg in the first few days after wounding and showed a gradual decline to 30 mmHg by days 4 to 5. The authors suggested that the decline in Po_2 in the early period would be sufficient to stimulate wound healing. Because our method of hypoxia measurement detected only Po_2 values < 10 mmHg, and we found little evidence of hypoxia on day 1, there appears to be a discrepancy between the earlier study and ours. The Po_2 measurements were performed by analyzing the Po_2 of fluid inside implanted Silastic catheters. By virtue of its size, this type of device provides an estimate of the average tissue Po_2, and such measurements are likely to be influenced strongly by vascular Po_2 in regions immediately adjacent to the catheter. However, values of 30 mmHg are not really hypoxic, if one considers the oxygen tension distribution when measured on a more microscopic scale. Using modern polarographic methods with electrodes that have minimal self-consumption artifact, Po_2 in normal tissues such as brain,[57] uterus,[58] skeletal muscles, and skin[59] drops to <15 mmHg. Some tissues, such as retina[60] and liver,[61] exist under chronically hypoxic conditions ($Po_2 \leq$ 10 mmHg). One could argue that a drop from 60 to 40 mmHg might be sufficient to stimulate angiogenesis and wound healing, but there is no direct evidence from the literature to support this conjecture. There have been several in vitro studies published evaluating the production and release of proangiogenic cytokines. In general, such studies involved a dramatic change in Po_2 (room air to 10 mmHg) during several hours. Under such conditions, cytokines such as VEGF,[62] basic fibroblast growth factor (bFGF),[63] TNFα,[6] and TGFβ[12] have been shown to be upregulated. However, these conditions are not comparable to the 30% drop reported by Chang et al. Studies are under way in our laboratory that address this concern by maintaining the cells at physiologic levels of oxygen (Po_2 15–30 mmHg) for a few cell cycles and then exposing them to hypoxia.

To summarize (Fig. 7), we have shown that there is no hypoxia during the early events of wound healing but that it is maximal in the most cellular phases of granulation. We found expression of proangiogenic cytokines in the provisional fibrin matrix during early wound healing, suggesting other trigger mechanisms for induction of these cytokines at this time point. However, the unique pattern of development and decline of hypoxia as wound cellularity and proliferation regress suggests its involvement in initiating apoptosis during the later stages of the healing process.

References

1. Dvorak HF. Tumors: wounds that do not heal. Similarities between tumor stroma generation and wound healing. N Engl J Med 1986; 315(26):1650–1659.
2. Folkman J. Angiogenesis in cancer, vascular, rheumatoid and other disease. Nat Med 1995; 1(1):27–31.
3. Haroon ZA, Peters KG, Greenberg CS, Dewhirst MW. Angiogenesis and oxygen transport in solid tumors. In: Teicher B, ed. Antiangio-

genic agents in cancer therapy. Totowa, NJ: Humana Press Inc.; 1999:3–21.
4. Minchenko A, Salceda S, Bauer T, Caro J. Hypoxia regulatory elements of the human vascular endothelial growth factor gene. Cell Mol Biol Res 1994; 40(1):35–39.
5. Patel B, Khaliq A, Jarvis-Evans J, et al. Oxygen regulation of TGF-beta 1 mRNA in human hepatoma (Hep G2) cells. Biochem Mol Biol Int 1994; 34(3):639–644.
6. Scannell G, Waxman K, Kaml GJ, et al. Hypoxia induces a human macrophage cell line to release tumor necrosis factor-alpha and its soluble receptors in vitro. J Surg Res 1993; 54(4):281–285.
7. Karakurum M, Shreeniwas R, Chen J, et al. Hypoxic induction of interleukin-8 gene expression in human endothelial cells. J Clin Invest 1994; 93(4):1564–1570.
8. Ninikoski J, Heughan C, Hunt TK. Oxygen and carbon dioxide tensions in experimental wounds. Surg Gynecol Obstet 1971; 133(6): 1003–1007.
9. Chang N, Goodson WHd, Gottrup F, Hunt TK. Direct measurement of wound and tissue oxygen tension in postoperative patients. Ann Surg 1983; 197(4):470–478.
10. Goodson WHd, Andrews WAS, Thakral KK, Hunt TK. Wound oxygen tension of large vs. small wounds in man. Surg Forum 1979; 30:92–95.
11. Knighton DR, Silver IA, Hunt TK. Regulation of wound-healing angiogenesis: effect of oxygen gradients and inspired oxygen concentration. Surgery 1981; 90(2):262–270.
12. Sakuda H, Nakashima Y, Kuriyama S, Sueishi K. Media conditioned by smooth muscle cells cultured in a variety of hypoxic environments stimulates in vitro angiogenesis. A relationship to transforming growth factor-beta 1. Am J Pathol 1992; 141(6):1507–1516.
13. Shweiki D, Itin A, Soffer D, Keshet E. Vascular endothelial growth factor induced by hypoxia may mediate hypoxia-initiated angiogenesis. Nature 1992; 359(6398):843–845.
14. Olive PL, Vikse C, Trotter MJ. Measurement of oxygen diffusion distance in tumor cubes using a fluorescent hypoxia probe. Int J Radiat Oncol Biol Phys 1992; 22(3):397–402.
15. Helmlinger G, Yuan F, Dellian M, Jain RK. Interstitial pH and Po_2 gradients in solid tumors in vivo: high-resolution measurements reveal a lack of correlation. Nat Med 1997; 3(2):177–182.
16. Chapman JD, Franko AJ, Sharplin J. A marker for hypoxic cells in tumours with potential clinical applicability. Br J Cancer 1981; 43(4): 546–550.
17. Gross MW, Karbach U, Groebe K, et al. Calibration of misonidazole labeling by simultaneous measurement of oxygen tension and labeling density in multicellular spheroids. Int J Cancer 1995; 61(4):567–573.
18. Raleigh JA, Miller GG, Franko AJ, et al. Fluorescence immunohistochemical detection of hypoxic cells in spheroids and tumours. Br J Cancer 1987; 56(4):395–400.
19. Cline JM, Thrall DE, Page RL, et al. Immunohistochemical detection of a hypoxia marker in spontaneous canine tumours. Br J Cancer 1990; 62(6):925–931.
20. Raleigh JA, Zeman EM, Rathman M, et al. Development of an ELISA for the detection of 2-nitroimidazole hypoxia markers bound to tumor tissue. Int J Radiat Oncol Biol Phys 1992; 22(3):403–405.
21. Lord EM, Harwell L, Koch CJ. Detection of hypoxic cells by monoclonal antibody recognizing 2-nitroimidazole adducts. Cancer Res 1993; 53(23):5721–5726.
22. Azuma C, Raleigh JA, Thrall DE. Longevity of pimonidazole adducts in spontaneous canine tumors as an estimate of hypoxic cell lifetime. Radiat Res 1997; 148(1):35–42.
23. Raleigh JA, Chou S-C, Arteel GE, Horsman MR. Comparisons among pimonidazole binding, oxygen electrode measurements and radiation response in C3H mouse tumors. Radiat Res 1999; 151:580–589.
24. Kennedy AS, Raleigh JA, Perez GM, et al. Proliferation and hypoxia in human squamous cell carcinoma of the cervix: first report of combined immunohistochemical assays. Int J Radiat Oncol Biol Phys 1997; 37(4):897–905.
25. Varia MA, Calkins-Adams DP, Rinker LH, et al. Pimonidazole: a novel hypoxia marker for complementary study of tumor hypoxia and cell proliferation in cervical carcinoma. Gynecol Oncol 1998; 71(2): 270–277.
26. Raleigh JA, Calkins-Adams DP, Rinker LH, et al. Hypoxia and vascular endothelial growth factor expression in human squamous cell carcinomas using pimonidazole as a hypoxia marker. Cancer Res 1998; 58(17):3765–3768.
27. Arteel GE, Raleigh JA, Bradford BU, Thurman RG. Acute alcohol produces hypoxia directly in rat liver tissue in vivo: role of Kupffer cells. Am J Physiol 1996; 271(3 Pt 1):G494–G500.
28. Arteel GE, Iimuro Y, Yin M, et al. Chronic enteral ethanol treatment causes hypoxia in rat liver tissue in vivo. Hepatology 1997; 25(4): 920–926.
29. Stachlewitz RF, Arteel GE, Raleigh JA, et al. Development and characterization of a new model of tacrine-induced hepatotoxicity: role of the sympathetic nervous system and hypoxia-reoxygenation. J Pharmacol Exp Ther 1997; 282(3):1591–1599.
30. Zhong Z, Arteel GE, Connor HD, et al. Cyclosporin A increases hypoxia and free radical production in rat kidneys: prevention by dietary glycine. Am J Physiol 1998; 275(Renal Physiol 44):F595–F604.
31. Cline JM, Thrall DE, Rosner GL, Raleigh JA. Distribution of the hypoxia marker CCI-103F in canine tumors. Int J Radiat Oncol Biol Phys 1994; 28(4):921–933.
32. Rojas A, Joiner MC, Hodgkiss RJ, et al. Enhancement of tumor radiosensitivity and reduced hypoxia-dependent binding of a 2-nitroimidazole with normobaric oxygen and carbogen: a therapeutic comparison with skin and kidneys. Int J Radiat Oncol Biol Phys 1992; 23(2):361–366.
33. Durand RE, Raleigh JA. Identification of nonproliferating but viable hypoxic cells in vivo. Cancer Res 1998; 58:3547–3550.
34. Olive PL. Distribution, oxygenation, and clonogenicity of macrophages in a murine tumor. Cancer Comm 1989; 1:93–100.
35. Hsu SM, Raine L, Fanger H. The use of antiavidin antibody and avidin-biotin-peroxidase complex in immunoperoxidase technics. Am J Clin Pathol 1981; 75(6):816–821.
36. Sheehan D, Hrapchak B. Theory and practice of histotechnology, 2nd ed. Columbus, OH: Battelle Press; 1980.
37. Freyer JP, Sutherland RM. A reduction in the in situ rates of oxygen and glucose consumption of cells in EMT6/Ro spheroids during growth. J Cell Physiol 1985; 124(3):516–524.
38. Howdieshell TR, Riegner C, Gupta V, et al. Normoxic wound fluid contains high levels of vascular endothelial growth factor. Ann Surg 1998; 228(5):707–715.
39. Banks RE, Forbes MA, Kinsey SE, et al. Release of the angiogenic cytokine vascular endothelial growth factor (VEGF) from platelets: significance for VEGF measurements and cancer biology. Br J Cancer 1998; 77(6):956–964.
40. Shoji M, Hancock WW, Abe K, et al. Activation of coagulation and angiogenesis in cancer: immunohistochemical localization in situ of clotting proteins and vascular endothelial growth factor in human cancer. Am J Pathol 1998; 152(2):399–411.
41. Gentry PA. The mammalian blood platelet: its role in haemostasis, inflammation and tissue repair. J Comp Pathol 1992; 107(3):243–270.
42. Mohle R, Green D, Moore MA, et al. Constitutive production and thrombin-induced release of vascular endothelial growth factor by human megakaryocytes and platelets. Proc Natl Acad Sci U S A 1997; 94(2):663–668.
43. Sporn MB, Roberts AB. Transforming growth factor-beta: recent progress and new challenges. J Cell Biol 1992; 119(5):1017–1021.
44. Derynck R. Transforming growth factor alpha. Cell 1988; 54(5):593–595.
45. Raines EW, Ross R. Platelet-derived growth factor. I. High-yield purification and evidence for multiple forms. J Biol Chem 1982; 257(9):5154–5160.

46. Knighton DR, Hunt TK, Thakral KK, Goodson WH 3rd. Role of platelets and fibrin in the healing sequence: an in vivo study of angiogenesis and collagen synthesis. Ann Surg 1982; 196(4):379–388.
47. Qi J, Kreutzer DL. Fibrin activation of vascular endothelial cells. Induction of IL-8 expression. J Immunol 1995; 155(2):867–876.
48. Contrino J, Goralnick S, Qi J, et al. Fibrin induction of tissue factor expression in human vascular endothelial cells. Circulation 1997; 96(2):605–613.
49. Qi J, Kreutzer DL, Piela-Smith TH. Fibrin induction of ICAM-1 expression in human vascular endothelial cells. J Immunol 1997; 158(4):1880–1886.
50. Ollivier V, Bentolila S, Chabbat J, et al. Tissue factor-dependent vascular endothelial growth factor production by human fibroblasts in response to activated factor VII. Blood 1998; 91(8):2698–2703.
51. Bochaton-Piallat ML, Gabbiani F, Redard M, et al. Apoptosis participates in cellularity regulation during rat aortic intimal thickening. Am J Pathol 1995; 146(5):1059–1064.
52. Desmouliere A, Badid C, Bochaton-Piallat ML, Gabbiani G. Apoptosis during wound healing, fibrocontractive diseases and vascular wall injury. Int J Biochem Cell Biol 1997; 29(1):19–30.
53. Desmouliere A, Redard M, Darby I, Gabbiani G. Apoptosis mediates the decrease in cellularity during the transition between granulation tissue and scar. Am J Pathol 1995; 146(1):56–66.
54. Bellamy CO. p53 and apoptosis. Br Med Bull 1997; 53(3):522–538.
55. Graeber TG, Osmanian C, Jacks T, et al. Hypoxia-mediated selection of cells with diminished apoptotic potential in solid tumours [see comments]. Nature 1996; 379(6560):88–91.
56. Carmeliet P, Dor Y, Herbert JM, et al. Role of HIF-1alpha in hypoxia-mediated apoptosis, cell proliferation and tumour angiogenesis. Nature 1998; 394(6692):485–490.
57. Feng ZC, Roberts EL Jr, Sick TJ, Rosenthal M. Depth profile of local oxygen tension and blood flow in rat cerebral cortex, white matter and hippocampus. Brain Res 1988; 445(2):280–288.
58. Hockel M, Schlenger K, Knoop C, Vaupel P. Oxygenation of carcinomas of the uterine cervix: evaluation by computerized O_2 tension measurements. Cancer Res 1991; 51(22):6098–6102.
59. Vaupel P, Schlenger KH, Hoeckel M, Okunieff P. Oxygenation of mammary tumors: from isotransplanted rodent tumors to primary malignancies in patients. Adv Exp Med Biol 1992; 316:361–371.
60. Linsenmeier RA, Braun RD. Oxygen distribution and consumption in the cat retina during normoxia and hypoxemia. J Gen Physiol 1992; 99(2):177–197.
61. Van Os-Corby DJ, Koch CJ, Chapman JD. Is misonidazole binding to mouse tissues a measure of cellular Po_2? Biochem Pharmacol 1987; 36(20):3487–3494.
62. Brown LF, Detmar M, Claffey K, et al. Vascular permeability factor/vascular endothelial growth factor: a multifunctional angiogenic cytokine. EXS 1997; 79:233–269.
63. Kuwabara K, Ogawa S, Matsumoto M, et al. Hypoxia-mediated induction of acidic/basic fibroblast growth factor and platelet-derived growth factor in mononuclear phagocytes stimulates growth of hypoxic endothelial cells. Proc Natl Acad Sci U S A 1995; 92(10):4606–4610. Raleigh, NC

APPENDIX 03

Plasma D-Dimer Levels in Operable Breast Cancer Patients Correlate With Clinical Stage and Axillary Lymph Node Status

By Kimberly Blackwell, Zishan Haroon, Gloria Broadwater, Donald Berry, Lyndsay Harris, J. Dirk Iglehart, Mark Dewhirst, and Charles Greenberg

Purpose: To investigate the relationship between preoperative plasma D-dimer levels and extent of tumor involvement in operable breast cancer patients.

Patients and Methods: A total of 140 preoperative plasma specimens were obtained from women scheduled to undergo diagnostic breast biopsies. Ninety-five patients in the initial group went on to undergo axillary lymph node dissection. Of the 140 patients from whom plasma samples were obtained, 102 were subsequently diagnosed with invasive breast carcinoma, nine were subsequently diagnosed with ductal carcinoma-in-situ, and 20 were subsequently diagnosed with benign breast disease. Plasma D-dimer levels were quantitated using a commercially available immunoassay kit (DIMERTEST; American Diagnostica, Greenwich, CT). The relationships between plasma D-dimer and other prognostic variables (tumor size, estrogen receptor, progesterone receptor, nuclear grade, histologic grade, lymphovascular invasion, and clinical stage grouping) were then examined using univariate and multivariate linear and logistic regression analyses.

Results: Median plasma D-dimer levels were significantly higher in patients with invasive carcinoma than those patients with either benign breast disease or carcinoma-in-situ ($P = .0001$). A significant relationship existed between the presence of elevated D-dimer (> 100 ng/mL) and involved axillary lymph nodes (χ^2 test; $P = .001$). Elevated D-dimer levels predicted positive lymph node involvement in both univariate regression ($P = .0035$) and multivariate linear regression ($P = .012$) models. In addition, elevated D-dimer levels predicted the presence of lymphovascular invasion in univariate logistic regression ($P = .0025$) and multivariate logistic regression analysis ($P = .0053$). Quantitative D-dimer levels were highly correlated with clinical stage grouping (analysis of variance test; $P = .002$).

Conclusion: Plasma D-dimer levels were markers of lymphovascular invasion, clinical stage, and lymph node involvement in operable breast cancer. This correlation suggests that detectable fibrin degradation, as measured by plasma D-dimer, is a clinically important marker for lymphovascular invasion and early tumor metastasis in operable breast cancer.

J Clin Oncol 18:600-608.

FIBRIN DEPOSITION and remodeling in the tumor extracellular matrix is an important initial step in tumor metastasis. For a tumor to successfully metastasize from its primary location, it must undergo several obligate steps, including the invasion into either the lymphatic or vascular lumen, transportation through the circulation, and establishment of viability in target tissues.[1] Cross-linked fibrin in the extracellular matrix serves as a stable framework for endothelial cell migration during angiogenesis and tumor cell migration during invasion. Extracellular remodeling of fibrin is essential for angiogenesis in tumors,[2] and activation of intravascular fibrin formation and degradation has been shown to occur in the plasma of breast cancer patients.[3,4] In addition, other indicators of fibrinolytic pathway activation, such as levels of plasminogen activator inhibitor and urokinase plasminogen activator, have been shown to have prognostic significance in patients with breast cancer.[5-8]

D-Dimer, a fibrin degradation product, is produced when factor XIIIa, a cross-linked fibrin, is degraded by plasmin generated from plasminogen by the action of serine protease tissue plasminogen activator. Investigation of human D-dimer levels has been made easier through the production of a specific monoclonal antibody that does not recognize degradation of fibrinogen or noncross-linked fibrin. Elevated D-dimer levels can be detected in the circulation, and elevated levels have been detected in patients with disseminated intravascular coagulation,[9,10] vaso-occlusive crisis in sickle cell disease,[11] thromboembolic events,[12-15] and myocardial infarction.[16]

D-Dimer levels are elevated in the plasma of various solid tumor patients, including lung,[17,18] prostate,[19,20] cervical,[21-23] and colorectal cancer patients.[24,25] In patients with

From the Divisions of Medical and Radiation Oncology, Duke University Comprehensive Cancer Center, Durham, NC.

Submitted March 12, 1999; accepted September 16, 1999.

Supported by grant no. CA-68438, a National Institutes of Health Specialized Program of Research Excellence grant in Breast Cancer at Duke University, Department of Defense grant no. 179717044, and National Cancer Institute grant no. CA-71753.

Address reprint requests to Charles Greenberg, MD, Department of Medicine and Pathology, Duke University Medical Center, Durham, NC 27710; email green032@mc.duke.edu.

0732-183X/00/1803-600

colorectal cancer, D-dimer levels have been shown to correlate with depth of tumor invasion at the time of surgical excision.[25] Plasma D-dimer levels have also been shown to directly correlate with other tumor markers, including CA-125 and carcinoembryonic antigen.[21,25] In patients with operable breast cancer, D-dimer levels have been shown to be elevated at time of diagnosis[26,27] and to decrease during adjuvant (epirubicin/cyclophosphamide) chemotherapy.[28] There still exists a gap in our knowledge regarding the relationship between quantitative D-dimer levels and extent of disease involvement in primary breast cancer. Our results suggest that a tight correlation exists between early tumor metastasis, lymphovascular invasion, and plasma D-dimer levels in operable breast cancer patients.

PATIENTS AND METHODS

Study Population

One hundred forty female patients seen for diagnostic surgical breast procedures were enrolled onto this study. Patients were eligible for participation if they had undergone a single needle biopsy or needle aspirate of their breast lesion but were excluded if they had undergone any more invasive procedure (excision or incisional biopsy, lumpectomy, or mastectomy.) The study sample consists of two separate consecutive patient populations. The first population (31 patients) had banked frozen plasma available and had been seen at Duke University Medical Center Surgical Oncology clinic from May 1994 through October 1995. Based on the promising results from the pilot population, we went on to prospectively enroll 109 patients from May 1997 to November 1998. Informed consent was obtained from all patients by the Duke University Medical Center Institutional Review Board.

Quantitative D-Dimer Level Determination

At time of enrollment, 5 mL of whole blood were drawn from the antecubital vein of patients using a tourniquet, 20-gauge Vacutainer needle and 3.8% sodium citrate Vacutainer collection tube (Becton Dickinson, Rutherford, NJ). All samples were centrifuged within 4 hours of venipuncture, and the plasma components were pipetted off and placed in snap-top plastic tubes. Centrifuged plasma was stored at −80°C until assays were run.

Quantitative D-dimer levels were obtained using the DIMERTEST immunoassay (American Diagnostica, Greenwich, CT). All samples were run in duplicate according to manufacturer's recommendations. This commercially available D-dimer monoclonal antibody recognizes an epitope that is a specific product of cross-linked fibrin that has been subsequently degraded by plasmin. Therefore, the plasma D-dimer assay does not recognize degradation of fibrinogen or noncross-linked fibrin. D-Dimer levels greater than 100 ng/mL were considered to be elevated, because this is the upper limit of normal using a 90% confidence limit from the mean of values obtained from healthy volunteers in our own laboratory.

Histopathologic Characterization

After enrollment onto the study, each patient either underwent excisional biopsy, lumpectomy, or modified radical mastectomy. Many patients had more than one pathologic breast specimen obtained after enrollment. Each specimen was paraffin-embedded and reviewed after hematoxylin and eosin staining. Hematoxylin and eosin staining were carried out, as described by Sheehan and Hrapchak.[29] Tissue specimens were examined for the following characteristics: presence or absence of invasive carcinoma, characterization of benign breast disease, tumor

Table 1. Patient Characteristics

Characteristic		Patients	
		No.	%
Age, years			
Median	54		
Range	33-74		
Patients with elevated D-dimer levels*		25†	19
D-dimer			
Mean	67.04		
Range	0-732.8		
Patients entered		140	
Patients analyzed		131	
Patients excluded from final analysis			
Concurrent pregnancy		2	
Concurrent CLL		1	
Bilateral breast malignancy		2	
Recent valve replacement, <2 weeks		1	
Neoadjuvant chemotherapy before plasma sample being obtained		1	
Plasma sample obtained after breast procedure performed		2	
Patients with Benign Breast Disease		29†	22
Ductal carcinoma-in-situ		9	
No pathologic abnormality		7	
Ductal hyperplasia		4	
Fibroadenoma		3	
Sclerosing adenosis		2	
Apocrine hyperplasia		1	
Atypical hyperplasia		1	
Lobular carcinoma-in-situ		1	
Intraductal papilloma		1	
Patients undergoing excisional biopsy only	77	59	
Patients undergoing modified radical mastectomy after biopsy	54	41	
Tumor size, cm			
Mean	1.94		
Range	0.2-10.5		
Patients who underwent lymph node dissection		95	13
No. of axillary nodes removed at time of dissection			
Median	13		
Range	1-37		
Patients with positive lymph nodes		33	35
Patients with negative lymph nodes		62	65
No. of positive axillary lymph nodes			
Mean	3.28		
Range	1-16		

Abbreviation: CLL, chronic lymphocytic leukemia.
*Elevated level: >100 ng/mL
†Out of no. of patients analyzed (n = 131).

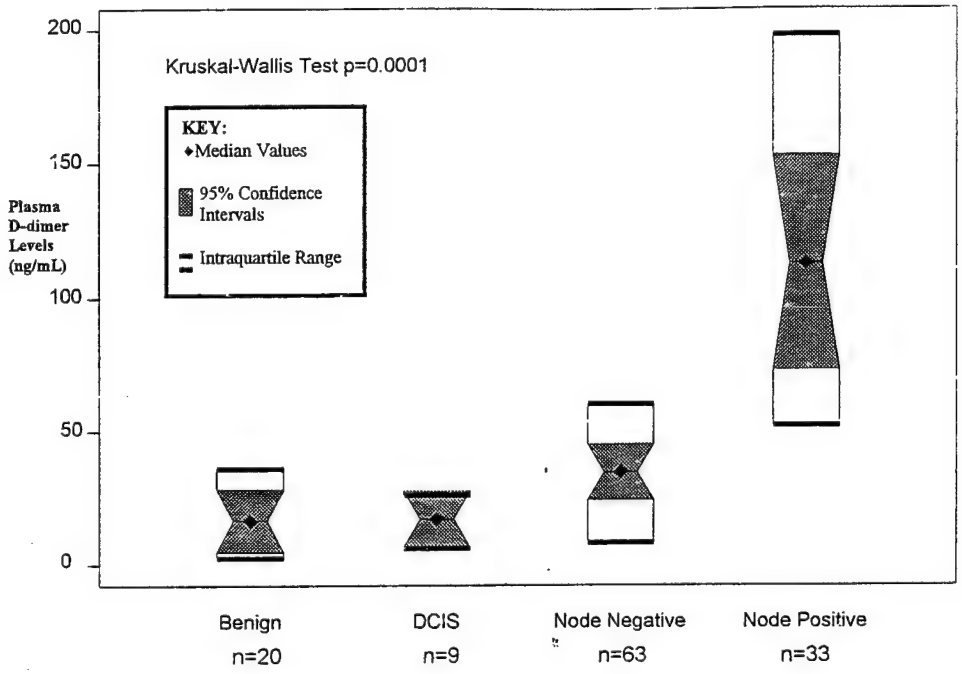

Fig 1. Plasma D-dimer levels by disease type.

size, nuclear grade, histologic grade, and lymphovascular invasion. If the specimen involved infiltrating carcinoma, estrogen and progesterone receptor expression were quantitated using image cytometry.[30] In cases with more than one pathologic specimen, the characteristics of the specimen with the largest amount of invasive disease was considered for the purposes of the analysis.

Patients who underwent axillary lymph node dissection had nodal tissue paraffin-embedded, hematoxylin and eosin stained, and microscopically examined for the presence of malignant cells by attending pathology staff at Duke University Medical Center. Subtotal involvement of the lymph node with malignant cells was considered positive for analysis purposes.

Clinical Staging

An observer unaware of D-dimer levels performed all clinical staging. Clinical staging was performed according to the 1998 American Joint Committee on Cancer staging system.[31] This staging system is based on all information available before first treatment and includes physical examination findings, imaging studies, operative findings, and pathologic findings. Stage grouping was performed, because of the small number of patients in each tumor-node-metastasis group, according to the American Joint Committee on Cancer guidelines as follows: stage I: T1N0M0; stage IIA: T0N1M0, T1N1M0, and T2N0M0; stage IIB: T2N1M0 and T3N0M0; stage IIIA: T0N2M0, T1N2M0, T2N2M0, T3N1M0, and T3N2M0; stage IIIB: T4Any NM0 and AnyTN3M0: and stage IV: AnyTAnyNM1.

Statistical Analysis

All statistical variables were examined in the pilot study and then in the prospective study separately. When results from the prospective trial were consistent with those in the pilot study, the data was examined as a single study population.

Study analysis included information regarding (1) D-dimer levels as a continuous and dichotomous variable (≤ 100 ng/mL or >100 ng/mL); (2) lymph node status as a continuous and dichotomous variable (positive/negative); (3) estrogen receptor status (positive/negative); (4) progesterone receptor status (positive/negative); (5) nuclear grade (well-differentiated [grade 1], intermediate [grade 2], and poorly differentiated [grade 3]); (6) histologic grade (well-differentiated [grade 1], intermediate [grade 2], and poorly differentiated [grade 3]); and (7) lymphovascular invasion (present/absent). Spearman correlation coefficients were used to examine the association between pairs of variables. Relationships between categorical variables were compared using χ^2 tests. Independent variables were used in univariate and multivariate linear and logistic regression models to predict D-dimer, lymph node involvement, and lymphovascular invasion.

RESULTS

Patient Characteristics

The characteristics of the study population are listed in Table 1. Of the 140 patients enrolled, nine were excluded from analysis after enrollment. Four patients were excluded after enrollment because of other concurrent conditions known to increase D-dimer levels, such as pregnancy (n = 2), chronic lymphocytic leukemia (n = 1), and recent (13 days prior) mechanical valve repair (n = 1). Two patients were excluded after enrollment because of bilateral breast malignancies, and three patients were excluded after enrollment because of already having undergone major breast surgical procedures (two patients had undergone lumpectomy) or because of having completed neoadjuvant chemo-

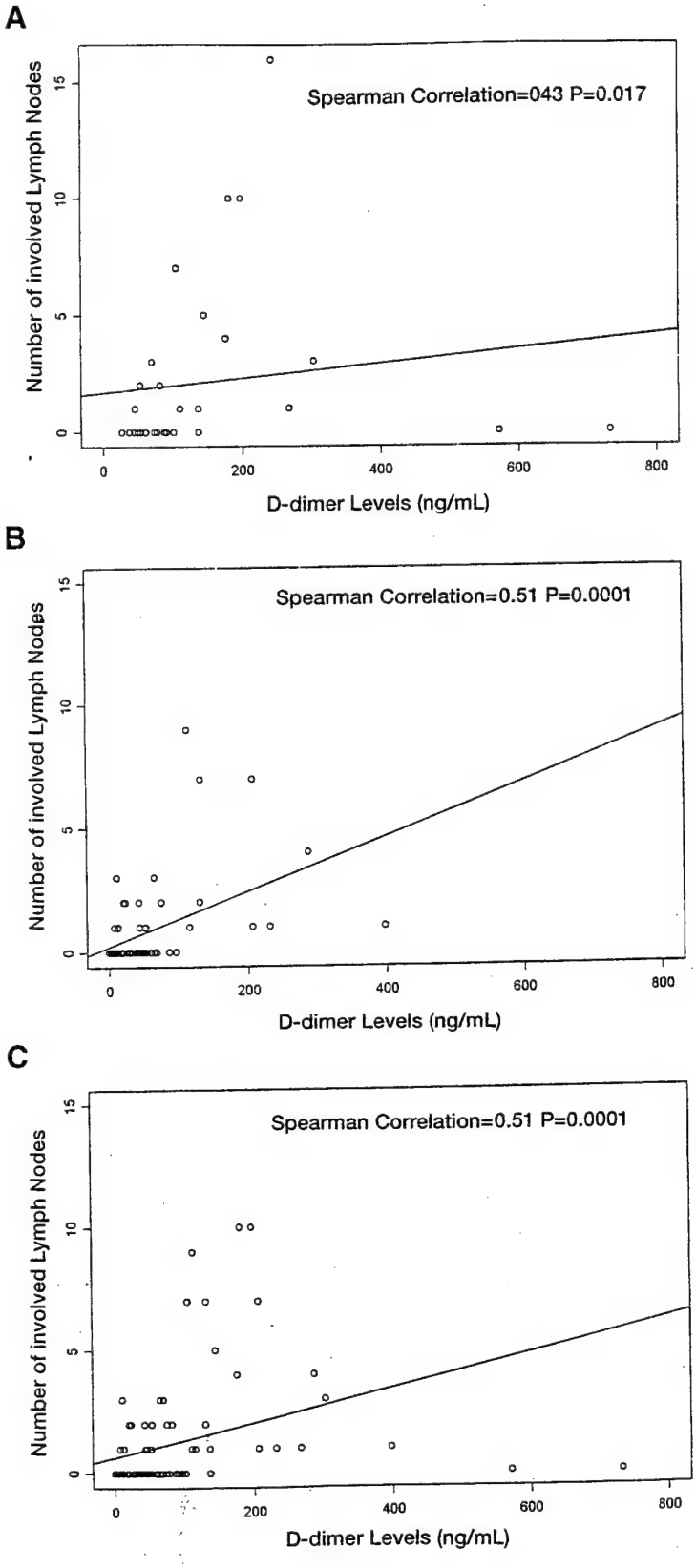

Fig 2. Correlation between D-dimer levels and number of involved lymph nodes; (A) pilot trial, (B) prospective trial, and (C) both trials.

Table 2. Plasma D-Dimer Levels and Histopathologic Correlates

	Pilot Trial (n = 31)		Prospective Trial (n = 64)		Combined Groups (n = 95)	
	Spearman Correlation	P	Spearman Correlation	P	Spearman Correlation	P
Lymph node status	0.43	.017	0.51	.0001	0.51	.0001
Tumor size	0.34	.058	0.09	.49	0.26	.008
Estrogen receptor status	−0.06	81	−0.32	.01	−0.27	.019
Progesterone receptor status	0.17	.53	0.02	.91	0.04	.73
Nuclear grade	0.07	.73	0.20	.16	0.16	.16
Histologic grade	−0.50	81	0.09	.53	−0.05	.70
Lymphovascular invasion	0.19	.39	0.38	.018	0.47	.0002

therapy (one patient). Three of the nine patients had elevated D-dimer levels (> 100 ng/mL).

Twenty-nine patients had benign breast disease at diagnosis. Seventy-seven patients (59%) underwent excisional biopsy as definitive surgical therapy. Fifty-four patients (41%) had modified radical mastectomy after biopsy. Sixty-one patients (73%) had axillary lymph node dissection with a median of 13 lymph nodes removed at the time of dissection. Thirty-three patients (35%) had involved lymph nodes, with the mean number of positive lymph nodes being 3.28 (range, one to 16 positive lymph nodes). Five patients (3%) had 10 or more involved lymph nodes. Five patients (3%) had five to nine involved lymph nodes. Three patients with 10 or more lymph nodes had preoperative documentation of palpable axillary lymph nodes. None of the patients with five to nine involved lymph nodes were noted preoperatively to have palpable lymph nodes.

Of patients with malignant disease, mean tumor size was 1.94 cm (range, 0.2 to 10.5 cm). Seven patients (5%) had tumors larger than 5 cm. No patients had clinical or pathologic evidence of chest wall or skin involvement. Twenty-five patients (19%) had elevated D-dimer levels (> 100 ng/mL). The mean D-dimer level in the study population was 67.04 ng/mL (SD = 8.87 ng/mL); the median D-dimer level was 37.25 ng/mL.

D-Dimer and Underlying Breast Disease

The distribution of D-dimer levels between patients with different types of underlying breast disease is shown in Fig 1. There was a significant difference between D-dimer levels in those patients with benign breast disease, ductal carcinoma-in-situ, lymph node–negative invasive carcinoma, and lymph node–positive invasive carcinoma (Kruskal-Wallis test, $P = .0001$). There was a statistically significant difference between median D-dimer levels in patients having positive nodes compared with those patients with no nodal involvement (Wilcoxon rank sum test, $P = .0001$).

D-Dimer and Histopathologic Variables

Of all histopathologic variables examined, D-dimer levels correlated strongest with the number of positive lymph nodes in the pilot group (Spearman correlation = 0.43; $P = .02$), the prospective group (Spearman correlation = 0.51; $P = .0001$), and the combined group (Spearman correlation = 0.51; $P = .0001$) (Fig 2). In the pilot group, D-dimer levels directly correlated with extent of lymph node involvement but not with tumor size, estrogen receptor status, progesterone receptor status, or lymphovascular invasion. In the prospective group, D-dimer levels correlated with extent of lymph node involvement, estrogen receptor status (Spearman correlation = −0.32; $P = .01$), and lymphovascular invasion (Spearman correlation = 0.38; $P = .02$), but not with tumor size or progesterone receptor status. In the combined (pilot and prospective) group, D-dimer levels correlated with extent of lymph node involvement, tumor size (Spearman correlation = 0.26; $P = .008$), lymphovascular invasion (Spearman correlation = 0.47; $P = .0002$), and estrogen receptor status (Spearman correlation = −0.27; $P = .019$), but not with progesterone receptor status (Spearman correlation = 0.04; $P = .73$) (Table 2)

D-Dimer and Clinical Stage

The results of correlation between D-dimer and clinical stage are listed in Table 3. No patients were stage IIIB or stage IV. There was a statistically significant difference in

Table 3. Correlation Between D-Dimer Levels and Clinical Stage Grouping

Clinical Stage Group	No. of Patients	Mean D-Dimer (ng/mL)
Stage I	40	34.29*
Stage IIA	29	103.42*
Stage IIB	14	119.37*
Stage IIIA	12	152.13*

*Analysis of variance test for differences between groups; $P = .002$.

Table 4. Correlation Between Elevated D-Dimer Levels and Involved Axillary Lymph Nodes

D-Dimer Level	No. of Involved Axillary Lymph Nodes		
	Negative	Positive	Total
Low, ≤ 100 ng/mL	57	14	71
Elevated, > 100 ng/mL	5	19	24
Total	62	33	95

D-dimer levels based on clinical stage grouping (analysis of variance test; $P = .002$).

D-Dimer and Lymph Node Involvement

When examined as a dichotomous variable (elevated = > 100 ng/mL; normal = ≤100 ng/mL), elevated D-dimer levels correlated strongly with the presence of positive lymph nodes (χ^2 test; $P = .001$) (Table 4). This correlation was seen regardless of group examined (pilot group: χ^2 test, $P = .02$ and prospective group: χ^2 test, $P = .001$).

Using the cutoff of 100 ng/mL, plasma D-dimer levels had a positive predictive value of 0.79 and a negative predictive value of 0.80 for predicting the extent of lymph node involvement. Likewise, elevated plasma D-dimer levels had a high specificity of 0.92 and moderate sensitivity of 0.58. A receiver operating characteristic (ROC) curve for D-dimer values in predicting lymph node involvement is shown in Fig 3.

Regression Modeling in Predicting D-Dimer Levels and Lymph Node Involvement

Presence of lymphovascular invasion and presence of positive lymph nodes were significant in predicting D-dimer levels in both univariate and multivariate linear regression models (Table 5). Elevated D-dimer levels and tumor size were significant in predicting the presence of positive lymph nodes in both univariate and multivariate logistic regression models (Table 6). Using logistic regression modeling, the probability of having involved lymph nodes can be predicted for a given tumor size. Table 7 lists the probability, according to D-dimer levels, of having positive lymph nodes for either a 1-cm primary tumor or a 2-cm primary tumor. Based on this model, a patient with a 2-cm tumor and an elevated level of D-dimer (200 ng/mL) was twice as likely (probability = 0.42) to have involved axillary lymph nodes as those patients with low levels of D-dimer (5 ng/mL; probability = 0.20).

DISCUSSION

For over 20 years, investigators have documented the importance of the fibrinolytic pathway in tumor angiogenesis and metastasis.[1-8,32-34] Indicators of fibrinolytic path-

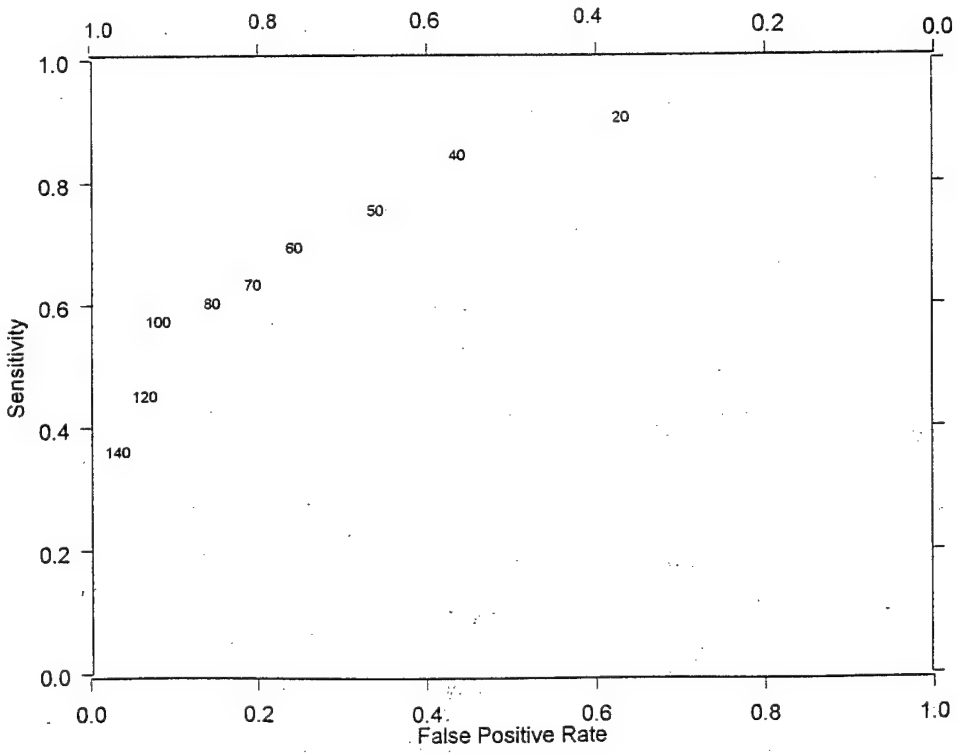

Fig 3. An receiver operating characteristic curve for D-dimer values in predicting lymph node involvement.

Table 5. Linear Regression Model Predicting D-Dimer Levels

Independent Variables	Univariate P	Multivariate P
Lymphovascular invasion	.0033	.01
No. of positive lymph nodes	.0035	.04

Table 6. Logistic Regression Model Predicting Positive Axillary Lymph Nodes

Independent Variables	Univariate P	Multivariate P
D-dimer levels	.0127	.0412
Tumor size	.0003	.0011
Nuclear grade	.01	NS
Histologic grade	.58	NS
Estrogen receptor	.13	NS
Progesterone receptor	.79	NS

Abbreviation: NS, not significant.

way activation, such as levels of plasminogen activator inhibitor and urokinase plasminogen activator, have been shown to have prognostic significance in patients with breast cancer.[5-8] Our study represents the first attempt to look at a product of fibrin degradation (D-dimer) as a specific marker for extent of disease in human breast cancer. Both of our study populations (pilot and prospective) were representative of mainstream clinical practices in terms of mean tumor size and lymph node involvement.[35] The patient population was skewed toward an increased percentage (78%) of malignant disease than that population usually seen for routine diagnostic surgical procedures. By carrying out the study in a referral center and allowing for previous outside needle biopsy diagnosis, we enrolled a larger percentage of patients with already known malignant disease than if the study had taken place in the community setting.

Previously, increased D-dimer levels have been demonstrated in a variety of intravascular and inflammatory conditions. Only 2% of patients in this study were prospectively excluded for concurrent conditions that could have elevated their D-dimer levels. Unrecognized conditions, such as asymptomatic venous thrombosis, certainly existed in our study population, and yet, D-dimer remained highly specific in detecting positive lymph nodes.

The process of metastasis involves multiple tumor-host interactions. To survive, metastatic cancer cells must leave the primary tumor, migrate into the lymphovascular system, and establish a new blood supply at their metastatic site. Fibrin remodeling is almost certainly involved in all steps of metastasis and has been proven to play a crucial role in new vessel formation.[36-39] This study confirms previous studies showing upregulated fibrinolytic activity (presence of plasma D-dimer) in malignant disease and increased levels of fibrinolytic activity (increased D-dimer levels) in metastatic disease. In addition, linear regression modeling showed a tight relationship between the presence of lymphovascular invasion and elevated D-dimer levels. This relationship suggests a possible, yet unproven, biologic mechanism for the entrance of D-dimer fragments into the circulation. Further research needs to be carried out looking at the mechanism by which fibrin degradation products enter the systemic circulation. Finally, research needs to be carried out looking at other levels of coagulation factors and their relationship with D-dimer levels.

Lymph node status in postmenopausal patients with smaller tumors determines treatment recommendations. Determining lymph node status via standard lymph node dissection creates many significant long-term side effects, including pain, numbness, and lymphedema. Many attempts have been made to predict lymph node status without undergoing a full lymph node dissection. Tumor size has been shown to predict lymph node status in numerous large studies,[35,40-42] and our combined study group results confirmed this finding. However, independently, our pilot study and prospective study failed to demonstrate a correlation between tumor size and axillary lymph node involvement. We believe this is because of the small number of patients in each study group and the large variance possible in tumor size.

Patients with tumors larger than 3 cm face a greater than 50% chance of having axillary lymph node involvement. Accurate tumor size is not available prospectively, and clinical examination has been shown by many authors to be nonspecific.[42,43] Many clinicians believe that premenopausal women with larger tumors should be spared the damaging effects of axillary lymph node dissection. How-

Table 7. Effects of Adding D-Dimer Levels to Known Tumor Size to Predict Lymph Node Involvement

D-Dimer Level (ng/mL)	1-cm Tumor		2-cm Tumor	
	Probability of Lymph Node Involvement	95% Confidence Interval	Probability of Lymph Node Involvement	95% Confidence Interval
5	0.12	0.06 -0.24	0.19	0.12 -0.32
50	0.15	0.09 -0.28	0.24	0.15 -0.35
100	0.19	0.11 -0.33	0.29	0.19 -0.41
150	0.24	0.13 -0.42	0.35	0.22 -0.51
200	0.29	0.14 -0.53	0.42	0.24 -0.62

ever, in patients with smaller tumors (< 1 cm), the risks and long-term morbidity of axillary lymph node dissection versus the benefits of knowing a patient's lymph node status are sometimes equivalent. Through the use of logistic regression modeling, our study shows that by holding tumor size constant at 1 cm, a healthy patient with an elevated D-dimer (200 ng/mL) is almost three times as likely to have positive lymph nodes as a patient with a low D-Dimer (5 ng/mL). This suggests that patients with small tumors and low D-dimer levels could possibly be spared the morbidity of an axillary lymph node dissection.

Given its sensitivity for predicting positive lymph node involvement, an important role of D-dimer could be in combination with other predictive factors in determining whether or not axillary lymph node dissection is necessary. This study clearly supports a role for plasma D-dimer levels in predicting clinically (lymph node status) and biologically (lymphovascular invasion) relevant factors in operable breast cancer. D-dimer can not be used alone in predicting lymph node status given its low negative predictive value. We are now investigating plasma D-dimer levels as a prognostic marker for operable breast cancer and the usefulness of combining plasma D-dimer levels with sentinel lymph node biopsy. Given the ease with which plasma D-dimer levels can be obtained, we are looking into the utility of adding quantitative D-dimer levels into models for predicting lymphovascular invasion and axillary lymph node involvement.

ACKNOWLEDGMENT

We thank Elizabeth Wildermann for her dedicated assistance in plasma collection.

REFERENCES

1. Fidler IJ, Ellis LM: The implications of angiogenesis for the biology and therapy of cancer metastasis. Cell 79:315-328, 1994

2. Dvorak HF, Brown LF, Detmar M, et al: Vascular permeability factor/vascular endothelial growth factor, microvascular hyperpermeability, and angiogenesis. Am J Pathol 146:1029-1039, 1995

3. Grohndahl-Hansen J, Agerlin N, Munkholm-Larsen P: Sensitive and specific enzyme-linked immunosorbent assay of urokinase-type plasminogen activator and its application in plasma from patients with breast cancer. J Lab Clin Med 111:42-51, 1988

4. Layer GT, Burnhard KH, Gaffney PJ, et al: Tissue plasminogen activators in breast cancer. Thrombosis Res 45:601-605, 1987

5. Spyratos F, Martin P-M, Hacene K, et al: Multiparametric prognostic evaluation of biological factors in primary breast cancer. J Natl Cancer Inst 84:1266-1272, 1992

6. Grondahl-Hansen J, Christensen IH, Rosenquist C, et al: High levels of urokinase-type plasminogen activator and its inhibitor PAI-1 in cytosolic extracts of breast carcinomas are associated with prognosis. Cancer Res 53:2513-2521, 1993

7. Janicke F, Schmitt M, Pache L, et al: Urokinase (uPa) and its inhibitor PAI-1 are strong and independent prognostic factors in node-negative breast cancer. Breast Cancer Res Treat 24:195-208, 1993

8. Duffy MJ, Reilly D, McDermott E, et al: Urokinase plasminogen activator as a prognostic marker in different subgroups of patients with breast cancer. Cancer 74:2276-2280, 1994

9. Wilde JT, Kitchen S, Kinsey S, et al: Plasma D-dimer levels and their relationship to serum fibrinogen/fibrin degradation products in hypercoaguable states. Br J Haematol 71:65-70, 1989

10. Bick RL, Baker WF: Diagnostic efficacy of the D-dimer assay in disseminated intravascular coagulation (DIC). Thromb Res 65:785-790, 1992

11. Devine DV, Kinney TR, Thomas Pfet al: Fragment D-dimer levels: An objective marker of vaso-occlusive crisis and other complications of sickle cell disease. Blood 68:317-319, 1986

12. Rowbotham BJ, Carroll P, Whitaker AN, et al: Measurement of crosslinked fibrin derivatives-use in the diagnosis of venous thrombosis. Thromb Haemost 57:59-61, 1987

13. Rowbotham BJ, Egerton-Vernon J, Whitaker AN, et al: Plasma cross linked fibrin degradation products in pulmonary embolism. Thorax 45:684-687, 1990

14. Carter CJ, Doyle DL, Dawson N, et al: Investigations into the clinical utility of latex D-dimer in the diagnosis of deep venous thrombosis. Thromb Haemost 69:8-11, 1993

15. Ginsberg JS, Kearon C, Douketis J, et al: The use of D-dimer testing and impedance plethysmographic examination in patients with clinical implications of deep vein thrombosis. Arch Intern Med 157:1077-1081, 1997

16. Francis CW, Connaghan DG, Scott WL, et al: Increased plasma concentration of crosslinked fibrin polymers in acute myocardial infarction. Circulation 75:1170-1175, 1987

17. Seitz R, Rappe N, Kraus M, et al: Activation of coagulation and fibrinolysis in patients with lung cancer: Relation to tumour stage and prognosis. Blood Coagul Fibrinolysis 4:249-254, 1993

18. Gabazza EC, Taguchi O, Yamakami T, et al: Evaluating prethrombotic state in lung cancer using molecular markers. Chest 103:196-200, 1993

19. Nakashima J, Tachibana M, Ueno M, et al: Tumor necrosis factor and coagulopathy in patients with prostate cancer. Cancer Res 55:4881-4885, 1995

20. Okajima K, Kohno I, Tsuruta J, et al: Direct evidence for systemic fibrinogenolysis in a patient with metastatic prostatic cancer. Thrombosis Res 66:717-727, 1992

21. Rella C, Coviello M, De Frenza N, et al: Plasma D-dimer measurement as a marker of gynecologic tumors: Comparison with CA 125. Tumori 79:347-51, 1993

22. Olt GJ, Greenberg C, Synan I, et al: Preoperative assessment of fragment D-dimer as a predictor of postoperative venous thrombosis. Am J Obstet Gynecol 162:772-775, 1990

23. Gadducci A, Baicchi U, Marrai R, et al: Pretreatment plasma levels of fibrinopeptide-A (FPA), D-dimer (DD), and von Willebrand factor (vWF) in patients with operable cervical cancer: Influence of surgical-pathological stage, tumor size, histologic type, and lymph node status. Gynecol Oncol 49:354-358, 1993

24. Edwards CM, Warren J, Armstrong L, et al: D-Dimer: A useful marker of disease stage in surgery for colorectal cancer. Br J Surg 80:1404-1405, 1993

25. Oya M, Akiyama Y, Yanagida T, et al: Plasma D-dimer level in patients with colorectal cancer: Its role as a tumor marker. Surg Today 28:373-378, 1998

26. McCollough P, Douglas J, Lowe GDO, et al: In vivo measurement of fibrin formation and fibrinolysis in operable breast cancer. Thromb Haemost 61:318-321, 1989

27. Mitter CG, Zielinski CC: Plasma levels of D-dimer: A crosslinked fibrin-degradation product in female breast cancer. J Cancer Res Clin Oncol 117:259-262, 1991

28. Tempelhoff GF, Dietrich M, Hommel G, et al: Blood coagulation during adjuvant epirubicin/cyclophosphamide chemotherapy in patients with primary operable breast cancer. J Clin Oncol 14:2560-2568, 1996

29. Sheehan D, Hrapchak B: Theory and Practice of Histotechnology (ed 2). Columbus, OH, Battelle Press, 1980

30. Layfield LJ, Saria EA, Conlon DH, et al: Estrogen and progesterone status determined by the Ventana ES 320 automated immunohistochemical stainer and the CAS 200 Image Analyzer in 236 early stage breast carcinomas. J Surg Oncology 61:177-184, 1996

31. American Joint Committee on Cancer: Cancer Staging Handbook (ed 5), in Fleming ID, Cooper JS, Henson DE, et al (eds). Philadelphia, PA, Lippincott-Raven, 1998

32. Dvorak HF: Tumors: Wounds that do not heal. N Engl J Med 315:1650-1659, 1986

33. Blood CA, Zetter BR: Tumor interactions with the vasculature: Angiogenesis and tumor metastasis. Biochim Biophys Acta 1032:89-118, 1990

34. Ausprunk DH, Folkman J: Migration and proliferation of endothelial cells in preformed and newly formed blood vessels during tumor angiogenesis. Microvasc Res 14:53-65, 1977

35. Carter C, Allen C, Henson D: Relation of tumor size, lymph node status, and survival in 24,740 breast cancer cases. Cancer 63:181-188, 1989

36. Nagy JA, Brown LF, Senger DR, et al: Pathogenesis of tumor stroma generation: A critical role for leaky blood vessels and fibrin deposition. Biochim Biophys Acta 948:305-326, 1988

37. Nagy JA, Morgan ES, Herzberg KT, et al: Pathogenesis of ascites tumor growth: Angiogenesis, vascular remodeling, and stroma formation in the peritoneal lining. Cancer Res 55:376-385, 1995

38. Brown LF, Van De Water L, Harvey VS, et al: Fibrinogen influx and accumulation of cross-linked fibrin in healing wounds and in tumor stroma. Am J Path 130:455-465, 1988

39. Shoji M, Hancock WM, Abe K, et al: Activation of coagulation and angiogenesis in cancer. Am J Path 152:399-411, 1998

40. Nemoto T, Vana J, Bedwani R: Management and survival of female breast cancer: Results of a national survey by the American College of Surgeons. Cancer 51:1333-1338, 1983

41. Fischer B, Slack N, Bross I: Cancer of the breast: Size of neoplasm and prognosis. Cancer 24:1071-1076, 1969

42. Schottenfeld D, Nash A, Robbins G: Ten-year results of the treatment of primary operable breast carcinoma. Cancer 38:1001-1012, 1976

43. Butcher H: Radical mastectomy for mammary carcinoma. Ann Surg 170:883-884, 1969

APPENDIX 04

0023-6837/99/7912-1679$03.00/0
LABORATORY INVESTIGATION

Vol. 79, No. 12, p. 1679, 1999
Printed in U.S.A.

Tissue Transglutaminase Is Expressed as a Host Response to Tumor Invasion and Inhibits Tumor Growth

Zishan A. Haroon, Thung-Shenq Lai, Joann M. Hettasch, Robert A. Lindberg, Mark W. Dewhirst and Charles S. Greenberg

Departments of Pathology (ZAH, MWD, CSG), Medicine (T-SL, JMH, CSG), and Radiation Oncology (RAL, MWD), Duke University Medical Center, Durham, North Carolina

SUMMARY: A stable extracellular matrix (ECM) constitutes an important part of host response mechanism against tumor growth and invasion. Tissue transglutaminase (TG), a calcium-dependent enzyme, can cross-link all major ECM proteins to form a stable ECM, because these cross-links are resistant to proteolytic and mechanical damage. TG can also enhance stability and strength of the ECM by its ability to facilitate the activation of transforming growth factor-β. We hypothesized that TG ECM-promoting abilities form an important part of the host response mechanism against tumor growth. Increased expression of TG was observed in the ECM of the host tumor interface of subcutaneously implanted rat mammary adenocarcinoma R3230 Ac. TG expression was also detected in the endothelial cells and macrophages. We also detected the cross-link product at the host tumor interface and within the tumor tissue, showing that TG was active. Western blots showed TG was degraded into three fragments of 55-, 50-, and 20-kDa forms. When recombinant wild-type TG was applied to R3230 Ac implanted in rat dorsal skin flap window chamber, it caused significant growth delay at day 7 compared with recombinant inactive TG controls. Collagen was detected in increased amounts in TG treated tumors, suggesting augmentation of production and stability of the ECM. We conclude that TG forms a distinct part of host response system against and acts to inhibit tumor growth. (*Lab Invest 1999, 79:1679–1686*).

The extracellular matrix (ECM) of the tumor plays an important role in the regulation of tumor growth, metastasis, and angiogenesis (Dano et al, 1999; Horton, 1995; Lukashev and Werb, 1998; Pepper et al, 1996; Taipale and Keski-Oja, 1997; Wernert, 1997). The ECM modulates tumor growth by (1) binding and storing cytokines; (2) providing a stable matrix for attachment and migration of cells; and (3) interacting with cell surface receptors that provide cell signals that control cell cycle, cell proliferation, and apoptosis pathways. Tumors are known to elicit a wound-healing response from the host tissues, resulting in formation of a granulation tissue at the advancing margins (Brown et al, 1989; Dvorak, 1986; Senger et al, 1994). The newly produced and remodeled ECM can either stimulate or inhibit tumor growth. The molecular mechanisms regulating the outcome between tumor and host factors in remodeling the ECM are just beginning to be defined.

Tissue transglutaminase (TG) is a calcium-dependent enzyme that covalently cross-links a wide variety of ECM proteins, producing a protease resistant matrix (Aeschlimann et al, 1996; Greenberg et al, 1991). TG expression has been shown in wounded tissues and at sites of inflammation and has been implicated in numerous interactions that stabilize ECM (Bowness and Tarr, 1997; Bowness et al, 1988; Weinberg et al, 1991). TG regulates the conversion of latent to active transforming growth factor-β (TGF-β) (Kojima et al, 1993), a cytokine that can modify epithelial growth, enhance synthesis of various ECM proteins and inhibitors of metalloproteases (Clark and Coker, 1998; Pepper, 1997; Taipale et al, 1998). TG could also cross-link elafin (Nara et al, 1994) and PAI-2 (Jensen et al, 1993), potent inhibitors of elastase and plasmin, respectively, to ECM molecules. Fibroblasts transfected with TG have been shown to have a distinctive spread morphology and increased resistance to protease digestion (Gentile et al, 1992). These TG activities, as part of the host response mechanisms, could alter the adhesive and invasive properties of malignant cells by modulating and influencing matrix production and stability of the host tissues. Thus, TG seems to be an important host factor that could play a role in tumor biology.

In an earlier study, we observed that TG antigen expression was associated with the neovasculature and the host's ECM surrounding human mammary tumors (Hettasch et al, 1996). The central hypothesis of our study was to ascertain whether TG in host tissue was involved in stabilizing the ECM around tumors. If stabilization occurred, we believed that

Received September 22, 1999.
This work was supported by Department of Defense Grant DAMD 179717044, Duke SPORE on Breast Cancer Grant P50 CA 68438, and National Institutes of Health Grants HL 38245 and HL 26309.
Address reprint requests to: Dr. C. Greenberg, Box 2603, MSRB, DUMC, Durham, North Carolina 27710. Fax: (919)684-4670; E-mail: green032@mc.duke.edu

addition of exogenous TG could inhibit tumor growth in a murine mammary carcinoma model. We found that TG antigen was localized to neovasculature and the ECM of rat R3230 Ac mammary tumor. TG expression was most intense at the interface between tumor and normal host tissue. The TG antigen expression pattern suggested TG was playing a role in regulating tumor growth. We transplanted R3230 Ac in the window chamber and subsequently recombinant TG was applied to the fascial surface of the window. We found that TG stimulated ECM formation and inhibited tumor growth.

Results

Light Microscopy

Subcutaneous tumor implants exhibited two distinct zones (Fig. 1A) in cross-sections stained with Masson trichrome, arbitrarily assigned as tumor core region (TCR) and host-tumor interface (HTI). The advancing margins at the HTI tissue showed extensive inflammatory reaction. There was also an increased amount of granulation tissue deposition consisting of endothelial cells, macrophages, and neutrophils interspersed among tumor and skeletal muscle cells in the HTI. The mammary tumor cells appeared granular and formed glandular clusters separated by thin bands of matrix and blood vessels in the TCR.

Localization, Expression, and Activity of TG

TG was expressed throughout the tumor and surrounding host tissue (Fig. 1B), although being more intense in HTI. TG antigen staining was present in the thin matrix, encapsulating the tumor islands in the TCR (Fig. 1C). The blood vessels present in the matrix in TCR also showed consistent expression of TG antigen. The few macrophages that were detected in this matrix exhibited TG expression. The tumor cells did not show any reactivity for the TG antigen, except in some instances where the tumor cells were adjacent to the matrix.

The host tissue initiated an intense wound-healing reaction to the tumor, resulting in granulation tissue formation all along the edges of the tumor tissue. HTI region was characterized by intense TG antigen staining that formed a TG-positive barrier between the normal and tumor tissues (Fig. 1D). TG antigen was expressed by endothelial cells, macrophages, skeletal muscle cells, and was also deposited in the ECM in the HTI region (Fig. 1E).

The presence of isopeptide bonds in tissues is a direct evidence for TG activity. The basement membranes of blood vessels, macrophages, smooth muscle cells, and ECM displayed consistent staining for isopeptide bonds, closely approximating TG distribution in the HTI and TCR (Fig. 1F). Factor XIIIa, a transglutaminase present in the blood, can also generate these isopeptide bonds. Compared with TG, factor XIIIa activity is restricted to areas of active thrombin formation, because thrombin is essential for factor XIII activation (Takahashi et al, 1986). Due to this critical limitation of factor XIIIa activity, we believe TG is more responsible for generation of these isopeptide bonds observed in our experimental model.

Detection of Macrophages and Active TGF-β

Because TG is expressed by macrophages and is directly involved in activation of TGF-β, we investigated the distribution of macrophages and TGF-β in relation to TG antigen staining. We found a high density of macrophages in the HTI region (Fig. 2A), and these cells also stained positive for TG antigen. The TCR staining pattern was largely devoid of macrophages. The few macrophages present stained positive for TG and were in the matrix surrounding necrotic areas. Active TGF-β staining was colocalized primarily in the endothelial cells with TG antigen reactivity in the HTI (Fig. 2B) and TCR.

Western Blots of the R3230 Ac Tumors

SDS-PAGE and quantitative immunoblotting demonstrated four distinct bands for TG antigen (Fig. 3, A and B). Quantitative analysis of the antigen revealed that more than 95% of the protein was rapidly degraded to 55-, 50-, and 20-kDa fragments from the full-length wild-type TG of 75 kDa.

Administration of Recombinant TG on R3230 Ac Implanted Dorsal Skin Flap Window Chamber

The R3230 Ac tumors treated with single dose of recombinant wild-type TG showed significant growth inhibition at day 7 after implantation compared with the control tumors treated with recombinant inactive TG (Fig. 4). The TG-treated tumors exhibited increased fibrosis in the surrounding matrix and around the tumor islands in both the TCR and HTI as indicated by intense staining of collagen fibers (Fig. 2, C to F). The mean size of TG-treated tumors was not significantly different from the controls at day 10, but some of the samples continued to show inhibition (data not shown).

Discussion

The host response to tissue injury caused by a tumor is characterized by complex and intricate mechanisms initiated to limit the growth and spread of tumors (Tabor, 1997). Host response mechanisms include increased activity of tumor suppressor genes, induction of cytokines that promote wound healing, stimulation of the immune system to resist foreign invasion, and production of a stable ECM. A stable ECM is intrinsically anti-angiogenic and growth inhibitory by virtue of being more protease resistant and mechanically resistant to disruption by the expanding tumor mass (Dano et al, 1999; Lochter et al, 1998; Werb et al, 1999). The formation of a stable ECM may be an effective barrier to growth and metastasis of tumors by restricting infiltration by tumor cells and growth of new blood vessels. The central hypothesis of this study was that host TG could enhance the formation

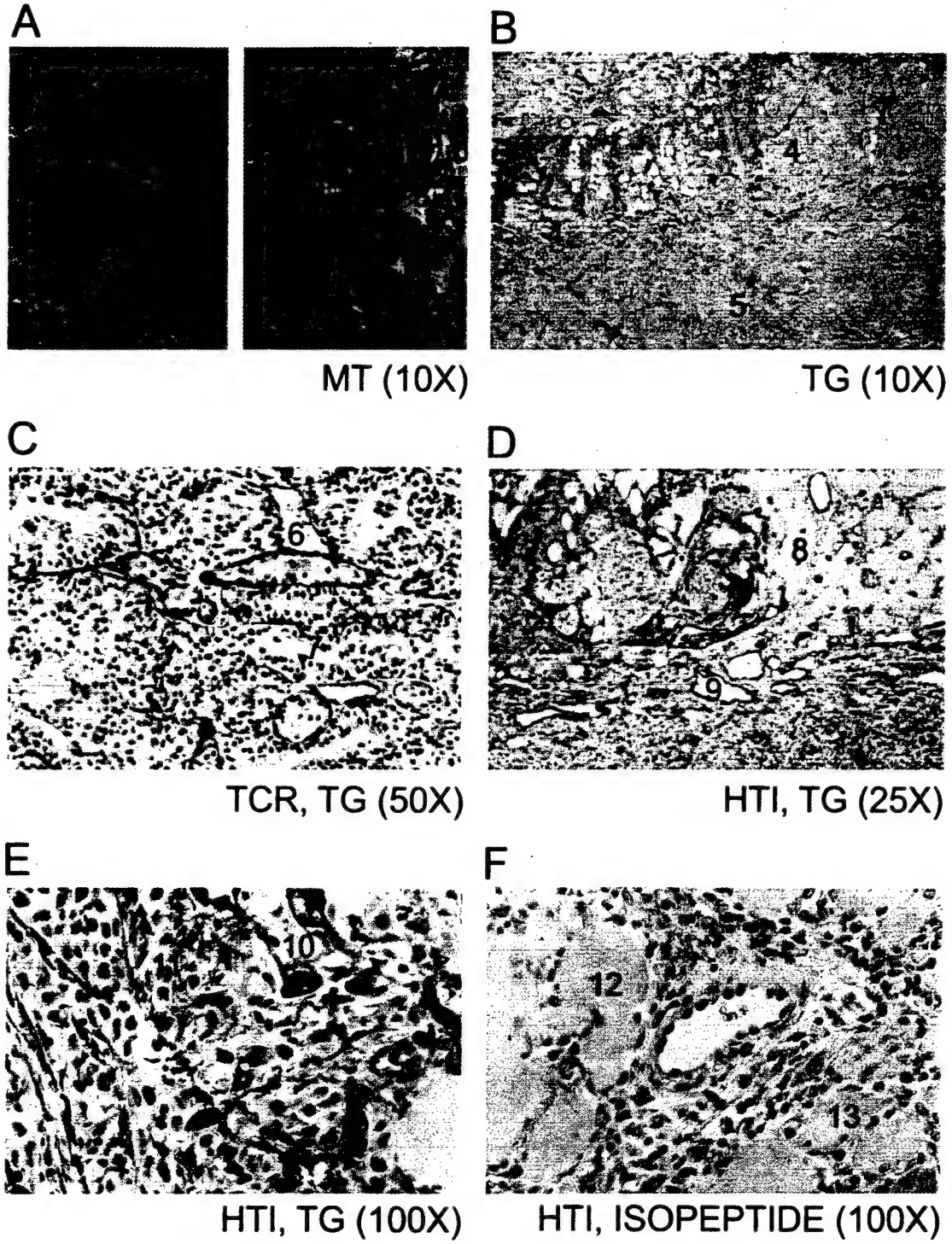

Figure 1.

Masson trichrome (*MT*) staining of the rat mammary adenocarcinoma R3230 Ac showing the basic histology and the two distinct regions of the tumor. A, Skeletal muscle cells (*A1*), blood vessels, macrophages, and collagen deposits (*A2*) can be observed in the host-tumor interface (*HTI*). In the tumor core region (*TCR*), glandular cell masses (*A3*) pack the interior of the tumor with some areas of necrosis. B, Tissue transglutaminase (*TG*) expression in the blood vessels and extracellular matrix (ECM) was intense in the HTI, forming a boundary between the tumor and host tissue (*B4*). In TCR, TG expression was markedly less, predominantly in blood vessels (*B5*). C, At higher magnification in TCR, TG could be seen in endothelial cells (*C6*) and also in the matrix between tumor islands. D and E, At higher magnifications in HTI, ECM (*D8* and *E11*), blood vessels (*D9*), and neovessels (*E10*) in the inflamed tissue exhibited TG expression. F, Isopeptide in HTI was detected in the basement membrane (*F12*) and ECM (*F13*).

of a stable ECM and modify tumor growth. The distribution of the TG antigen and isopeptide bonds in rat mammary tumor model and inhibition of tumor growth by administration of recombinant TG supports this hypothesis. TG seems to be a part of the host injury response machinery that works to inhibit growth of tumors by maintaining the integrity of the host tissues.

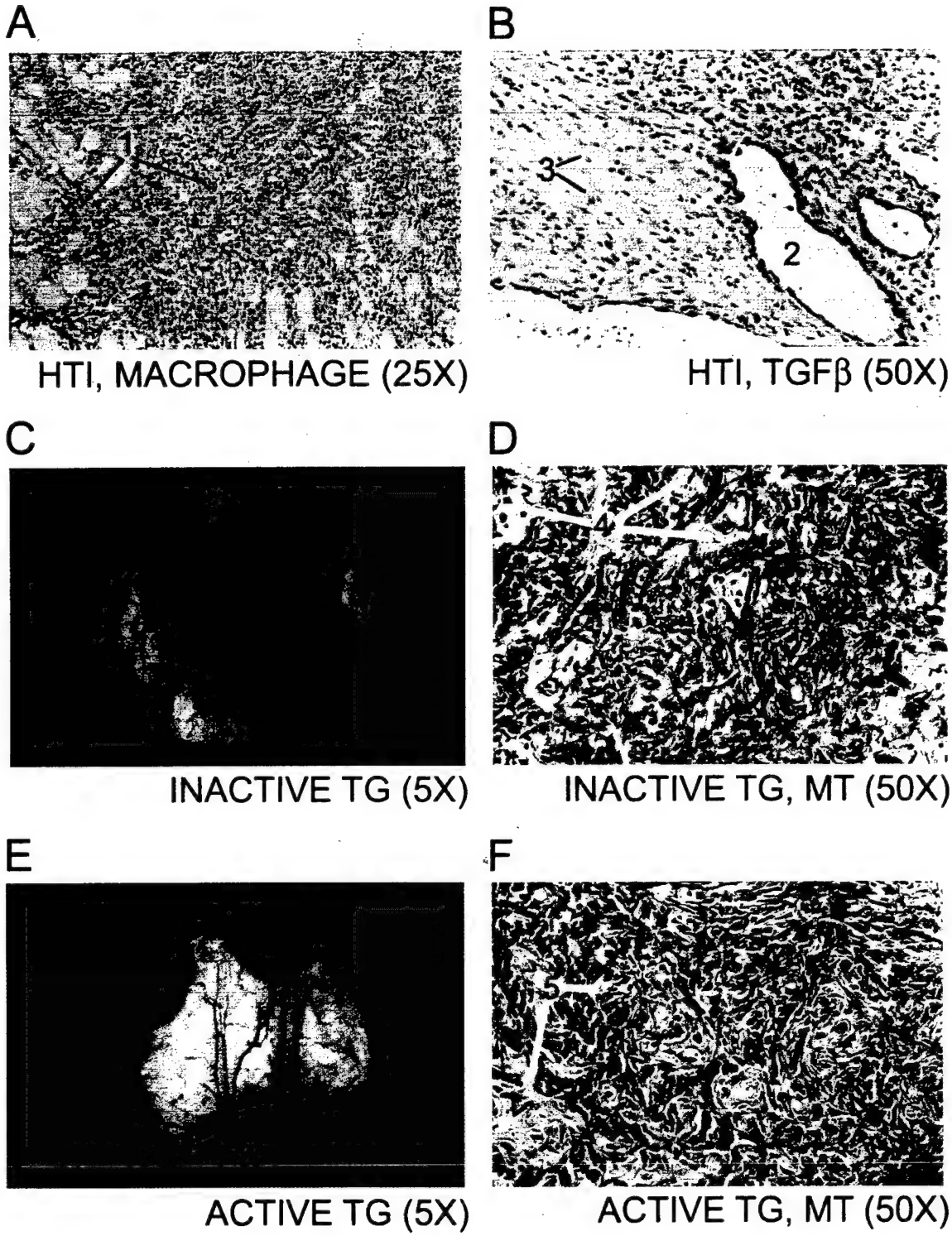

Figure 2.

A, Macrophage distribution (*A1*) was intense in HTI, being dispersed widely throughout the inflammatory interface. B, TGF-β was detected in the blood vessels (*B2*) and ECM (*B3*) in the HTI. C, A rat dorsal skin flap window chamber implanted with R3230 Ac and treated with recombinant inactive TG at day 10 (tumor boundary marked by *arrows*). D, Masson trichrome stain for this tumor showed little collagen deposition (*D4*, green strands) in the ECM. E, R3230 Ac implanted in window chamber and treated with recombinant active TG shows marked inhibition at day 10 after surgery. F, Increased amounts of collagen (*F5*) was detected by Masson trichrome in the ECM of TG-treated tumor.

TG can cross-link several major constituents of the ECM, including fibronectin (Martinez et al, 1994), collagen (Mosher and Schad, 1979), fibrin (Greenberg et al, 1987), fibrinogen (Martinez et al, 1989), vitronectin (Sane et al, 1988), and laminin/nidogen (Aeschlimann and Paulsson, 1991). TG can cross-link these matrix proteins with each other to form a protease-resistant barrier that would be a formidable obstacle to growth

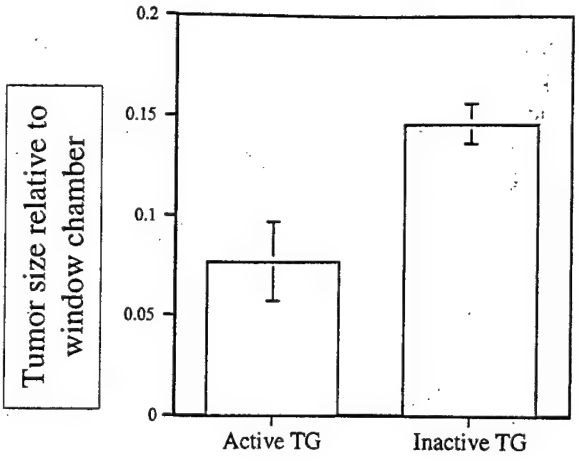

Figure 3.

A, Western blot of R3230 Ac tumor. Lane 1 shows the recombinant human TG at 80 kDa. Rat wild-type TG is shown at 75 kDa. Three fragmented forms of TG were detected at 55:50 and 20 kDa. B, Graphic representation of the cumulative data ($n = 4$) shows 55-kDa form as the dominant isoforms of TG, whereas full-length TG accounted for only 9% of the total protein.

of blood vessels and limit tumor progression as part of host response mechanism. We identified both expression and activity of TG in the matrix surrounding the tumor. However, despite the host response, tumor progression was not halted perhaps in part by the ability of the tumor to produce factors that inactivate the TG. The majority of the TG antigen in the tumor tissue was degraded, suggesting that tumor-associated proteases could cleave and inactivate the TG. TG when exposed to extracellular levels of calcium ions is protease sensitive and readily degraded by several serine proteases (Lai et al, 1998). The tumors' production of proteases may overwhelm the ability of TG to inhibit growth by cross-linking the host's ECM. That a single administration of recombinant TG to the tissue surrounding a tumor implanted in window chambers resulted in the enhanced production of ECM and an inhibition of tumor growth indicates that TG expression by the host has the ability to restrict tumor growth. However, the tumor seems to have a potent mechanism that can overwhelm the host response and allow the tumor to expand.

During malignant transformation, the acquisition of high protease activity by the tumor cells is essential for breakdown of basement membrane and matrix that accompany tumor cell migration, proliferation, expansion, and the development of a tumor blood supply that promotes metastasis (Benaud et al, 1998; Dano et al, 1999; Lochter et al, 1998). Antiproteases such as maspin were recognized recently as tumor suppressor genes in their ability to restrict the effectiveness of this proteolytic cascade (Sager et al, 1997). TG is known to cross-link antiproteases such as PAI-2 (Jensen et al, 1993) and Elafin (Nara et al, 1994) to ECM, making them readily available for interaction with proteases. The antitumor effect observed in tumor implanted window chambers could be due, in part, to the elevated antiprotease response mediated by TG.

We also observed a distinct fibrotic reaction in the tumors treated with TG and this could be due to the ability of the TG to enhance the rate of synthesis of ECM molecules. The cytokine TGF-β was identified as possessing distinct antitumor activity that may be due to its effect on the host production of a stable ECM (Clark and Coker, 1998; Taipale et al, 1998). TG in conjunction with urokinase plasminogen activator receptor, mannose-6-phosphate receptor and plasminogen can function at the cell surface to activate latent TGF-β (Kojima et al, 1993). The ability of TG to generate TGF-β imparts another mechanism that can assist the host's injury response system to limit tumor growth. TGF-β stimulates matrix production increases expression of tissue inhibitors of metalloproteinases and other protease inhibitors that would allow the newly synthesized matrix molecules to accumulate (Clark and Coker, 1998). The increased levels of collagen observed in the recombinant active TG treated indicate that TG can promote this reaction in the host tissues. We also detected the coexpression of the TG antigen and active TGF-β at sites within the TCR and HTI regions of the mammary tumor.

The ability of the tumor to overwhelm the host's ability to repair damaged tissues is essential for its survival (Dvorak, 1986; Nagy et al, 1989). In this study, we provide direct evidence that the induction of the TG gene occurs in response to the expanding tumor. Furthermore, the host tissues can use active TG to produce a stable ECM that restricts tumor expansion and limits angiogenesis. The TG-matrix–stabilizing mechanism has limited capacity, because the tumor tissues seem to degrade and inactivate TG by the expression of proteases. Future studies will investigate how overexpression of TG at sites of tumor growth can be enhanced to restrict the growth and metastasis of tumor cells.

Materials and Methods

Animal Protocols

The Duke Institutional Animal Care and Use Committee approved all animal protocols.

Tumor Implantation

Pieces (0.1 mm^3) of rat mammary adenocarcinoma R3230 Ac tumors (syngeneic) were surgically implanted in the subcutaneous tissue of the thigh from a donor rat. These tumors were grown to an average size of 1 cm^3 and then surgically removed from the rat. The tumor was cut in half, and the tissue was either snap frozen in liquid nitrogen for Western blots or fixed in 10% neutral buffered formalin and paraffin embedded for immunohistochemistry studies.

Window Chambers

Dorsal skin flap window chambers were used as described by Papenfuss (Papenfuss et al, 1979). Briefly, Fisher 344 rats were anesthetized, and the skin over the back was depilated and surgically prepared.

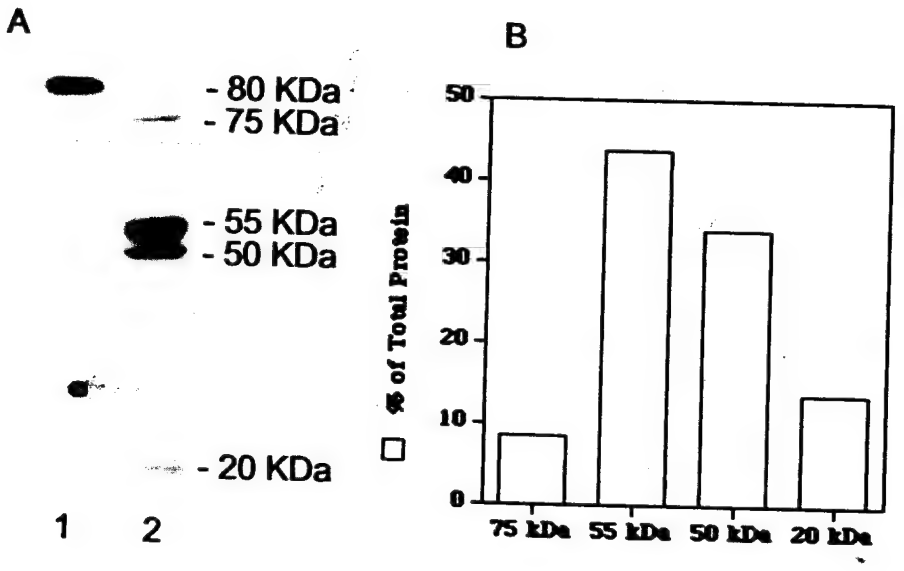

Figure 4.

Recombinant active TG-treated R3230 Ac tumors showed significant growth inhibition ($p = 0.04$, Student's two tail t test) against recombinant inactive TG-treated control cells at day 7. Error bars ± SEM, $n = 6$.

The skin flap was pulled dorsally away from the back. Two opposing 1-cm diameter windows were created on each side of the flap by surgically resecting the epidermis. One to two fascial planes were left, which contained a few preformed vessels. A 0.1-mm^3 piece of mammary adenocarcinoma (R3230 Ac) from a donor animal was transplanted near vessels with active flow. The resultant tissue window was protected by glass coverslips and held away from the body of the animal by an anodized aluminum superstructure. This device provided protection against desiccation and infection as the tumor grew. This tumor tissue window created a visual field through which the process of tumor growth could be observed noninvasively (Dewhirst et al, 19961999). A single dose of recombinant human TG (Lai et al, 1996) (0.5 ml of 39.0 μM solution) was applied topically on the day of surgery. Recombinant human inactive TG (mutation Cys277Ala) was used as a control. Rats were killed at day 10. Photographs were taken at days 0, 3, 7, and 10 after surgery to document the growth of the tumor implants. Quantitation of tumor growth was provided by measuring tumor size at the above mentioned time point. The tumor size was measured as a fraction of the window size through computer image analysis.

Immunohistochemistry

Immunohistochemistry was carried out by using procedures described by Hsu et al (Hsu et al, 1981). Briefly, paraffin-embedded tissues were sectioned (5 microns), and antigen retrieval was performed by using citrate buffer from Biogenex (San Ramon, California). Tissues were treated with primary antibody against tissue transglutaminase (TG100, 1:10, endothelial cell marker, nonreactive to factor XIIIa, unpublished data) (Neomarkers, Fremont, California), ED1-macrophage marker (MCA341, 1:100) (Serotec, Oxford, United Kingdom), isopeptide (814 MAM, 1:75, nonreactive to glutamine and lysine, (Roch et al, 1991) (CovalAB, Oullins, France), Panspecific TGF-β (AB-100-NA, 1:100, recognizes the active forms of TGF-β1, 2, and 5) (R&D, Minneapolis, Minnesota). Secondary and tertiary antibodies were provided in a kit (314KLD) (Innovex, Richmond, California), and the location of the reaction was visualized with 3,3′-diaminobenzidine tetrahydrochloride (Sigma, St. Louis, Missouri). Slides were counterstained with hematoxylin and mounted with coverslips. Controls for the immunohistochemistry were treated with normal mouse serum or mouse IgG and rabbit IgG and were negative in any reactivity. Masson trichrome staining was carried out as described by Sheehan and Hrapchak (Sheehan and Hrapchak, 1980).

Western Blot

Subcutaneous implanted tumors were homogenized in 2 ml of cold lysis buffer containing the proteolytic inhibitor cocktail 1697498 (Boehringer-Mannheim, Mannheim, Germany) followed by sonification. The blots were performed with four different tumor tissues. They were then centrifuged, supernatant was removed, and protein content was determined according to manufacturer's instructions (Bradford Reagent, Bio-Rad, Hercules, California). Gel electrophoresis of the extracted tissue samples (50 μg/ml) was performed on an 8.5% polyacrylamide gel by using the buffer system of Laemmeli. After electrophoresis, the proteins were transferred to nitrocellulose (0.2 μm). After the transfer was complete, the nitrocellulose membrane was blocked for 1 hour with 5% nonfat milk dissolved in 20 mM Tris-HCl, pH 7.4, 150 mM NaCl, 0.5% Tween 20. The TG antigen was detected by incubation for 1 hour by using a monoclonal antibody for TG (TG 100, CUB 7402, Neomarkers) diluted

1:1000, followed by incubation for 1 hour with sheep anti-mouse IgG conjugated to horseradish peroxidase. The TG antigen was visualized by using chemiluminescence reagents (ECL, Amersham Corp., Arlington Heights, Illinois) and a 30-second exposure to autoradiography film. The amount of protein on the blot was estimated with a densitometer. The data in Figure 3A shows one sample blot, and Figure 3B has the cumulative data for the four blots in a graphical presentation.

References

Aeschlimann D and Paulsson M (1991). Cross-linking of laminin-nidogen complexes by tissue transglutaminase. A novel mechanism for basement membrane stabilization. J Biol Chem 266:15308–15317.

Aeschlimann D, Mosher D, and Paulsson M (1996). Tissue transglutaminase and factor XIII in cartilage and bone remodeling. Semin Thromb Hemost 22:437–443.

Benaud C, Dickson RB, and Thompson EW (1998). Roles of the matrix metalloproteinases in mammary gland development and cancer. Breast Cancer Res Treat 50:97–116.

Bowness JM and Tarr AH (1997). Increase in transglutaminase and its extracellular products in response to an inflammatory stimulus by lipopolysaccharide. Mol Cell Biochem 169:157–163.

Bowness JM, Tarr AH, and Wong T (1988). Increased transglutaminase activity during skin wound healing in rats. Biochim Biophys Acta 967:234–240.

Brown LF, Dvorak AM, and Dvorak HF (1989). Leaky vessels, fibrin deposition, and fibrosis: A sequence of events common to solid tumors and to many other types of disease. Am Rev Respir Dis 140:1104–1107.

Clark DA and Coker R (1998). Transforming growth factor-beta (TGF-beta). Int J Biochem Cell Biol 30:293–298.

Dano K, Romer J, Nielsen BS, Bjorn S, Pyke C, Rygaard J, and Lund LR (1999). Cancer invasion and tissue remodeling: Cooperation of protease systems and cell types. APMIS 107:120–127.

Dewhirst MW, Ong ET, Braun RD, Smith B, Klitzman B, Evans SM, and Wilson D (1999). Quantification of longitudinal tissue pO_2 gradients in window chamber tumours: Impact on tumour hypoxia. Br J Cancer 79:1717–1722.

Dewhirst MW, Ong ET, Rosner GL, Rehmus SW, Shan S, Braun RD, Brizel DM, and Secomb TW (1996). Arteriolar oxygenation in tumour and subcutaneous arterioles: Effects of inspired air oxygen content. Br J Cancer Suppl 27:S241–S246.

Dvorak HF (1986). Tumors: Wounds that do not heal. Similarities between tumor stroma generation and wound healing. N Engl J Med 315:1650–1659.

Gentile V, Thomazy V, Piacentini M, Fesus L, and Davies PJ (1992). Expression of tissue transglutaminase in Balb-C 3T3 fibroblasts: Effects on cellular morphology and adhesion. J Cell Biol 119:463–474.

Greenberg CS, Achyuthan KE, Borowitz MJ, and Shuman MA (1987). The transglutaminase in vascular cells and tissues could provide an alternate pathway for fibrin stabilization. Blood 70:702–709.

Greenberg CS, Birckbichler PJ, and Rice RH (1991). Transglutaminases: Multifunctional cross-linking enzymes that stabilize tissues. FASEB J 5:3071–3077.

Hettasch JM, Bandarenko N, Burchette JL, Lai TS, Marks JR, Haroon ZA, Peters K, Dewhirst MW, Iglehart JD, and Greenberg CS (1996). Tissue transglutaminase expression in human breast cancer. Lab Invest 75:637–645.

Horton MA (1995). Interactions of connective tissue cells with the extracellular matrix. Bone 17:51S–53S.

Hsu SM, Raine L, and Fanger H (1981). Use of avidin-biotin-peroxidase complex (ABC) in immunoperoxidase techniques: A comparison between ABC and unlabeled antibody (PAP) procedures. J Histochem Cytochem 29:577–580.

Jensen PH, Lorand L, Ebbesen P, and Gliemann J (1993). Type-2 plasminogen-activator inhibitor is a substrate for trophoblast transglutaminase and factor XIIIa. Transglutaminase-catalyzed cross-linking to cellular and extracellular structures. Eur J Biochem 214:141–146.

Kojima S, Nara K, and Rifkin DB (1993). Requirement for transglutaminase in the activation of latent transforming growth factor-beta in bovine endothelial cells. J Cell Biol 121:439–448.

Lai TS, Slaughter TF, Koropchak CM, Haroon ZA, and Greenberg CS (1996). C-terminal deletion of human tissue transglutaminase enhances magnesium-dependent GTP/ATPase activity. J Biol Chem 271:31191–31195.

Lai TS, Slaughter TF, Peoples KA, Hettasch JM, and Greenberg CS (1998). Regulation of human tissue transglutaminase function by magnesium-nucleotide complexes. Identification of distinct binding sites for Mg-GTP and Mg-ATP. J Biol Chem 273:1776–1781.

Lochter A, Sternlicht MD, Werb Z, and Bissell MJ (1998). The significance of matrix metalloproteinases during early stages of tumor progression. Ann N Y Acad Sci 857:180–193.

Lukashev ME and Werb Z (1998). ECM signalling: Orchestrating cell behaviour and misbehaviour. Trends Cell Biol 8:437–441.

Martinez J, Rich E, and Barsigian C (1989). Transglutaminase-mediated cross-linking of fibrinogen by human umbilical vein endothelial cells. J Biol Chem 264: 20502–20508.

Martinez J, Chalupowicz DG, Roush RK, Sheth A, and Barsigian C (1994). Transglutaminase-mediated processing of fibronectin by endothelial cell monolayers. Biochemistry 33:2538–2545.

Mosher DF and Schad PE (1979). Cross-linking of fibronectin to collagen by blood coagulation Factor XIIIa. J Clin Invest 64:781–787.

Nagy JA, Brown LF, Senger DR, Lanir N, Van de Water L, Dvorak AM, and Dvorak HF (1989). Pathogenesis of tumor stroma generation: A critical role for leaky blood vessels and fibrin deposition. Biochim Biophys Acta 948:305–326.

Nara K, Ito S, Ito T, Suzuki Y, Ghoneim MA, Tachibana S, and Hirose S (1994). Elastase inhibitor elafin is a new type of proteinase inhibitor which has a transglutaminase-mediated anchoring sequence termed "cementoin." J Biochem (Tokyo) 115:441–448.

Papenfuss HD, Gross JF, Intaglietta M, and Treese FA (1979). A transparent access chamber for the rat dorsal skin fold. Microvasc Res 18:311–318.

Pepper MS (1997). Transforming growth factor-beta: Vasculogenesis, angiogenesis, and vessel wall integrity. Cytokine Growth Factor Rev 8:21–43.

Pepper MS, Montesano R, Mandriota SJ, Orci L, and Vassalli JD (1996). Angiogenesis: A paradigm for balanced extracellular proteolysis during cell migration and morphogenesis. Enzyme Protein 49:138–162.

Roch A, Noel P, El-Aloui S, Charlot C, and Quash G (1991). Differential expression of isopeptide bonds Nε (γ glutamyl) lysine in benign and malignant breast lesions: An immunohistochemical study. Int J Cancer 48:215–220.

Sager R, Sheng S, Pemberton P, and Hendrix MJ (1997). Maspin. A tumor suppressing serpin. Adv Exp Med Biol 425:77–88.

Sane DC, Moser TL, Pippen AM, Parker CJ, Achyuthan KE, and Greenberg CS (1988). Vitronectin is a substrate for transglutaminases. Biochem Biophys Res Commun 157: 115–120.

Senger DR, Brown LF, Claffey KP, and Dvorak HF (1994). Vascular permeability factor, tumor angiogenesis and stroma generation. Invasion Metastasis 14:385–394.

Sheehan D and Hrapchak B (1980). Theory and practice of histotechnology, 2nd ed. Columbus, OH: Battelle Press.

Tabor E (1997). Liver tumors and host defense. Semin Liver Dis 17:351–355.

Taipale J and Keski-Oja J (1997). Growth factors in the extracellular matrix. FASEB J 11:51–59.

Taipale J, Saharinen J, and Keski-Oja J (1998). Extracellular matrix-associated transforming growth factor-beta: Role in cancer cell growth and invasion. Adv Cancer Res 75:87–134.

Takahashi N, Takahashi Y, and Putnam FW (1986). Primary structure of blood coagulation factor XIIIa (fibrinoligase, transglutaminase) from human placenta. Proc Natl Acad Sci U S A 83:8019–8023.

Weinberg JB, Pippen AM, and Greenberg CS (1991). Extravascular fibrin formation and dissolution in synovial tissue of patients with osteoarthritis and rheumatoid arthritis. Arthritis Rheum 34:996–1005.

Werb Z, Vu TH, Rinkenberger JL, and Coussens LM (1999). Matrix-degrading proteases and angiogenesis during development and tumor formation. APMIS 107:11–18.

Wernert N (1997). The multiple roles of tumour stroma. Virchows Arch 430:433–443.

APPENDIX 05

TG Transfected 4T1 Mammary Carcinoma Shows Paradoxical Effects on Metastasis Depending on Site of Implantation

(This study is still in progress and we hope to finalize it in December and would forward the manuscript for DOD record)

Earlier work involving TG transfection in tumor cell lines have showed that TG transfected tumor cell lines growth inhibition (1). It has also been reported that the amount of TG expression in tumor cell lines is inversely proportional to their metastatic potential. Our goal was to assess the effect of TG transfection on metastasis and tumor growth in a highly metastatic mammary carcinoma cell line at different transplantation sites.

Methods:

Transplantations: Nude mice were given a tail vein (Intravenous IV) injection of 10^5 cells transfected with either GFP-TG or GFP alone as control. The mice were sacrificed when they showed physical signs of distress/tumor load i.e. $\geq$ 20% weight loss, labored breathing and slow activity. For ectopic transplantation, 10^6 cells transfected with GFP-TG or GFP alone were first mixed in matrigel and then transplanted in the subcutaneous fascia in the hind leg. Mice were sacrificed every week to follow the process of tumor growth and metastasis at the histological level also. Tumors size was measured on a weekly basis. In all experiments, lung and tumor tissue was preserved for immunohistochemical analysis.

Transfections: Prepare cells, 50-80% full (0.1-0.5 million cells per well 24 hours before transfection). Prepare reagent A in tube 1, TG Plasmid DNA-1-3ug, OPTI-MEM-100ul.

Prepare reagent B in tube 2, LIPOFECTAMINE-10ul, OPTI-MEM-100ul. Combine B with A in tube 1, mix gently. Incubate for about 1 hour at room temperature. When mixture A+B is ready, rinse cells once with PBS, then twice with OPTI-MEM. Add 0.8ml OPTI-MEM in tube 1, mix gently. Add the whole mixture (A+B+OPTI-MEM) into 35mm-well and cover the cells evenly. Incubate in normal condition for 5-10 hours. In time, add 1ml OPTI-MEM and 200ul FBS per well. Incubate in normal condition for 12-24 hours. Replace medium with fresh complete growth medium (10% FBS, 1%Antibiotic) and add G418.

Results and Discussion:

Tail-vein (IV) Injections: GFP-TG transfected 4T1 cells showed enhanced metastasis as compared to GFP alone. On gross examination, the GFP-TG lungs appeared riddled with mets as compared to GFP alone. The lifetime of the GFP-TG mice was also reduced to more than 60% as compared to GFP alone mice since almost all the GFP-TG mice died at week 2 and GFP alone were doing well at week 3 post injection. On histological examination, GFP-TG mets more numerous and seemed to creep along the septa of the lung and give a matted appearance.

Ectopic Transplantation: GFP-TG tumors grew at a much slower pace than GFP alone. They also exhibited intense central necrosis and only the outer margin had live tumor cells. GFP-TG tumors grew in perfect spheres as compared to multiple tumor masses in case of GFP alone. On an average, tumor size of GFP alone was 3-4 times larger than GFP-TG. GFP tumors developed mets by week 2 and all of the animals died by week 3. On the other hand, GFP-TG bearing mice were alive at week 4 and there were very few mets in the lungs of these animals.

This pattern of these results may seem paradoxical at first but is perhaps due to a similar mechanism of action. TG transfected cells have been shown to have a high degree of adhesiveness and they also spread very effectively (2, 3). This property can impart positive attribute for the metastasizing cells since the most difficult part of metastasis is attachment at distant sites. Any cell which has advantage here will be better adapted to grow. Meanwhile, this enhanced adhesiveness can cause a primary tumor mass to grow in a tightly packed manner that makes the first part of metastasis very difficult i.e. detachment and access to blood vessels. The idea of these tumors growing in a tight sphere which is highly crosslinked is further promoted by the fact that these tumor show extensive necrosis in the middle which may be due to the intense pressure imposed by such a structure.

Thus, it seems that TG's ability to cross link major ECM and cell membrane proteins can have diverse effects on tumor growth and metastasis. TG expression in primary tumor seems to limit the growth and metastasis potential of the tumors. On the other hand, mets with high expression of TG seem to have a distinct advantage in metastasis.

1. Johnson, T. S., C. R. Knight, S. el-Alaoui, S. Mian, R. C. Rees, V. Gentile, P. J. Davies, and M. Griffin. (1994). Transfection of tissue transglutaminase into a highly malignant hamster fibrosarcoma leads to a reduced incidence of primary tumour growth. Oncogene. 9 (10):2935-42.

2. Gentile, V., V. Thomazy, M. Piacentini, L. Fesus, and P. J. Davies. (1992). Expression of tissue transglutaminase in Balb-C 3T3 fibroblasts: effects on cellular morphology and adhesion. J Cell Biol. 119 (2):463-74.

3. Zirvi, K. A., J. P. Keogh, A. Slomiany, and B. L. Slomiany. (1993). Effects of exogenous transglutaminase on spreading of human colorectal carcinoma cells. Cancer Biochem Biophys. 13 (4):283-94.

APPENDIX 06

1 Angiogenesis and Oxygen Transport in Solid Tumors

Zishan A. Haroon, Kevin G. Peters, Charles S. Greenberg, and Mark W. Dewhirst

CONTENTS

1. INTRODUCTION

Angiogenesis, the formation of new vessels from existing microvasculature, is a tremendously complex and intricate process, essential for embryogenesis and development of multicellular organisms *(1)*, but it occurs only rarely in adult tissues in a tightly controlled manner during normal wound healing and the female reproductive cycle (corpus luteum, placenta, and uterus) *(2)*. When these tight controls are breached, the result is unchecked angiogenesis, which has been implicated in the development and progression of a variety of diseases (Table 1). The prevalence of pathologic angiogenesis in human diseases, and the significant mortality associated with these disorders, underscore the importance and emergence of antiangiogenesis therapy as a major clinical tool. In the case of solid malignancies, the generation of proangiogenic substances is in part caused by the pathologic microenvironment that develops in response to uncoordinated vascular production.

A common consequence of the abnormal microvascular structure and function that exist in tumors is hypoxia, which is known to induce a number of factors involved in regulating angiogenesis. Thus, hypoxia may prove to be a common initial signal for tumor vessel formation. There are other microenvironmental factors that may also play a role in the process as well, including endogenous levels of nitric oxide (NO). This chapter presents an overview of the features of normal and pathologic angiogenesis, with an emphasis on the role of hypoxia and dysfunctional vasculature during the angiogenic process in tumors.

From: *Antiangiogenic Agents in Cancer Therapy*
Edited by: B. A. Teicher © Humana Press Inc., Totowa, NJ

Table 1
List of Major Diseases in Which Angiogenesis Plays a Role in Pathogenesis

Inflammatory diseases:
Arthritis, chronic inflammations, inflammatory bowel diseases, psoriasis
Neoplasms:
Breast, bladder, colon, glioblastoma, hemangioblastoma, lung, melanoma, neuroblastoma, pancreas, renal, uterine–cervix
Ocular diseases:
Age-related macular degeneration, proliferative retinopathy (diabetic)

2. NORMAL ANGIOGENESIS

Normal angiogenesis is a multistep, tightly orchestrated process that occurs predominantly during physiologic events involving tissue repair and/or remodeling (wound healing, placental development, and so on) *(3)*. Tissue repair and remodeling involves continuous feedback and interaction between endothelial cells and the extracellular matrix (ECM) in a process that has been termed "dynamic reciprocity" by Clark *(4)*. Similarly, vascular remodeling is accomplished by targeted apoptosis and proliferation, deposition of matrix and its stabilization, and organization by enzymatic crosslinking and proteolysis.

Normal angiogenesis involves an initial localized breakdown of the basement membrane in the parent vessel that is mediated by proteases *(3,5*; Fig. 1]. Endothelial cells then migrate into the perivascular space and adjoining matrix, and form a capillary sprout. These sprouts elongate by further endothelial migration at the tip, and proliferation at the base, to replace the migrated cells. Subsequently, remodeling occurs, and these cords anastamose to form a loop, basement membrane is laid out, and a patent vessel is formed.

2.1. Molecular Mediators of Angiogenesis

Although many angiogenic substances have been identified, polypeptide growth factors, such as fibroblast growth factor (FGF), vascular endothelial growth factor (VEGF), and platelet-derived growth factor (PDGF) seem to be the most potent ones (Table 2). It is interesting to note that the aforementioned growth factors signal through receptor tyrosine kinases *(6)*. VEGF, also known as vascular permeability factor, is a multifunctional cytokine that is upregulated in response to hypoxia, and is considered one of the most potent proangiogenic molecules *(7)*.

Apart from activating endothelial cells to proliferate and express matrix metalloproteinases, plasminogen activators, and tissue factor, the most prominent effect of VEGF is induction of vascular hyperpermeability. It has been consistently observed that hyperpermeability to plasma proteins is associated with both pathological and physiological angiogenesis *(8)*. This association may have two very important implications for angiogenesis: First, it leads to the formation of a provisional fibrin matrix, which provides the primary scaffold for assembly of elements necessary for neovascularization *(8)*. The provisional fibrin matrix probably provides a more fluid matrix that is supportive of the angiogenic process. Second, another suggestion for hyperpermeability's role in angiogenesis has been proposed by Folkman *(9)*, which relates to the observation that confluent endothelial cells are refractory to mitogenic stimuli. The vasodilation and hyperpermeability that precede angiogenesis may subject endothelial cells to stretch and decrease confluence, which increases reactivity to proangiogenic mitogens.

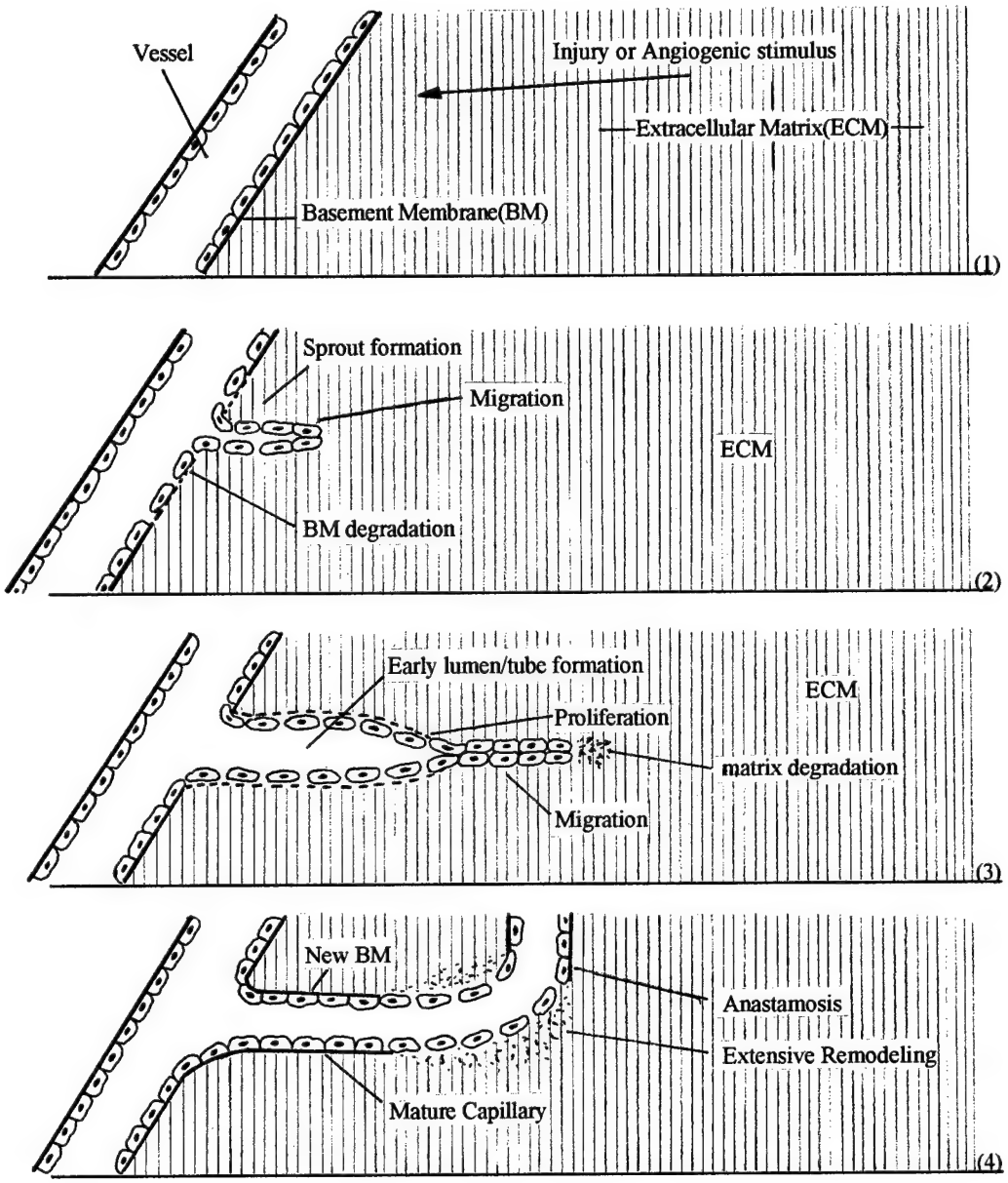

Fig. 1. A general mechanism of normal angiogenesis process. (1) Injury or tissue repair activates the endothelial cells. (2) Results in basement membrane degradation by proteases, and initial sprout formation by migration of endothelial cells. (3) Endothelial cells continue to migrate at the tip, with controlled matrix degradation. Proliferation occurs proximal to migration with formation of the primitive tube. (4) Extensive remodeling occurs all along the new capillary; new basement membrane is laid out to form a mature capillary as it anastamoses with other sprouts.

Normal angiogenesis involves complex interactions among endothelial cells, inflammatory cells, and ECM. These precisely controlled interactions involve ECM proteolysis during basement membrane degradation, invasion of the provisional fibrin matrix, and remodeling of the matrix and vessels *(10)*. These proteolytic activities also activate and/

Table 2
Prominent Molecules That Have Been Shown to Possess Proangiogenic Properties

Angiogenin
Fibroblast growth factors (acidic and basic)
Heparin
Hepatocyte growth factor (scatter factor)
Insulin-like growth factors
Interleukin-8
Platelet-activating factor
Platelet-derived endothelial cell growth factor
Platelet derived growth factor-BB
Transforming growth factor-α
Transforming growth factor-β
Tumor necrosis factor-α
Vascular endothelial growth factor

Table 3
Role of Balanced Proteolysis in Angiogenesis

Migratory path formation and remodeling:
Basement membrane degradation
Controlled ECM degradation involved during migration/invasion of endothelial and inflammatory cells into matrix
Anastamoses and capillary lumen/tube formation
Release of cytokines:
Release of bound basic FGF and VEGF
Activation of TGF-β from latent to active form
Degradation products with angiogenesis modulating capability:
Angiostatin (plasminogen)
Collagen derived peptides
Endostatin (collagen XVIII)
Fibrin and fibronectin fragments
16-kDa fragment of prolactin

or release important angiogenic cytokines, such as transforming growth factor-β (TGF-β), VEGF, and basic fibroblast growth factor (bFGF) *(11)*. In addition, biologically active degradation products of ECM, such as angiostatin from plasminogen, are generated, which regulate angiogenesis *(12)*. A balance of proteases and antiproteases, in a tightly regulated temporospatial pattern, is required for proper neovessel formation and remodeling/maturation (Table 3). Cytokines that regulate proteolytic activity during normal angiogenesis include bFGF, VEGF, TGF-β, hepatocyte growth factor (HGF), tumor necrosis factor-α (TNF-α), and interleukin-1 (IL-1) *(13)*.

Although endothelial cells provide the foundation for neovasculature, angiogenesis also involves complex interactions with fibroblasts and inflammatory cells, such as macrophages and mast cells. The role these inflammatory cells play during angiogenesis is further strengthened by the fact that many proinflammatory cytokines, such as interleukin-8 (IL-8) and TNF-α, induce angiogenesis *(14,15)*. Macrophages *(16)* and mast cells *(17)*

are involved during induction and propagation of the angiogenic cascade, and mediate their effects through secretion of cytokines and growth factors (including VEGF), release of proteases, and activation of fibroblasts. Fibroblasts are chiefly responsible for production of ECM and release of matrix metalloproteinases (MMPs) for selective degradation and organization of the ECM *(4)*.

Migration of endothelial and inflammatory cells forms an indispensable part of the angiogenic cascade. Migration is a multistep process that begins with a strong directional stimulus to migrate, and is followed by coordinate expression of receptors and matrix molecules to facilitate movement. TGF-β, VEGF, bFGF, and PDGF provide the chemotactic signals *(18)*, and chemokines provide chemokinetic signals *(14)* for both inflammatory and endothelial cells in induction of angiogenesis. The best-characterized receptors that are involved in migration during angiogenesis are integrins β_1, $\alpha_v\beta_3$, and $\alpha_v\beta_5$ *(19)*. Although the evidence is still sketchy, it is becoming apparent that particular integrins are upregulated, and are required for the angiogenic effects of specific cytokines, such as $\alpha_v\beta_3$ for bFGF and $\alpha_v\beta_5$ for VEGF *(20)*.

The final steps in physiologic angiogenesis include transforming loosely associated endothelial cells and ECM into mature and patent vessels with intact basement membranes. Current evidence suggests that vessel maturation may be driven by novel molecular mediators, such as angiopoietins and their Tie family of receptors.

Angiopoietin-1 and -2 have recently been described as ligands for an endothelial-cell-specific tyrosine kinase receptor, Tie-2 *(21)*. Tie 2 receptors are essential for embryonic angiogenesis, since knock-outs of this receptor are embryonic lethal, with profound defects in assembly of microvessels, and it is proposed that the activity of the Tie-2 receptor is located downstream from VEGF on the angiogenic cascade *(22)*. The presence of the Tie-2 receptor on endothelial cells during angiogenesis in a variety of settings *(23)*, combined with evidence for constitutive angiopoietin 1 expression by vascular smooth muscle cells and/or pericytes, suggest that they may be involved in a regulated feedback system to modulate and steer the vessel maturation and organization process *(21)*. Meanwhile, angiopoietin-2 acts as a natural antagonist to Angiopoietin-1 and Tie-2, to provide a critical balance during induction of angiogenesis, vascular remodeling, and maturation *(21)*. Thus, angiopoietins and Tie-2 demonstrate a complex and intertwined relationship among themselves and their environment, and also exhibit the ability to regulate the angiogenic process.

3. TUMOR ANGIOGENESIS

Although developmental (embryonic) and disease-associated (pathologic) angiogenesis share many mechanistic features, as first suggested by Haddow *(24)* and later by Dvorak *(25)*, they probably differ regarding to regulatory controls *(26)*. As described above, tissue repair is normally a self-limiting process that occurs in response to hypoxia generated at the site of tissue injury. In contrast, progressive tumor growth creates ongoing hypoxia and acidosis, which do not recede as they would after injury (Fig. 2). Moreover, tumor vessels fail to mature into a normally functioning vasculature. In this manner, a positive feedback loop is created as continued tumor proliferation, handicapped by a disorganized vasculature, again outstrips its supply, which leads to continuing hypoxemia and angiogenesis (Fig. 3).

It is of interest to note that production of several of the proangiogenic compounds are regulated by hypoxia, including VEGF, bFGF, TGF-β, TNF-α, and IL-8 (Table 4).

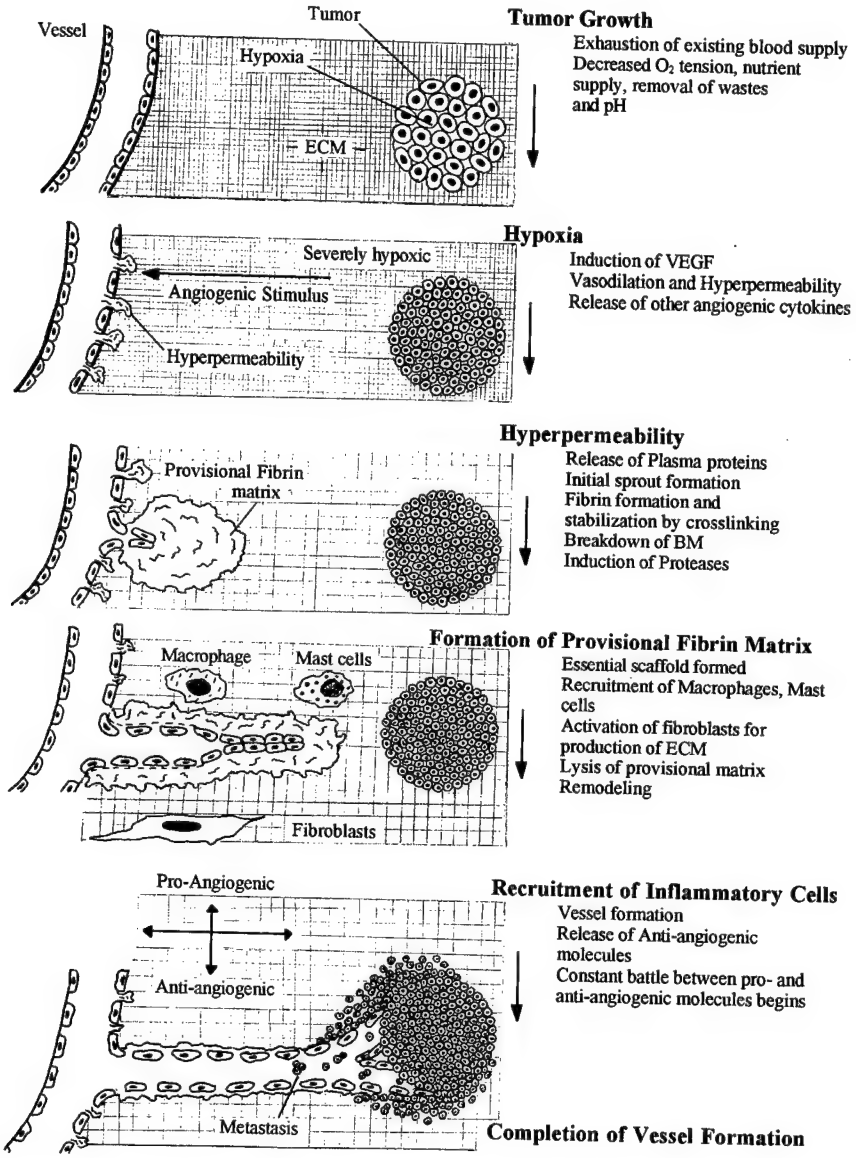

Fig. 2. A flow chart showing the current understanding of the process of tumor angiogenesis.

Furthermore, the presence of tumor hypoxia has been tied to more aggressive phenotypes in murine tumor models, as well as in human tumors. For example, in human cervix cancer and soft tissue sarcomas, presence of hypoxia prior to the start of therapy has been tied to a greater likelihood for distant metastases *(36,37)*. Additionally, the presence of tumor regions with high vascular density predicts for poorer overall survival in carcinoma of the breast, and in prostate cancer *(38)*. Taken together, these data strongly suggest that hypoxia upregulates angiogenesis, which in turn provides vascular access for metastasis.

Oncogenic transformations of tumor cells may also play a direct role in induction and propagation of angiogenesis, through production of angiogenic factors. It has been shown

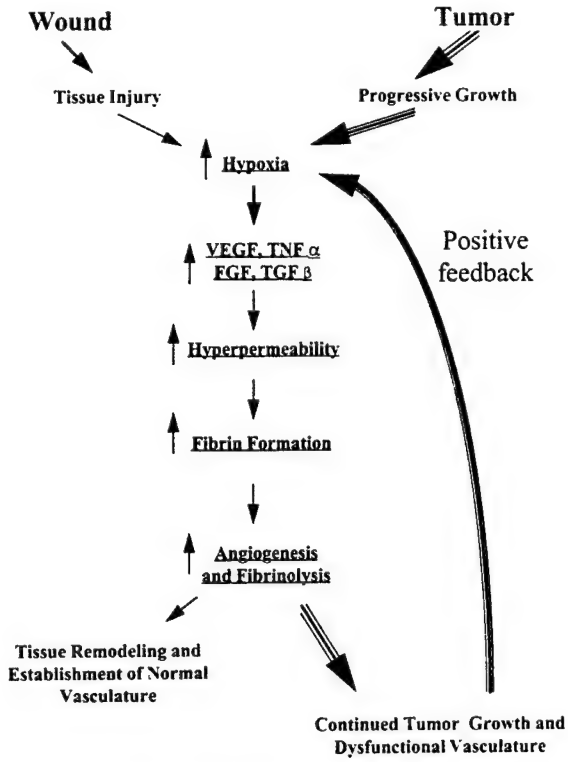

Fig. 3. Both normal tissue repair/remodeling mechanisms (wound healing) and tumors share common pathways to stimulate angiogenesis. Tissue repair, being a self-limited process, leads to regeneration of normal vasculature; tumor-induced angiogenesis produces a dysfunctional vasculature, which, coupled with progressive growth of tumor cells, results in continuing hypoxemia and angiogenesis.

Table 4
List of Proangiogenic Cytokines and Receptors Whose Expression Is Modulated by Hypoxia

Cytokine or receptor	*Hypoxia level*		*Gene expression*
	PO_2	*Time*	
Angiopoietin 1	NS	18 h	↓ *(27)*
aFGF, bFGF	2.0%	24 h	↑ *(28)*
Flk-1/KDR	2.0/2.0%	24/24 h	↓/↑ *(29[a],30[b])*
Flt-1	2.0%	24 h	↑ *(30)*
Interleukin-8	2.0%	24 h	↑ *(31)*
PDGF-A, PDGF-B	1.0%	16 h	↑ *(32)*
TGF-β	0.0%	24 h	↑ *(33)*
TNF-α	1.0%	24 h	↑ *(34)*
VEGF	1.0%	06 h	↑ *(35)*

↑, increase, ↓, decrease, NS, not specified.
*a*Reoxygenation performed in the experiments.
*b*Conflicting data has been reported in the papers.

Table 5
Short List of Molecules That Exhibit Potent Antiangiogenesis Activity

Angiostatin
Endostatin
Interferon-α
Metalloproteinase inhibitors
Platelet factor 4
Somatostatin
Thrombospondin

that VEGF expression is induced by mutant H- or K-*ras* oncogenes, as well as v-*src* and v-*raf,* in transformed fibroblasts and epithelial cells *(39)*. Other angiogenic growth factors, such as TGF-β and TGF–α, have also been shown to be upregulated by mutant ras *(39)*. These effects may be mediated through a ras-raf-MAP kinase signal transduction pathway, which results in activation of promoter regions of genes of angiogenic growth factors. Several of these proangiogenic cytokines have been shown to be produced by the same tumor *(40)*. This evidence points to a potential pitfall in approaching antiangiogenesis therapy directed against a singular angiogenic cytokine.

Aggressive neovascularization also leads to production and generation of numerous antiangiogenic compounds (Table 5). These substances are vital in regulating the process of angiogenesis, and are discussed in detail in later chapters.

4. TUMOR PATHOPHYSIOLOGY LEADING TO HYPOXIA

It is generally believed that hypoxia in tumors develops in two ways. The first form, referred to as chronic hypoxia, has classically been thought to result from long diffusion distances between tumor vessels *(41)*. The second form, known as perfusion limited, or acute, hypoxia, has been attributed to transient blockages in, or collapse of, tumor vessels *(42)*. This chapter will distinguish between these two forms of hypoxia in the following manner: Cells that are chronically hypoxic exist in an environment where the PO_2 is <10 mmHg for many hours at a time. Such cells may never experience a normoxic condition once they become hypoxic. Cells that are acutely hypoxic exist in an environment where the PO_2 is <10 mmHg for many minutes at a time. These cells probably experience many cycles of hypoxia and reoxygenation. Mechanistic understanding of the relative importance of the factors leading to both forms of hypoxia may lead to additional lines of investigation regarding microenvironmental control of gene expression in tumors.

4.1. Origins of Chronic Hypoxia

The balance between how much oxygen is delivered and how much is consumed leads to the oxygen concentration that is found in tissue. Several factors contribute to the development of chronic hypoxia, including longitudinal gradients of PO_2, irregular vascular geometry and low vascular density, altered blood viscosity, and oxygen consumption that is out of balance with supply. Of these factors, oxygen consumption has the most dynamic effect on tissue PO_2.

4.1.1. Deficiencies in Tumor Oxygen Supply Longitudinal Gradients

It is now well recognized that tumor microvessels can be hypoxic, even when there is movement of red cells through the vessel *(43,44)*. The most likely origin of intravascular hypoxia comes from longitudinal or axial gradients in oxygen tension, which are defined as declines in oxygen tension along the vascular tree. Two features of longitudinal gradients lead to intravascular hypoxia in tumors. First, tumor-feeding arterioles are more deoxygenated than comparable arterioles in normal tissues. Dewhirst et al. *(45)* reported that the PO_2 of tumor-feeding arterioles averaged 60% that of comparable arterioles of normal granulating tissues, yielding an average PO_2 of 32 mmHg, when aortic blood gas PO_2 averaged near 100 mmHg. The relative deoxygenation of these arterioles is probably caused by one or more factors: tissue pH—there is a right shift of the hemoglobin saturation curve as the arteriole enters a region of tissue acidosis (a typical condition in tumors); higher oxygen consumption—it is likely that the arterioles pass through a region of high cell proliferation, where the oxygen consumption rate may be very high. It is well established that longitudinal gradients occur in normal tissues as well, but such conditions do not normally lead to vascular hypoxia, probably because of the normal abundance of arteriolar supply *(46)*.

It has been estimated recently that the majority of oxygen transport in normal tissues actually occurs at the level of the terminal arteriole, rather than in capillaries *(46)*. There are arteriolar supply vessels to tumors, but they typically do not enter the tumor parenchyma *per se,* unless the tumor happens to grow around them *(47)*. Thus, oxygen transport in tumors cannot occur via arterioles. This means that the majority of oxygen transport is delivered via capillaries or veins, and it is likely that the blood must travel unusually long distances in postarteriolar microvessels before exiting the tumor *(48)*. There are several sets of data to support this hypothesis. Using phosphorescence quench imaging, it has been shown that longitudinal gradients exist in skin window chamber tumors, where those microvessels nearest the arterioles are much better oxygenated than vessels most distant from the arterioles *(49)*. The most distant vessels appear to be hypoxic (PO_2 averaging <10 mmHg). Studies with oxygen microelectrodes *(43)* and phosporescence quench imaging studies of Helmlinger et al. *(44)* have independently demonstrated the presence of hypoxemic tumor microvessels, in the absence of vascular stasis. Collectively, these data substantiate the notion that vascular hypoxia in tumors occurs because of the relative lack of arterioles. Vascular hypoxia, of the type described here, does not occur in normal tissues.

4.1.2. Altered Blood Viscosity

The vascular hypoxia found in tumors was speculated to be responsible for altered blood viscosity, which could contribute to sluggish flow that is often found in tumors. Using a viscometer, suspension viscosity was found to be increased by 40% when PO_2 and pH were decreased below 10 mmHg and 6.8, respectively. This effect was caused by shrinking of red cells. When the calcium channel blocker, flunarizine (5–10 mg/L-1), was co-administered with red cell suspensions, viscosity returned to control levels *(50)*. When the effect of flunarizine was examined in vivo, the drug improved blood flow and oxygenation, selectively, in the center of tumors, where microvessels are more hypoxic *(51)*. In summary, the reduced vascular oxygenation observed in tumors leads to rheologic changes in red cells that increase viscosity and decrease tumor blood flow. This leads to a viscous cycle, as the resultant reduction in blood flow further exacerbates the vascular

hypoxemia. The use of agents, such as flunarizine, could break this cycle, and at least restore viscosity to normal limits.

4.1.3. Vascular Geometry

The classic theory, which originated with Thomlinson and Grey, is that chronic hypoxia develops because intervascular distances are too long in tumors *(41)*. However, the irregular geometry of vascular networks is also important. Dewhirst et al. *(52)* have performed simulations of oxygen transport in two microvascular networks. The simulations were done using microvessel flow velocities and hematocrits that are typical for the R3230Ac tumor line growing in skin window chambers. Oxygen consumption rates were assumed to be in the midrange of what has been measured for this tumor line. Two models were compared (actual geometry shown in Fig. 4A). The Greens' function model utilizes the actual microvascular geometry; the Krogh cylinder model assumes that all of the vessels are straight and parallel. In simulations, the Krogh cylinder model predicted no regions of tissue with PO_2 <10 mmHg; the Green's function model predicted substantial regions of hypoxia (Fig. 4B). These represent scenarios in which there is adequate vascular density, but the chaotic nature of the vascular geometry creates hypoxia *(47,53)*.

The presence of highly disordered vascular networks also leads to plasma channels. These are vessels that do not contain appreciable red cells, but do carry plasma. In the skin-fold chamber tumor model, it has been estimated that 8–9% of all microvessels have this characteristic *(54)*. These channels probably develop because of the abnormal branching angles and altered rheology of red cells. Both of these conditions will tend to favor concentration of red cells in vessels with the lowest flow resistance.

4.1.4. Oxygen Demand vs Oxygen Supply

Microregional measurements of oxygen consumption have been performed by fitting the profile of oxygen tension between vessels to a diffusion equation *(52)*. For the R3230 Ac tumor, oxygen consumption rates were observed in the range of what has been measured in murine and human tumor xenografts *(48,55)*, averaging 1.5 mL O_2/100 g/min (range 0.8–2.2 mL/100 g/min). The oxygen consumption rates that have been measured in tumors are in the midrange of what has been reported for normal tissues *(48)*. Thus, one cannot make the claim that tumor hypoxia is the result of oxygen consumption rates that are abnormally elevated.

The Green's function method described above has also been used to compare the relative importance of tissue perfusion, oxygen content, and oxygen consumption in controlling tumor oxygenation (Fig. 4C; *48,56)*. The object of the simulations was to

Fig. 4. Three-dimensional vascular architecture and its effects on oxygen transport. **(A)** Three-dimensional reconstruction of a microvascular network in a window-chamber tumor, as determined using confocal microscopy. **(B)** Comparison of the distribution of PO_2 values for actual geometry vs the same vascular density, but with evenly spaced, parallel vessels (Krogh cylinder simulation). The irregular geometry leads to hypoxia (PO_2 values < 10 mmHg), but no hypoxia is predicted for the Krogh cylinder simulation. **(C)** Relative effects of microvascular perfusion, oxygen content, and oxygen consumption rate on hypoxic fraction. This simulation indicates that the most sensitive parameter for reduction of hypoxia is manipulation of oxygen consumption rate. (Reproduced with permission from ref. *48*)

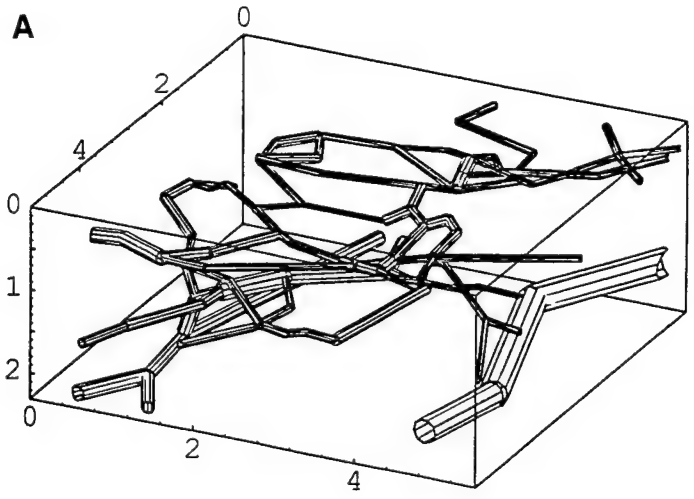
A
0
2
4
0
1
2
0
2
4

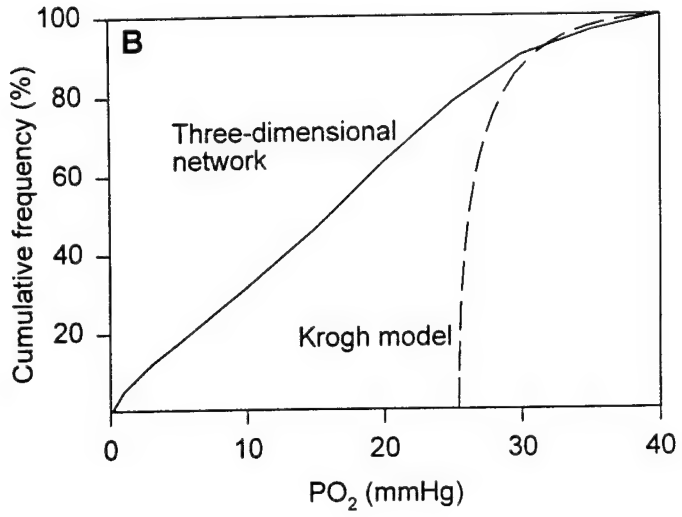
B
100
80
60
40
20
Cumulative frequency (%)
Three-dimensional network
Krogh model
0
10
20
30
40
PO_2 (mmHg)

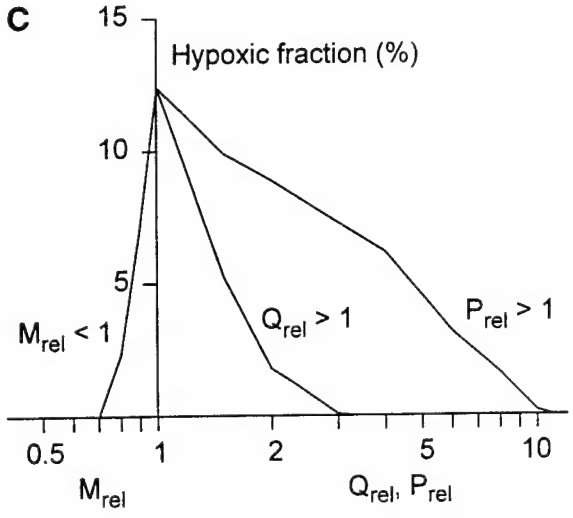
C
15
10
5
Hypoxic fraction (%)
M_{rel} < 1
Q_{rel} > 1
P_{rel} > 1
0.5
1
2
5
10
M_{rel}
Q_{rel}, P_{rel}

determine how much perfusion, oxygen content, or consumption rate would have to be changed, to eliminate hypoxia in the simulated region. Under two baseline conditions of oxygen consumption, the most efficient method to reduce hypoxia was via reduction in oxygen consumption rate. In one example, the relative efficiency of changing oxygen consumption vs oxygen content of blood was a factor of 30. To be specific, an 11-fold increase in oxygen content would be needed to eliminate hypoxia, compared with a 30% reduction in oxygen consumption rate. Thus, even though oxygen consumption is not greatly elevated, relative to many normal tissues, it still has the most significant impact on tissue oxygenation in tumors.

4.2. Acute Hypoxia

Until recently, the commonly held view has been that acute hypoxia results primarily from vascular stasis, and that this occurs from one of three causes: vascular collapse, leukocyte plugging, or impingement of tumor cells in the vascular lumen. Although these factors may play a role in vascular stasis, they are not the only cause for acute hypoxia. Using window chamber tumors to study the kinetics of tumor microvessel flow, total vascular stasis was observed in approx 5% of vessel segments, and the duration of stasis was <20 s *(57)*. These data are similar in magnitude to prior reports by Chaplin et al. using matched dye methods *(58)*. Based on these observations, it seems that total vascular stasis is not the most common source of transient hypoxia.

Flow instabilities are a rather common phenomenon, and there is strong evidence that instabilities in tumor perfusion, short of vascular stasis, can lead to transient hypoxia *(60)*. Trotter et al. performed a series of studies in murine tumors using, pairs of intravenously administered fluorescent dyes to monitor functional vessels *(59)*. They noted differences in staining intensity around groups of vessels, and theorized that this may be caused by fluctuations in blood flow rate within small networks of vessels. They also suggested that such behavior could lead to transient hypoxia, without a requirement of total vascular stasis. Temporal variations in perfusion have been seen in both experimental and human tumors, using laser Doppler flowmetry *(60,61)*. Similarly, the temperature of murine tumors has been shown to be temporally unstable, which must be related to variations in perfusion rate *(62)*. These data suggest that variations in blood flow rate occur in tumors, but until recently there was no direct proof that such variations in flow could lead to transient hypoxia.

This issue was also addressed by simultaneously monitoring microvessel red cell flux and PO_2 for periods up to 1 h, using window chamber tumors by Kimura et al. *(57)*. In most cases, the red cell flux in groups of microvessels was unstable, and the variations in red cell flux could be as much as several orders of magnitude, but more commonly is in the range of a factor of two. The Green's function method was used to simulate the effects of a twofold change in red cell flux on tissue PO_2 distribution. The simulation showed that as much as 25% of the tumor region could fluctuate above and below a hypoxic threshold, under these conditions. Considering the fact that the observed fluctuations were of at least this order of magnitude in nearly all vessels studied, the investigators concluded that transient hypoxia must be a common phenomenon, and that it is most frequently brought on by fluctuation in blood flow, rather than by total vascular stasis.

More recently, temporal instabilities of PO_2 and perfusion in hind limb tumors have been investigated *(63)*. To accomplish this task, 10-μm diameter recessed-tip electrodes and laser Doppler probes were introduced into tumors, and monitored continuously for

Table 6
Temporal Observations of Intermittent Hypoxia in R3230 Ac Flank Tumors *(63)*

Parameter	*PO_2 < 5 mmHg*
Fraction of experiments never hypoxic	5/13
Fraction of experiments always hypoxic	3/13
Median number of hypoxic events/h	3.9 (0.9–17.9)[a]
Median % time hypoxic	60.1 (16.2–84.7)[a]
Median duration of hypoxic episodes (min)	7.4 (0.9–44.7)[a]

[a]Numbers in parentheses indicate range of data.

periods ranging from 60 to 120 min. The observed fluctuations in PO_2 were similar in kinetics to those previously published for laser Doppler flowmetry by Chaplin and Hill *(60,61)*, and were consistent with Kimura and Braun *(57,63)* in the window chamber model (Table 6). In these studies, some measurements never dropped below a threshold value of 10 mmHg, and others remained below this threshold for periods up to 90 min of observation. The remaining experiments, however, demonstrated temporal variations above and below this threshold.

It has been reported that hypoxia might create negative selection pressure on cells with wild-type p53 suppressor gene, since activation of p53 leads to apoptosis *(64)*. Thus, cells with mutant forms of p53 would gain a survival advantage over cells with wild-type p53. The instabilities in tumor oxygenation perhaps suggest a more sinister effect of hypoxia *(57,63)*. If the process of oxygen transport is as unstable as these results would indicate, then it is possible that, once a tumor becomes vascularized, it is subjected to repeated cycles of ischemia-reperfusion injury. Since the primary bioactive product of this process is superoxide anion *(65)*, it is possible that mutagenic events leading to tumor progression could result. Recent evidence for the mutagenic effects of hypoxia reoxygenation injury comes from the work of Reynolds et al. *(66)*. In these studies, a phage shuttle vector reporter system was transfected into the tumorigenic cell line, LN12. In tissue culture under normoxic conditions the incidence of mutations averaged $<2 \times 10^{-5}$, even after more than 20 passages. However, the incidence increased by a factor of four after one episode of hypoxia/reoxygenation, and doubled again after another episode. The incidence was much higher when the tumor was grown in vivo, compared with in vitro culture, as well.

The causes of acute hypoxia are not well defined at this time. Certainly, all of the factors that contribute to chronic hypoxia will also contribute to acute hypoxia, since they create the baseline conditions that exist without blood flow fluctuations. Factors that may contribute to flow fluctuations include arteriolar vasomotion *(54)*, rapid vascular remodeling *(67)*, and other hemodynamic effects *(68,69)*.

It is clear from the above discussion that tumor hypoxia is a complex and dynamic process that is the result of several factors. Chronic hypoxia probably develops as a result of exaggerated longitudinal gradients, leading to intravascular hypoxia; irregular vascular geometry and/or long intervascular distances; irregular vascular branching patterns; and rheologic effects, leading to plasma channels and oxygen consumption rates that are out of balance with oxygen delivery. These features, combined with the dynamic nature of tumor blood flow, lead to an overall pattern of hypoxia that is both chronic and acute (Fig. 5).

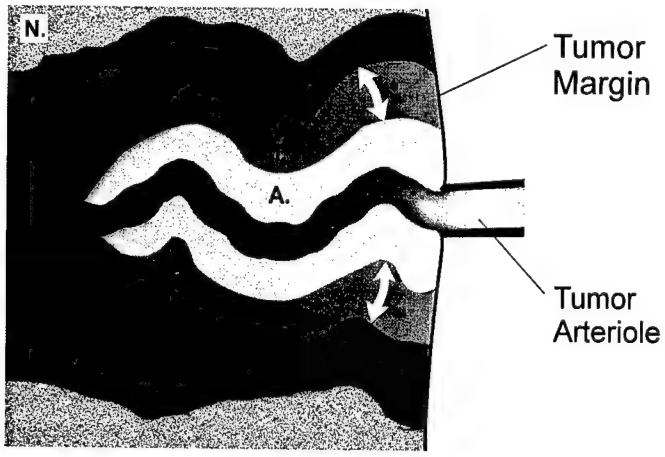

Fig. 5. Composite working model for interrelationships between chronic and acute hypoxia. Arrows indicate diffusion distance of oxygen that is influenced by instabilities in red cell flux. At the extremes, there are regions of vascular hypoxia where such fluctuations are of little consequence, since tissues immediately surrounding the vasculature would be hypoxic (C = chronically hypoxic). Conversely, there are regions near well-oxygenated vessels that are unaffected by changes in red cell flux (A = aerobic). It is likely, however, that large regions of tumor will lie between these extremes, and will be subjected to periodic fluctuations in PO_2 that lead to hypoxia reoxygenation injury. I = intermittently hypoxic; N indicates regions of necrosis.

It is of interest to note that many of the genes involved in regulation of angiogenesis are regulated by hypoxia (Table 4). However, there is very little information on whether such genes are also regulated by hypoxia reoxygenation injury, particularly with the kinetics shown in this chapter. Clearly this is an important area for future investigation.

5. NITRIC OXIDE

There is increasing evidence that tumors produce varying levels of NO *(70)*. A number of studies have been published that have investigated the effects of NO on angiogenesis. Consistently the story is emerging that NO definitely has an effect, but whether it up- or downregulates the process is controversial. It is important to note that the hyperpermeability of vascular endothelium that is stimulated by VEGF occurs via stimulation of NO synthesis *(71)*. Evidence for a proangiogenic effect of NO comes from the following observations: Exposure of glioblastoma and hepatocellular carcinoma cell lines to SNAP and NOR3 (both NO donor compounds) increased VEGF production, primarily by stabilizing mRNA levels *(72)*; use of NO donors leads to increased angiogenesis in the cornea pocket assay, when angiogenesis is stimulated by substance P *(73)*; use of NO donors stimulates proliferation of coronary postcapillary endothelial cells, in vitro *(74)*; and the human breast tumor line, DLD1, which was transfected with the NO synthase gene, grew more quickly and had better-vascularized tumors than the parent line *(75)*. There are also data that indicate that NO downregulates angiogenesis. Examples of such evidence include: VEGF production by arterial smooth muscle cells is downregulated by NO (in this case, the inhibition occurs by inhibition of AP1 binding to the VEGF promoter *[76]*); production of VEGF and its receptors are downregulated when NO is added to the perfusate of ex vivo perfused lungs, and angiogenesis is inhibited in the chick

corioallantoic membrane when exposed to exogenous NO, and is upregulated when NO synthase inhibitors are used *(77,78)*; primary tumor growth and metastasis frequency are lowered in the Lewis lung tumor model when animals are administered NO donor drugs *(79)*; proliferation and migration of endothelial cells is inhibited in vitro in the presence of NO donor drugs *(80,81)*.

The data that are available thus far suggest that NO has both positive and negative effects on angiogenesis. However, two sets of data in tumor models suggest that it plays a positive role in stimulating angiogenesis *(75,79)*. Clearly, the issue is very complicated, and additional work is needed to further elucidate the role that it plays in tumor angiogenesis.

6. SUMMARY

There is no question that there is a complex interrelationship between tumor hypoxia and tumor angiogenesis. A question that remains unanswered is whether the hypoxia in tumors is responsible for abnormal angiogenesis, or whether the abnormal angiogenesis is responsible for hypoxia. In all likelihood, dysfunction in both processes feed on each other to continue the process of tumor growth. At issue, then, is whether there is any benefit to be gained from trying to modulate tumor hypoxia as part of antiangiogenesis therapy. Presumably, if one were to improve tumor oxygenation by some means, there might be a reduction in the angiogenic stimulus, but, under such conditions, additional tumor cell growth might be favored. Alternatively, pharmacologic manipulation designed to increase tumor hypoxia may stimulate more angiogenesis, thus stimulating additional tumor growth. If either of these types of manipulations were combined with antiangiogenesis therapy, it is difficult to predict what the net result would be on tumor growth and metastasis. Alternatively, it is not clear what the physiologic consequences of antiangiogenesis therapy are on tumor oxygenation. Will the use of antiangiogenic agents exacerbate hypoxia, leading to altered cytokine expression, additional intermittent hypoxia, and tumor progression? Clearly additional studies are needed to begin to unravel these complex processes, since the answers may have important implications in how to implement these exciting new forms of therapy.

ACKNOWLEDGMENTS

The authors acknowledge the detailed art work provided by Irram Haroon. This work was supported by grants from the National Institutes of Health CA40355, CA 71753, the Duke Specialized Program of Research Excellence on Breast Cancer P50 CA 68438, and Department of Defense DAMD 179717044.

REFERENCES

1. Hamilton, W. J., Boyd, J. D., and Mossman, H. W. (1962) *Human Embryology*, William and Wilkins, Baltimore.
2. Folkman, J. and Shing, Y. (1992) Angiogenesis. *J. Biol. Chem.* **267,** 10,931–10,934.
3. Blood, C. A. and Zetter, B. R. (1990) Tumor interactions with the vasculature: angiogenesis and tumor metastasis. *Biochim. Biophys. Acta* **1032,** 89–118.
4. Clark, R. A. F. (1996) Wound repair: overview and general considerations, in *Molecular and Cellular Biology of Wound Repair*, 2nd ed. (Clark, R. A. F., ed.), Plenum, New York, pp. 1–50.
5. Ausprunk, D. H. and Folkman, J. (1977) Migration and proliferation of endothelial cells in preformed and newly formed blood vessels during tumor angiogenesis. *Microvasc. Res.* **14,** 53–65.

6. Mustohen, T. and Alitalo, K. (1995) Endothelial receptor tyrosine kinases involved in angiogenesis. *J. Cell Biol.* **129,** 895–898.
7. Brown, L. F., Detmar, M., Claffey, K, Nagy, J. A., Feng, D., Dvorak, A. M., and Dvorak, H. F. (1997) Vascular permeability factor/vascular endothelial growth factor: a multifunctional angiogenic cytokine. *EXS. Regul. Angiogenesis* **79,** 233–269.
8. Dvorak, H. F., Brown, L. F., Detmar, M., and Dvorak, A. M. (1995) Vascular permeability factor/ vascular endothelial growth factor, microvascular hyperpermeability, and angiogenesis. *Am. J. Pathol.* **146,** 1029–1039.
9. Folkman, J. (1997) Angiogenesis and angiogenesis inhibition: an overview. *EXS Regul. Angiogenesis* **79,** 1–7.
10. Pepper, M. S., Montesano, R., Mandriota, S. J., Orci, L., and Vassalli, J-D (1996) Angiogenesis: a paradigm for balanced extracellular proteolysis during cell migration and morphogenesis. *Enzyme Protein* **49,** 138–162.
11. Flaumenhaft, R. and Rifkin, D. B. (1992) Extracellular regulation of growth factor action. *Mol. Biol. Cell.* **3,** 1057–1065.
12. O'Reilly, M. S., Holmgren, L., Shing, Y., Chen, C., Rosenthal, R. A., Moses, M., et al. (1994) Angistatin: a novel angiogenesis inhibitor that mediates the suppression of metastases by a Lewis lung carcinoma. *Cell* **79,** 315–328.
13. Mignatti, P. and Rifkin, D. B. (1996) Plasminogen activators and matrix metalloproteinases in angiogenesis. *Enzyme Protein* **49,** 117–137.
14. Hu, D. E., Hori, Y., and Fan, T. P. (1993) Interleukin-8 stimulates angiogenesis in rats. *Inflammation* **17(2),** 135–143.
15. Adams, D. H. and Lloyd, A. R. (1997) Chemokines: leucocyte recruitment and activation cytokines. *Lancet* **349,** 490–495.
16. Polverini, P. J. (1997) Role of macrophages in angiogenesis-dependent disease. *EXS Regul. Angiogenesis* **79,** 11–28.
17. Meininger, C. J. (1995) Mast cells and tumor associated angiogenesis. *Chem. Immunol.* **62,** 239–257.
18. Battegay, E. J. (1995) Angiogenesis: mechanistic insights, neovascular diseases, and therapeutic prospects. *J. Mol. Med.* **73,** 333–346.
19. Brooks, P. C. (1996) Role of integrins in angiogenesis. *Eur. J. Cancer* **32A,** 2423–2429.
20. Varner, J. A. (1997) The role of vascular cell integrins $\alpha_v\beta_3$ and $\alpha_v\beta_5$ in angiogenesis. *EXS Regul. Angiogenesis* **79,** 361–390.
21. Maisonpierre, P. C., Suri, C., Jones, P. F., Bartunkova, S., Wiegand, S., Radziejewski, C., et al. (1997) Angiopoietin-2, a natural antagonist for Tie2 that disrupts *in vivo* angiogenesis. *Science* **277,** 55–60.
22. Sato, T. N., Tazawa, Y., Deutsch, U., Wolburg, H., Risau, W., and Qin, Y. (1995) Distinct roles of the receptor tyrosine kinases Tie-1 and Tie-2 in blood vessel formation. *Nature* **376,** 70–74.
23. Wong, A. L., Haroon, Z. A., Werner, S., Dewhirst, M. W., Greenberg, C. S., and Peters, K. G. (1997) Expression and phosphorylation of Tie-2 in adult rat tissue suggest a dual role in angiogenesis and vascular maintenance. *Circ. Res.* **81,** 567–574.
24. Haddow, A. (1972) Molecular repair, wound healing, and carcinogenesis: tumor production a possible overhealing? *Adv. Cancer Res.* **16,** 181–234.
25. Dvorak, H. F. (1986) Tumors: wounds that do not heal. *New Eng. J. Med.* **315(26),** 1650–1659.
26. van Hinsbergh, V. W. M., Koolwijk, P., and Hanemaaijer, R. (1997) Role of fibrin and plasminogen activators in repair-associated angiogenesis: *in vitro* studies with human endothelial cells. *EXS Regul. Angiogenesis* **79,** 391–411.
27. Enholm, B., Paavonen, K., Ristimaki, A., Kumar, V., Gunji, Y., Klefstrom, J., et al. (1997) Comparison of VEGF, VEGF-B, VEGF-C and Angiogenesis-1 mRNA regulation by serum, growth factors, oncoproteins and hypoxia. *Oncogene* **14,** 2475–2483.
28. Kuwabara, K., Ogawa, S., Matsumoto, M., Koga, S., Clauss, M., Pinsky, D., et al. (1995) Hypoxia-mediated induction of acidic/basic fibroblast growth factor and platelet-derived growth factor in mononuclear phagocytes stimulates growth of hypoxic endothelial cells. *Proc. Natl. Acad. Sci. USA* **922,** 4606–4610.
29. Waltenberger J., Mayr, U., Pentz, S., and Hombach, V. (1996) Functional upregulation of the vascular endothelial growth factor receptor KDR by hypoxia. *Circulation* **94,** 1647–1654.
30. Detmar, M., Brown, L., Berse, B., Jackman, R., Elicker, B., Dvorak, H., and Claffey, K. (1997) Hypoxia regulates the expression of VPF/VEGF and its receptors in human skin. *J. Inves. Dermatol.* **108,** 263–268.

31. Karakurum, M., Shreeniwas, R., Chen, J., Pinsky, D., Yan, S.-D., Anderson, M., et al. (1994) Hypoxic induction of interleukin-8 gene expression in human endothelial cells. *J. Clin. Invest.* **93,** 1564–1570.
32. Gleadle, J., Ebert, B., Firth, J., and Ratcliffe, P. (1995) Regulation of angiogenic growth factor expression by hypoxia, transition metals, and chelating agents. *Am. J. Physiol.* **268,** C1362–C1368.
33. Patel, B., Khaliq, A., Jarvis-Evans, J., Mcleod, D., Mackness, M., and Boulton, M. (1994) Oxygen regulation of TGF β1 mRNA in human hepatoma (HEP G2) cells. *Biochem. Mol. Biol. Int.* **34,** 639–644.
34. Sampson, L. and Chaplin, D. (1996) The influence of oxygen and carbon dioxide tension on the production of TNF α by activated macrophages. *Br. J. Cancer* **74(Suppl. XXVII),** S133–S135.
35. Minchenko, A., Salceda, S., Bauer, T., and Caro, J. (1994) Hypoxia regulatory elements of the human VEGF gene. *Cell Mol. Biol. Res.* **40,** 35–39.
36. Brizel, D. M., Scully, S. P., Harrelson, J. M., Layfield, L., Bean, J., Prosnitz, L., and Dewhirst, M. (1996) Tumor oxygenation predicts for the likelihood of distant metastases in human soft tissue sarcoma. *Cancer Res.* **56,** 941–943.
37. Hockel, M., Schlenger, K., Aral, B., Mitze, M., Schaffer, U., and Vaupel, P. (1996) Association between tumor hypoxia and malignant progression in advanced cancer of the uterine cervix. *Cancer Res.* **56,** 4509–4515.
38. Weidner, N., Semple, J. P., Welch, W. R., and Folkman, J. (1991) Tumor angiogenesis and metastasis-corelation in invasive breast carcinoma. *N. Engl. J. Med.* **324,** 1–8.
39. Rak, J., Filmus, J., Finkenzeller, G., Grugel, S., Marme, D., and Kerbel, R. S. (1995) Oncogenes as inducers of tumor angiogenesis. *Cancer Metastasis Rev.* **14,** 263–277.
40. Relf, M., LeJeune, S., Scott, P., Fox, S., Smith, K., Leek, R., et al. (1997) Expression of the angiogenic factors VEGF, acidic and basic FGF, TGF β-1, platelet-derived endothelial cell growth factor, placenta growth factor, and pleiotrophin in human primary breast cancer and its relation to angiogenesis. *Cancer Res.* **57,** 963–969.
41. Thomlinson, R. H. and Gray, L. H. (1955) Histological structure of some human lung cancers and the possible implications for radiotherapy. *Br. J. Cancer* **9,** 539–549.
42. Overgaard, J. and Horsman, M. R. (1996) Modification of hypoxia-induced radioresistance in tumors by the use of oxygen and sensitizers. *Semin. Radiat. Oncol.* **6,** 10–21.
43. Dewhirst, M. W., Ong, E. T., Klitzman, B., Secomb, T., Vinuya, R., Dodge, R., Brizel, D., and Gross, J. (1992) Perivascular oxygen tensions in a transplantable mammary tumor growing in a dorsal flap window chamber. *Radiat. Res.* **130,** 171–182.
44. Helmlinger, G., Yuan, F., Dellian, M., Jain, R. K. (1997) Interstitial pH and PO2 gradients in solid tumors in vivo: high-resolution measurements reveal a lack of correlation. *Nature Med.* **3,** 177–182.
45. Dewhirst, M. W., Ong, E. T., Rosner, G. L., Rhemus, S., Shan, S., Braun, R., Brizel, D., and Secomb, T. (1996) Arteriolar oxygenation in tumour and subcutaneous arterioles: effects of inspired air oxygen content. *Br. J. Cancer* **74(Suppl. XXVII),** S241–S246.
46. Intaglietta, M., Johnson, P. C., and Winslow, R. M. (1996) Microvascular and tissue oxygen distribution. *Cardiovasc. Res.* **32,** 632–643.
47. Vaupel, P., Kallinowski, F., and Okunieff, P. (1989) Blood flow, oxygen, nutrient supply and metabolic microenvironment of human tumors: a review. *Cancer Res.* **49,** 6449–6465.
48. Secomb, T. W., Hsu, R., Braun, R. D., Ross, J. R., Gross, J., and Dewhirst, M. (1997) Theoretical simulation of oxygen transport to tumors by three-dimensional networks of microvessels. *Adv. Exp. Biol. Med.*, in press.
49. Dewhirst, M., Ong, E., Smith, B., Evans, S., Secomb, T., and Wilson, D. (1996) Longitudinal gradients of vascular PO_2 in R3230AC tumor microvessels in dorsal flap window chambers, in *Sixth World Congress for Microcirculation* (Messmer, K. and Kubler, W., eds.), Monduzzi Editore S. p. A., Bologna, Italy, pp. 343–346.
50. Kavanagh, B. D., Coffey, B. E., Needham, D., Hochmuth, R., and Dewhirst, M. (1993) The effect of flunarizine on the viscosity of human and rat erythrocyte suspensions in conditions of extreme hypoxia and lactic acidosis. *Br. J. Cancer* **67,** 734–741.
51. Dewhirst, M. W., Ong, E. T., Madwed, D., Klitzman, B., Secomb, T., Brizel, D., et al. (1992) Effects of the calcium channel blocker flunarizine on the hemodynamics and oxygenation of tumor microvasculature. *Radiat. Res.* **132,** 61–68.
52. Dewhirst, M. W., Secomb, T. W., Ong, E. T., Hsu, R., and Gross, J. (1994) Determination of local oxygen consumption rates in tumors. *Cancer Res.* **54,** 3333–3336.
53. Secomb, T. W., Hsu, R., Dewhirst, M. W., Klitzman, B., and Gross, J. F. (1993) Analysis of oxygen transport to tumor tissue by microvascular networks. *Int. J. Radiat. Oncol. Biol. Phys.* **25,** 481–489.

54. Dewhirst, M. W., Kimura, H., Rehmus, S. W. E., Braun, R., Papahadjopoulos, D., Hong, K., and Secomb, T. (1996) Microvascular studies on the origins of perfusion-limited hypoxia. *Br. J. Cancer* **74,** S247–S251.
55. Kallinowski, F., Schlenger, K. H., Runkel, S., Kloes, M., Stohrer, M., Okunieff, P., and Vaupel, P. (1989) Blood flow, metabolism, cellular microenvironment, and growth rate of human tumor xenografts. *Cancer Res.* **49,** 3759–3764.
56. Secomb, T. W., Hsu, R., Ong, E. T., Gross, J., and Dewhirst, M. (1995) Analysis of the effects of oxygen supply and demand on hypoxic fraction in tumors. *Acta Oncol.* **34,** 313–316.
57. Kimura, H., Braun, R. D., Ong, E. T., Hsu, R., Secomb, T., Papahadjopoulos, D., Hong, K., and Dewhirst, M. (1996) Fluctuations in red cell flux in tumor microvessels can lead to transient hypoxia and reoxygenation in tumor parenchyma. *Cancer Res.* **56,** 5522–5528.
58. Chaplin, D. J., Durand, R. E., and Olive, P. (1986) Acute hypoxia in tumors: implications for modifiers of radiation effects. *Int. J. Radiat. Oncol. Biol. Phys.* **12,** 1279–1282.
59. Trotter, M. J., Olive, P. L., and Chaplin, D. J. (1990) Effect of vascular marker Hoechst 33342 on tumour perfusion and cardiovascular function in the mouse. *Br. J. Cancer* **62,** 903–908.
60. Chaplin, D. J. and Hill, S. A. (1995) Temporal heterogeneity in microregional erythrocyte flux in experimental solid tumors. *Br. J. Cancer* **71,** 1210–1213.
61. Hill, S. A., Pigott, K. H., Saunders, M. I., Powell, M., Arnold, S., Obeid, A., et al. (1996) Microregional blood flow in murine and human tumours assessed using laser Doppler microprobes. *Br. J. Cancer* **74,** S260–S263.
62. Li, X., Brown, S. L., and Hill, R. P. (1992) Factors influencing the thermosensitivity of two rodent tumors. *Radiat. Res.* **130,** 211–219.
63. Dewhirst, M. W., Braun, R. D., and Lanzen, J. L. (1998) Temporal changes in PO_2 of R3230 Ac tumors, in Fischer-344 rats. *Int. J. Radiat. Oncol. Biol. Phys.*, submitted.
64. Graeber, T. G., Osmanian, C., and Jacks, T. (1996) Hypoxia-mediated selection of cells with diminished apoptotic potential in solid tumours [see comments]. *Nature* **379,** 88–91.
65. Welbourn, C. R. B., Goldman, G., Paterson, I. S., Valeri, C., Shepro, D., and Hechtman, H. (1991) Pathophysiology of ischemia reperfusion injury-central role of the neutrophil. *Br. J. Surg.* **78,** 651.
66. Reynolds, T. Y., Rockwell, S., and Glazer, P. M.(1996) Genetic instability induced by the tumor microenvironment. *Cancer Res.* **56,** 5754–5757.
67. Patan, S., Munn, L. L., and Jain, R. K. (1996) Intussusceptive microvascular growth in a human colon adneocarcinoma xenograft: a novel mechanism of tumor angiogenesis. *Microvasc. Res.* **51,** 260–272.
68. Kiani, M. F., Pries, A. R., Hsu, L. L., Saralius, H., and Cokelet, G. (1994) Fluctuations in microvascular blood flow parameters caused by hemodynamic mechanisms. *Am. J. Physiol.* **266,** H1822–H1828.
69. Schmidt-Schoenbein, G. W., Skalak, R., Usami, S., and Chien, S. (1980) Cell distribution in capillary networks. *Microvasc. Res.* **19,** 18–44.
70. Tozer, G. M. and Everett, S. A. (1997) Nitric oxide in tumour biology and cancer therapy. Part 1. Physiological aspects. *Clin. Oncol.* **9,** 282–293.
71. Wu, H. M., Huang, Q., Yuan, Y., and Granger, H. J. (1996) VEGF induces NO-dependent hyperpermeability in coronary venules. *Am. J. Physiol.* **271,** H2735–H2739.
72. Chin, K., Kurashima, Y., Ogura, T., Tajiri, H., Yoshida, S., and Esumi, H. (1997) Induction of vascular endothelial growth factor by nitric oxide in human glioblastoma and hepatocellular carcinoma cells. *Oncogene* **15,** 437–442.
73. Ziche, M., Morbidelli, L., Masini, E., Amerini, S., Granger, H. J., Maggi, C. A., Geppetti, P., and Ledda, F. (1994) Nitric oxide mediates angiogenesis in vivo and endothelial cell growth and migration in vitro promoted by substance P. *J. Clin. Invest.* **94,** 2036–2044.
74. Morbidelli, L., Chang, C. H., Douglas, J. G., Granger, H. J., Ledda, F., and Ziche, M. (1996) Nitric oxide mediates mitogenic effect of VEGF on coronary venular endothelium. *Am. J. Physiol.* **270,** H411–H415.
75. Jenkins, D. C., Charles, I. G., Thomsen, L. L., Moss, D. W., Holmes, L. S., Baylis, S. A., et al. (1995) Roles of nitric oxide in tumor growth. *Proc. Natl. Acad. Sci. USA* **92,** 4392–4396.
76. Tsurumi, Y., Murohara, T., Krasinski, K., Chen, D., Witzenbichler, B., Kearney, M., Couffinhal, T., and Isner, J. M. (1997) Reciprocal relation between VEGF and NO in the regulation of endothelial integrity. *Nature Med.* **3,** 879–886.
77. Tuder, R. M., Flook, B. E., and Voelkel, N. F. (1995) Increased gene expression for VEGF and the VEGF receptors KDR/Flk and Flt in lungs exposed to acute or to chronic hypoxia. Modulation of gene expression by nitric oxide. *J. Clin. Invest.* **95,** 1798–1807.

78. Pipili-Synetos, E., Sakkoula, E., Haralabopoulos, G., Andriopoulou, P., Peristeris, P., and Maragoudakis, M. E. (1994) Evidence that nitric oxide is an endogenous antiangiogenic mediator. *Br. J. Pharmacol.* **111,** 894–902.
79. Pipili-Synetos, E., Papageorgiou, A., Sakkoula, E., Sotiropoulou, G., Fotsis, T., Karakiulakis, G., and Maragoudakis, M. E. (1995) Inhibition of angiogenesis, tumour growth and metastasis by the NO-releasing vasodilators, isosorbide mononitrate and dinitrate. *Br. J. Pharmacol.* **116,** 1829–1834.
80. Yang, W., Ando, J., Korenaga, R., Toyo-oka, T., and Kamiya, A. (1994) Exogenous nitric oxide inhibits proliferation of cultured vascular endothelial cells. *Biochem. Biophys. Res. Commun.* **203,** 1160–1167.
81. Lau, Y. T. and Ma, W. C. (1996) Nitric oxide inhibits migration of cultured endothelial cells. *Biochem. Biophys. Res. Commun.* **221,** 670–674.